Fatigue life assessment on composite concrete-steel bridges

Author:

Gonzalo Jurado

Supervisors:

Prof. Luis Borges
Prof. Carlos Rebelo
Prof. Helena Gervasio

University of Coimbra

ACKNOWLEDGEMENTS

This work has been carried out under the supervision of Prof. Luís Borges, Prof. Carlos Rebelo and Prof. Helena Gervásio and I would like to thank them for all their help and encouragement.

I would like to thank Prof. Luís Simões da Silva, director of ISISE, for his support and for granting me the opportunity to work in an outstanding research environment. To the administrative staff (Manuela, Vera and Bárbora) whose cooperation and assistance throughout the program have been greatly appreciated.

My special gratitude goes to my family for their patience and constant support. They have guided, encouraged, loved and consoled me through it all. I love you more than words can express.

To my friends, those who, despite the physical distance, have always been there for me when I needed them the most. The warmth of their words in moments of despair has meant everything to me. Thank you.

My time during SUSCOS program has been memorable thanks to all my colleagues. I would like to thank all of you for the good times we spent both at the university and outside. It has been an incredible experience and I owe it to you.

Finally, to my dear friend who is watching me from heaven.

Coímbra, 31 January 2017 Gonzalo Jurado

'Life is not waiting for the storm to pass, it's learning how to dance in the rain'.

- Vivian Greene.

ABSTRACT

Fatigue is an important consideration in the design of bridges, especially those made of steel. Cycles resulting from the passage of a truck over a bridge depend essentially on bridge type, detail location, span length and vehicles axles configuration. Moreover, as bridges form the keystone of transport networks, their safe operation with minimal maintenance closures is paramount for efficient operation. Yearly increases in the volume of heavy traffic mean a higher number of fatigue damaging load cycles, which leads to taking appropriate measures and finding sustainable solutions, with reduced environmental, economic and social impacts.

This work is focused on developing a software tool for the design and assessment of composite concrete-steel bridges under fatigue, according to Eurocodes. The type of bridge used for this project is limited to a road-girder-bridge. Design approaches include both the damage equivalent factor method and the damage accumulation method. For the latter, an algorithm was developed which simulates truck passages over a bridge model and calculates fatigue load effects using the axle positions recorded in real time. This information could serve as an identification tool for bridges where fatigue is likely to be a problem and could form part of a full bridge management framework in the future.

Furthermore, the program is applied into a real case study, in order to compare the results and evaluate its efficiency and accuracy. Finally, conclusions are drawn and future work is proposed, leaving space for improvements and new challenges.

TABLE OF CONTENTS

LIST OF FIGURES

LIST OF TABLES

1   INTRODUCTION AND OBJECTIVES

Bridges are critical elements within a road network and their safe operation with minimal maintenance closures is paramount for efficient operation. Bridge managers must operate, maintain, and improve their structures whilst providing safety and comfort for the user and adhering to limited financial resources. An increasing part of work on the roadway infrastructures concerns the assessment and maintenance of existing structures.

Fatigue evaluation is an important task in design of bridges because the metallic members of bridges are subjected to variable amplitude loading due to passage of traffic on the bridge. For fatigue evaluation, stress ranges and number of cycles play an important role and should be determined as accurately as possible. However, they are highly dependent of different parameters like bridge type, detail location, span length and vehicles axles configuration. For example, considering the negative moment at the mid support of a two-span continuous bridge and assuming large spans for simplicity, two cycles occur due to passage of one truck. Also, the problem becomes more complicated, assuming presence of more than one truck over the bridge.

The main goals of this research plan are the follows:

I.   Assessment of the structural performance of composite concrete-steel bridges over time, focusing of fatigue behavior;

II.   Development of a probabilistic approach for the fatigue assessment of bridges taking into account traffic variation over time and a S-N probabilistic curve;

III. Development of a software tool for the implementation of the developed approach.

Two types of fatigue assessment were included: the simple equivalent factor method and the more detailed damage accumulation method.

Moreover, a traffic simulation module which provides a flexible configuration was developed for this purpose. This module allows determining the maximum values of the internal forces by simulating various traffic load models on several types of two lane bridge (bidirectional traffic) as well as two-lane highway bridges (unidirectional traffic). Furthermore, the program is prepared to determine stress histograms as well as cumulative damage on the detail under study.

The thesis is organised in 3 main chapters: first, there is some literature review, where general theoretical concepts as well as some research on the topic are presented; then, the program as a software tool is introduced, taking note to its structure and operation; and, finally, the program is applied to a real case study in order to compare the results and analyse its accuracy. In the end, some conclusions and future improvements are mentioned.

2   LITERATURE REVIEW

2.1   FATIGUE LOAD MODELS IN EUROCODES

2.1.1   Introduction

Load effects generated by traffic loads on bridges are generally very complex. Not only are the stress ranges generated by these loads of variable amplitudes, but also other parameters that might affect the fatigue performance of bridge details such as the mean stress values and the sequence of loading cycles are rather stochastic.

In order to treat such complex loading situations there is a need to represent the "real" traffic loads in terms of one or more equivalent load models. Expressed in terms of load effects (i.e. stresses and deformation) the variable amplitude stress ranges generated by real traffic loads on bridges should be represented as one or more equivalent constant amplitude stress ranges, which are easier to treat in a design situation. In doing so, the fatigue damage generated by these equivalent load models should be equivalent to that caused by the real traffic load on bridges. The fatigue load models in EN 1990 and EN 1991-2 were derived on the basis of these principles.

In summary, the procedure used to derive the fatigue load models in Eurocode (illustrated graphically in Figure 2.1) is the following:

1. Selection of typical bridges for simulating bridge responses to traffic flow;

2. Selection of typical structural details for fatigue analysis along with their fatigue resistance curves;

3. Using measured traffic data and the influence line for each studied detail, perform a simulation of bridge response to obtain the stress history relevant for fatigue design of the detail;

4. Employing an appropriate cycle counting method to transform the stress history into a stress histogram with a number of constant amplitude stress ranges;

5. Applying damage accumulation rule (e.g. Palmgren-Miner rule) to obtain an equivalent stress range $\Delta\sigma_E$, causing the same damage as the stress histogram generated in the traffic simulation.

6. Deriving damage-equivalent fatigue load models, which generate a comparable damage to that caused by $\Delta\sigma_E$.

It goes without saying that an accurate determination of fatigue load models requires an appropriate selection of the geometry of the load model vehicles, its axle loads, axle spacing as well as the composition of traffic and its dynamic effects. All these factors have been considered in the derivation of traffic load models for bridges in Eurocode. A more detailed description of how traffic load models for road bridges was performed can be found in [3].

2.1.2   Fatigue load models for road bridges

The fatigue load models for road bridges recommended in EN 1991-2 were derived according to the procedure presented in the previous section. In EN 1991-2, there are totally five recommended fatigue load models to reflect the actual load conditions accurately when designing road bridges against fatigue. These fatigue load models have been defined and calibrated based on a wide range of European traffic data measurements in which the traffic measured during the two measurement periods, the years 1977 – 1982 and 1984 – 1988. These measurements were recorded on various types of roads and bridges in different European countries [3].

The Auxerre traffic has been chosen as the basis for the derivation of the load models for road bridges in
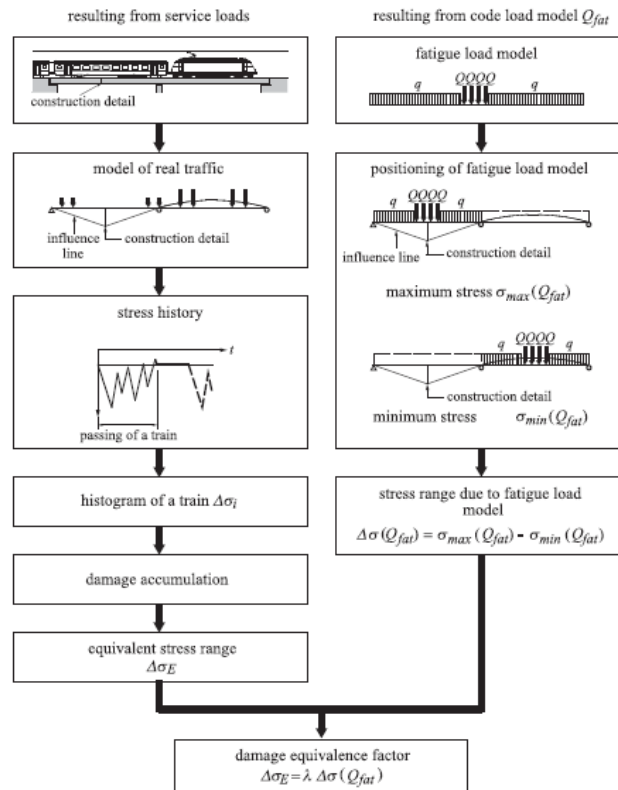
Figure 2.1: Damage equivalent factor (Hirt, 2006).

EN 1991-2. The Auxerre traffic displays neither the largest axle loads nor the longest measurement. However, it has the largest frequency of large axle loads which is an essential factor to derive a characteristic design load for fatigue design of bridges. Another reason for choosing the Auxerre traffic as a common "European traffic" is that the extrapolation method used to determine characteristic values needed a sample of uniform traffic, which was provided by this traffic composition.

All in all, five different load models are proposed in EN 1991-2 for road traffic. The choice of appropriate load model depends on the fatigue verification method used in design. In addition, the use of a specific load model might lead to conservative results in a specific case, while another load model might be more appropriate in a specific situation. In the following sections, a more detailed description of each load model is presented and comments are made on the application of these load models when appropriate.

2.1.2.1 Fatigue Load Model 1 (FLM 1)

Fatigue load model 1 (FLM 1) is intended to be used to check an "infinite fatigue design" situation, i.e. to check whether the fatigue life of the bridge may be considered infinite. This load model generates a "constant amplitude" stress range which is the algebraic difference between the minimum and maximum stress obtained from positioning the load model in the corresponding tow positions.

FLM 1 is directly derived from the characteristic load model 1 (LM 1) used in the ULS design by multiplying the concentrated axle loads (Q_{ik}) by 0.7 and the weight density of the uniformly distributed loads (q_{ik}, q_{rk}) by 0.3. Thus, FLM 1 is composed of both concentrated and uniformly distributed loads. Fatigue verification with FLM 1 is performed by comparing the stress range generated by this model to the Constant Amplitude Fatigue Limit (CAFL). Therefore fatigue design using FLM 1 would yield a very heavy structure.

The characteristic LM 1 is composed of double-axle concentrated loads (called the Tandem System) applied in conjunction with a uniformly distributed load (UDL). This load model was developed using measured traffic data on the motorway (A6) Paris-Lyon near Auxerre. The vehicle geometry and the axle loads are specified in EN 1991-2. As shown in Figure 2.2, the amount of uniformly distributed load applied on bridge lanes including remaining area is the same except for lane number 1, in which a higher fatigue load is recommended.

2.1.2.2 Fatigue Load Model 2 (FLM 2)

Fatigue load model 2 (FLM2) is defined as a set of frequent lorries in Table 4.6 of EN 1991-2. In this table, the set of frequent vehicles is composed of five standard lorries, which represent the most common lorries in Europe. Each lorry is presented with its specific arrangement of axle spacing, axle loads and wheel types for the frequent loading. The loads in fatigue load model 2 and the set of standard lorries was established using the measured traffic data on motorway (A6) Paris-Lyon at Auxerre.

Some notes on the application of FLM1 and FLM2:

- Similar to FLM 1, fatigue load model 2 is intended to be used to determine the maximum and minimum stresses when designing for an unlimited fatigue life. The stress range generated by each lorry should be compared to the CAFL in the fatigue verification.
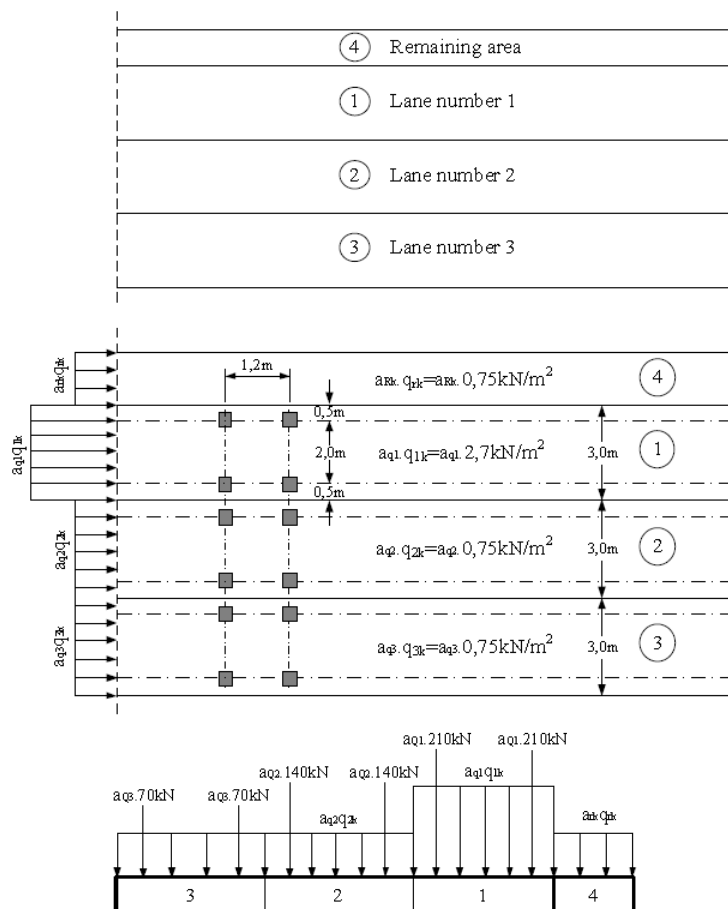
Figure 2.2: Fatigue load model 1 according to EN 1991-2 (Al-Emrani et al., 2014).

- FLM 2 is intended to be used in situations where the presence of more than one vehicle over the bridge can be neglected. This is the situation for bridge details with short influence lines,

e.g. local bending effects in orthotropic steel bridge decks. The fatigue verification should therefore be performed for each vehicle in the traffic set as – dependent on the length of influence line for the particular detail – an axle load, a bogie axle or an entire vehicle may cause a loading cycle. Thus for such situations, FLM 2 deliver more accurate results than FLM 1.

- Fatigue verification applying FLM 1 and FLM 2 is performed by checking that the stress range (the algebraic difference between the maximum and minimum stress) for the detail and load effect under consideration does not exceed the CAFL. This exerts a limitation on the application of these two load models as for some details, such as welded details loaded in shear, a constant amplitude fatigue limit is not defined in the code.

2.1.2.3 Fatigue Load Model 3 (FLM 3)

Fatigue Load Model 3 (FLM 3) is composed of a single vehicle with four axles of 120kN each (the total weight of the vehicle being 480kN). The vehicle geometry and the axle loads are specified in EN 1991-2 and reproduced in Figure 2.3.

Similar to FLM 1 and FLM 2, FLM 3 was also derived using the measured traffic data on the motorway Paris-Lyon at Auxerre. The total weight of the vehicle in FLM3 is slightly higher than the measured total weight in the Auxerre traffic, which was 469kN. On the other hand, the single axle load of 120kN in FLM 3 is lower than the measured maximum axel load which was 131kN.
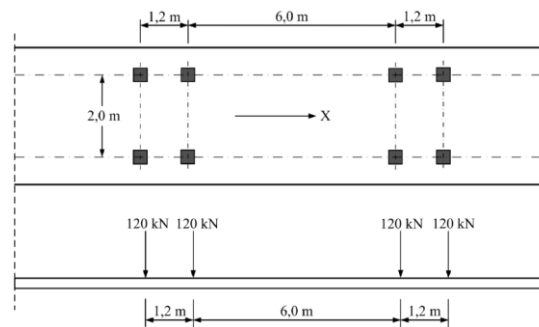
Figure 2.3: Fatigue load model 3 according to EN 1991-2 (Al-Emrani et al., 2014).

FLM 3 is used to verify the fatigue life of the investigated details by calculating the maximum and minimum stresses resulting from the longitudinal and transversal location of the load model. The model is thus intended to be used with the simplified λ–method, i.e. to verify that the computed stress range is equal to or less than the fatigue strength of the detail under study. The model is sufficiently accurate for road bridges with spans longer than 10 m, but has an inclination to yield conservative results for shorter spans [4].

FLM 3 crosses the bridge in the mid-line of the slow traffic lane defined in the project. A second 4 axles vehicle, with a reduced load of 36 kN per axle, can follow the first one with a minimum distance equal to 40 m. This can govern the fatigue design of a structural detail located on an intermediate bridge support, each adjacent span being loaded by one of the two lorries.

Since verification can be made with respect to finite fatigue life, there is a need for specifying a number of cycles, which is expressed as a traffic category on the bridge. A traffic category should be defined by at least (EN 1991-2):

- the number of slow lanes,
- the number N_{obs} of heavy vehicles (maximum gross vehicle weight more than 100kN), observed or estimated, per year and per slow lane (i.e. a traffic lane used predominantly by lorries).

Indicative values are given in EN 1991-2 and reproduced in Table 2.1, but the national annexes may define traffic categories and numbers of heavy vehicles.

Traffic categories		N_{obs} per year and per slow lane
1	Roads and motorways with 2 or more lanes per direction with high flow rates of lorries	$2.0 \cdot 10^6$
2	Roads and motorways with medium flow rates of lorries	$0.5 \cdot 10^6$
3	Main roads with low flow rates of lorries	$0.125 \cdot 10^6$
4	Local roads with low flow rates of lorries	$0.05 \cdot 10^6$

Table 2.1: Indicative numbers of heavy vehicles expected per year and per slow lane (EN 1991-2).

On each fast lane (i.e. a traffic lane used predominantly by cars), additionally, 10% of N_{obs} may be taken into account.

It should be noted that there is no general relation between traffic categories for fatigue verifications and the ultimate strength loading classes and associated adjustment factors. Furthermore, within this fatigue load model are already included effects of the flowing traffic, such as the pavement quality and dynamic responses of the bridges.

2.1.2.4 Fatigue Load Model 4 (FLM 4)

Fatigue load model 4 (FLM 4) is a set of 5 different lorries with different geometry and axle loads, which are intended to simulate the effects of "real" heavy traffic loads on road bridges, see Table 2.2. The properties of the lorries in FLM4 are consistent with the most common heavy vehicles on European roadways and are assumed to be representative for standard lorries in Europe. EN 1991-2 provides also the properties of each lorry by the number of axles and spacing represented with an equivalent load for each axle. Different traffic types are accounted for by defining different composition of lorries as percentage of the heavy traffic volume. For the application of fatigue load model 4 on road bridges, a definition of the total annual number of lorries crossing the road bridge (N_{obs}) has also been defined by the code.

FLM 4 is mainly intended to be used in the time-history analysis in association with a cycle counting procedure to assemble stress cycle ranges when assessing the fatigue life of the structure. In other words, FLM 4 is recommended to be used with the cumulative damage assessment concept.

Some notes on the application of FLM3 and FLM4:

- Since both FLM 3 and FLM 4 are meant to be used for fatigue verification with finite fatigue life (i.e. for a specific design life), the number of cycles needs to be specified somehow (observe that this was not needed for FLM 1 & FLM 2 as they are meant to verify that the fatigue life of the bridge is infinite).

- With slow lane it is meant traffic lanes used predominantly by heavy vehicles. With heavy vehicles it is meant lorries with a gross weight higher than 100kN.

- Except for the additional vehicle that might need to be considered in FLM 3 (for moment over intermediate supports in continuous bridges), each vehicle in FLM 3 and FLM 4 should cross the bridge "alone", i.e. in the absence of any other traffic vehicles.
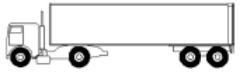
Vehicle type				Traffic type		
				Lorry percentage		
Lorry	Axle spacing [m]	Equivalent axle loads [kN]	Wheel type *	Long distance	Medium distance	Local traffic
	4,5	70 130	A B	20,0	40,0	20,0
	4,20 1,30	70 120 120	A B B	5,0	10,0	5,0
	3,20 5,20 1,30 1,30	70 150 90 90 90	A B C C C	50,0	30,0	5,0
	3,40 6,00 1,80	70 140 90 90	A B B B	15,0	15,0	5,0
	4,80 3,60 4,40 1,30	70 130 90 80 80	A B C C C	10,0	5,0	5,0

Table 2.2: Set of equivalent lorries specified for FLM4 (source EN 1991-2, Table 4.7).

* The type and size of wheels is given in Table 4.8 in EN 1991-2

2.1.2.5 Fatigue Load Model 5 (FLM 5)

Fatigue load model 5 (FLM 5) is based on recorded road traffic and a direct application of measured traffic data. This load model is intended to be used to accurately verify the fatigue strength of cable-stayed or suspended bridges, other complex and important bridges or bridges with "unusual" traffic. Fatigue verification with FLM 5 requires traffic measurement data, an extrapolation of this data in time and a rather sophisticated statistical analysis. EN 1991-2 provides additional information in this respect in its Annex B.

2.1.3 Summary

The fatigue load models recommended in EN 1991-2 for road bridges are based on reference influence surfaces for different types of bridge structures, i.e. simply supported and continuous bridges for span length between 3m and 200 m. These load models can be divided in two main groups depending on the required fatigue life. The first group is used to verify infinite fatigue life. This group contains of FLM 1 and FLM 2. The second group of the fatigue load models is aimed for performing fatigue assessing for given fatigue design life using the damage accumulation method based on Palmgren-Miner rule or the damage equivalent concept, also called simplified λ-coefficient method. In this group, FLM 3 is applied when performing the damage equivalent concept and FLM 4 when performing the cumulative damage concept. The grouping of the fatigue load models for road bridges are compiled in Figure 2.4 below.
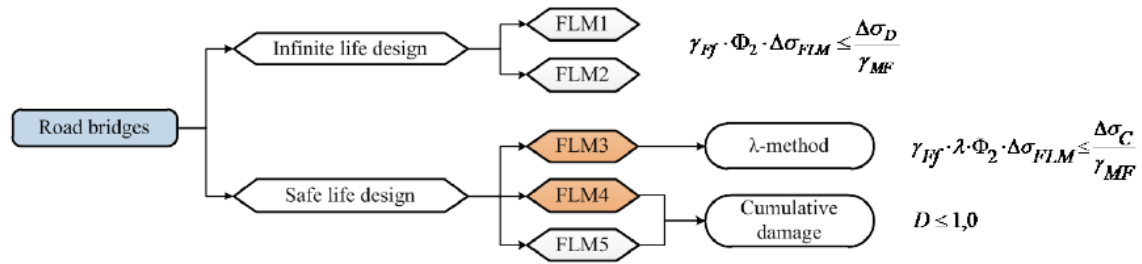
Figure 2.4: Fatigue load models for road bridges according to EN 1991-2 (Al-Emrani et al., 2014).

2.2   NOMINAL STRESSES IN STEEL AND CONCRETE COMPOSITE BRIDGES

2.2.1   Nominal stresses

The first step for determining the nominal stresses in a structural detail is to perform the elastic global cracked analysis of the composite steel and concrete bridge according to EN 1994-2, and to calculate the internal forces and moments for the basic SLS combination of the non-cyclic loads which is defined in EN 1992-1-1, 6.8.3:

$$G_{k,sup}\left(or\ G_{k,inf}\right) + (1\ or\ 0)S + 0.6T_k \qquad \text{(Eq. 2.1)}$$

where

G_k characteristic nominal value of the permanent actions effects,

S characteristic value of the effects of the concrete shrinkage,

T_k characteristic value of the effects of the thermal gradient.

The non-structural bridge equipments (safety barriers, asphalt layer etc.) have to be calculated by integrating an uncertainty on the characteristic value of the corresponding action effects. The corollary is that two values of the internal forces and moments, a minimum and a maximum one, have to be considered in every cross section of the composite bridge. Each bound of this basic envelope should be considered independently for adding the effects of the fatigue load model (usually FLM3 from EN 1991-2) in the combination of actions.

For the second step of the calculation of the nominal stresses, the bridge design specifications should settle the number and the location of the slow traffic lanes on the bridge deck. These assumptions are then used for calculating the transversal distribution coefficient for each lane. The FLM3 crossing the bridge in the slow lane induces a variation of the internal forces and moments in the bridge, which should be added to the maximum (resp. minimum) bound of the envelope for the basic SLS combination of non-cyclic actions. Two different envelopes, named case 1 and 2 in the following, are then defined:

- Case 1:

$$min\left[G_{k,sup}\left(or\ G_{k,inf}\right) + (1\ or\ 0)S + 0.6T_k\right] + FLM3 \qquad \text{(Eq. 2.2)}$$

- Case 2:

$$max\left[G_{k,sup}\left(or\ G_{k,inf}\right) + (1\ or\ 0)S + 0.6T_k\right] + FLM3 \qquad \text{(Eq. 2.3)}$$

The calculation of the nominal stresses should be performed for each bound of these two cases (it means that 4 different values of the internal forces and moments have to be considered, finally leading to 2 values for the stress range). The stress calculation should take the construction sequences into account and if one of these bending moments induces a tension in the concrete slab, the corresponding stress value should be calculated with the cracked properties of the cross section resistance.

In this work and according to the Eurocode notations, for both previous cases, the bounds of the envelope for the bending moment are noted by pairs $M_{Ed,max,f}$ and $M_{Ed,min,f}$ respectively.

2.2.2 Stress ranges

According to EN 1994-2, 6.8.4 and EN 1992-1, 6.8.3, the non-cyclic variable actions and the maximum and minimum values for permanent actions are taken as a frequent combination of actions with the cyclic load, as follows:

$$M_{Ed,max,f} = M_{c,max,Ed} + M_{FLM3,max} \qquad \text{(Eq. 2.4)}$$

$$M_{Ed,min,f} = M_{c,min,Ed} + M_{FLM3,min} \qquad \text{(Eq. 2.5)}$$

Considering $M_{Ed,min}$ corresponds to bending moments that induce compression in the slab $M_{Ed,max}$ corresponds to negative moments, which result in tension in the slab.

$M_{c,Ed}$ is the value of the bending moment applied in the composite structure, resulting from a frequent combination of actions.

Three different situations are considered for the stress range calculation as follows:

i) $M_{Ed,max,f}$ and $M_{Ed,min,f}$ cause tensile stresses in the concrete slab.

The effect of the basic SLS combination for non-cyclic loads disappears from the stress range, which should be calculated using the mechanical properties of the composite cross section with cracked concrete (structural steel + reinforcement):

$$\sigma_{max,f} - \sigma_{min,f} = \left(M_{FLM3,max} - M_{FLM3,min} \right) \cdot \frac{v_2}{Iy_2} \qquad \text{(Eq. 2.6)}$$

where:

v_2 distance from the neutral axis to the relevant fibre,

Iy_2 second moment of area of the cracked concrete composite cross section around its strong axis.

M_{FLM3} bending moment (minimum or maximum) due to fatigue load model FLM3.

ii) $M_{Ed,max,f}$ and $M_{Ed,min,f}$ cause compression stresses in the concrete slab.

The effect of the basic SLS combination for non-cyclic loads also disappears from the stress range, which should be calculated using the mechanical properties of the composite cross section with uncracked concrete (structural steel + concrete):

$$\sigma_{max,f} - \sigma_{min,f} = \left(M_{FLM3,max} - M_{FLM3,min} \right) \cdot \frac{v_1}{Iy_1} \qquad \text{(Eq. 2.7)}$$

where v_1 is the distance from the neutral axis to the relevant fibre and Iy_1 is the inertia of the uncracked concrete composite cross section, calculated with the short term modular ratio $n_0 = E_a / E_{cm}$.

iii) $M_{Ed,max,f}$ causes tensile stresses and $M_{Ed,min,f}$ causes compression stresses in the concrete slab.

In this situation, the composite part of the bending moment from the basic SLS combination for non-cyclic loads, $M_{c,Ed}$, influences the stress range according to the following equation:

$$\sigma_{max,f} - \sigma_{min,f} = \left(M_{FLM3,max} + M_{C,Ed,max} \right) \cdot \frac{v_2}{Iy_2} - \left(M_{FLM3,min} + M_{C,Ed,min} \right) \cdot \frac{v_1}{Iy_1} \qquad \text{(Eq. 2.8)}$$

$M_{c,Ed}$ is normally split up into several action effect cases for which the corresponding stresses should be evaluated with the proper elastic modular ratio n_L. In order to simplify the calculations, the short-term elastic modulus ratio n_0 may also be used for all the action effects.

2.2.3 Stress ranges in shear connectors

In steel and concrete composite structures subjected to fatigue loadings, one important issue is the fatigue verification of the connection. In this specific case, the stresses acting in the detail are:

- a direct stress range in the steel beam flange, to which the stud connectors are welded,

- a shear stress range in the weld of each of the stud connectors due to the composite action effect between the concrete slab and the steel beam.

The method for determining the direct stress range in the flange has been shown in section 2.2.2. The method for determining the shear stress and shear stress ranges is according to EN 1994-2, 6.8.5.5 and 6.8.6.2. The shear stresses at the steel-concrete interface are calculated using the properties of the cross section with uncracked concrete (in opposition to the direct stress calculations). As a consequence, the basis SLS combination of non-cyclic loads has no influence on the shear stress range, which is only induced by the FLM3 crossing and computed, as usual, as the difference between the two extreme values.

The longitudinal shear force per unit length is computed as follows:

$$v_L = \frac{S_{V1} \cdot V_{Ed}}{Iy_1} \qquad \textit{(Eq. 2.9)}$$

where:

V_{Ed} design value of the longitudinal shear force computed from a global cracked concrete analysis.

S_{V1} first moment of area of the concrete slab (taking the shear lag effect into account by means of an effective width) with respect to the centroid of the uncracked composite cross section.

Iy_1 second moment of area of the uncracked concrete composite cross section.

The expression for the shear stress range is:

$$\Delta\tau = \frac{\Delta v_{L,FLM3}}{A_{stud} \cdot n_{stud}} \qquad \textit{(Eq. 2.10)}$$

where:

$\Delta v_{L,FLM3}$ longitudinal shear force per unit length at the steel-concrete interface due to FLM3 crossing.

A_{stud} shear area of a connector.

n_{stud} number of shear studs per unit length.

2.3 FATIGUE DESIGN METHODS

Eurocode allows for the application of two principal methods for the fatigue design of bridges: The equivalent damage method, also known as the λ-coefficient method, and the more general cumulative damage method. The background and the application of these two methods are presented in this chapter.

2.3.1 The concept of equivalent stress range

As was mentioned in the previous chapter, load effects generated by traffic loads on bridges are generally very complex. The stress ranges generated by these loads are usually of variable amplitudes which are relatively difficult to treat in design situations. There is, therefore, a need to represent the fatigue load effects caused by the "actual" variable amplitude loading in term of an equivalent constant amplitude load effects.

The treatment of such complex fatigue loading situation is usually treated in the following main steps:

1. Transformation of the variable amplitude loading into a representative constant amplitude loading. This is usually done by some kind of cyclic counting method.

2. Using the new set of representative constant amplitude loading to perform the fatigue design or analysis. This is done either:

   - directly, by applying the Palmgren-Miner damage accumulation rule, or

   - by using the equivalent stress range concept.

The rules concerned with the fatigue design of bridges in Eurocode allow for the application of any of these two methods. The simplified λ-method in Eurocode is an adaption of the general equivalent stress range concept corrected by various λ-factors, while a direct application of the Palmgren-Miner rule can alternatively be used. As was discussed in the previous chapter, specific fatigue load models have been derived and implemented in Eurocode for each of these two methods.

The principles of the damage accumulation rule (Palmgren-Miner) state that a structural steel detail subjected to a given stress histogram will fail in fatigue when the damage factor D reaches a specific value. In EN 1993-1-9, the value of the damage factor D was set to unity. Thus:

$$D = \sum_i D_i = \sum_i \frac{n_i}{N_i} \qquad \text{(Eq. 2.11)}$$

$$N_i = N_C \cdot \left(\frac{\Delta\sigma_C / \gamma_{Mf}}{\gamma_{Ff} \cdot \Delta\sigma_i} \right)^m \qquad \text{(Eq. 2.12)}$$

and n_i being the total number of loading cycles in the stress histogram.

The fatigue damage caused by a number of loading blocks with constant amplitude loading can also be represented by an equivalent stress range. The definition of equivalent stress range is that constant amplitude stress range which if applied with the same total number of loading cycles of the variable stress range (Σn_i) would cause the same total damage as the variable amplitude loading block.

If one, for simplicity, assumes an S-N curve with a constant slope of 3, an expression for the equivalent stress range can be derived as follows in for any load spectrum:

$$\Delta\sigma_E = \left[\frac{\sum_{i=1}^{n} n_i \cdot \Delta\sigma_i{}^m}{\sum_{i=1}^{n} n_i} \right]^{\frac{1}{m}} \qquad \text{(Eq. 2.13)}$$

In Eurocode, fatigue verification based on the simplified λ-method adopts an equivalent stress concept, where the stresses obtained from relevant load models in EN 1991-2 are modified with various λ-factors in order to be expressed as an equivalent stress range at 2 million cycles ($\Delta\sigma_{E,2}$). This transformation from $\Delta\sigma_E$ to $\Delta\sigma_{E,2}$ can be easily obtained from:

$$\frac{\Delta\sigma_{E,2}{}^m}{2E6} = \frac{\Delta\sigma_E{}^m}{N} \qquad \text{(Eq. 2.14)}$$

giving:

$$\Delta\sigma_{E,2} = \Delta\sigma_E \cdot \left(\frac{N}{2E6}\right)^{1/m}$$

(Eq. 2.15)

Doing so, the fatigue verification is reduced to a direct comparison between the equivalent stress range at 2 million cycles and the fatigue class (or fatigue strength) of the detail:

$$\gamma_{Ff} \cdot \Delta\sigma_{E,2} \leq \frac{\Delta\sigma_C}{\gamma_{Mf}}$$

(Eq. 2.16)

2.3.2 Fatigue design with the λ-coefficient method

The λ-coefficient method is a conventional simplified fatigue assessment method, which is based on comparing an equivalent stress range with the studied detail category. The basic idea with this method is that the fatigue damage caused by the stress range spectrum is associated with an equivalent stress range $\Delta\sigma_E$ or an equivalent stress range at 2 million stress cycles, $\Delta\sigma_{E,2}$. The latter is – per definition – the fatigue strength. The method was derived originally for railway bridges, but applies also for road bridges. The purpose of this method is to convert fatigue verifications using λ−coefficients into a conventional fatigue resistance control, i.e. stress range check.

The conventional fatigue resistance control is on the basis of conditioning a lower or equal maximum stress range to the detail capacity stress range (see (Eq. 2.17)). The maximum stress range is the stress obtained from the fatigue load models which were originally derived to be used with this method (seen in previous chapter).

The fatigue verification is expressed as:

$$\gamma_{Ff} \cdot \lambda \cdot \Phi \cdot \Delta\sigma_{FLM} \leq \frac{\Delta\sigma_C}{\gamma_{Mf}}$$

(Eq. 2.17)

where:

γ_{Ff} is the partial safety factor for fatigue loading

γ_{Mf} is the partial safety factor for fatigue resistance

λ is the fatigue damage equivalent factor related to 2E6 cycles

ϕ is the dynamic factor

$\Delta\sigma_{FLM}$ is the stress range due to the fatigue load model (see 2.2.2)

$\Delta\sigma_C$ is the reference stress range value of the fatigue strength

The λ-coefficient is obtained considering four different λ-coefficients as follows:

$$\lambda = \lambda_1 \cdot \lambda_2 \cdot \lambda_3 \cdot \lambda_4 \leq \lambda_{max}$$

(Eq. 2.18)

where:

λ_1 is the span factor taking into account the length of the span and the structure type

λ_2 is the volume factor taking into account the traffic volume

λ_3 is the time factor taking into account the design life of the bridge

λ_4 is the lane factor taking into account the traffic on more than one lane

λ_{max} is the maximum damage equivalent factor taking into account the fatigue limit

The λ factors are in more detail described in the following sections.

Figure 2.5 presents an overview of the application of the λ-coefficient method with the relevant parts of Eurocode involved in the fatigue verification with this method.
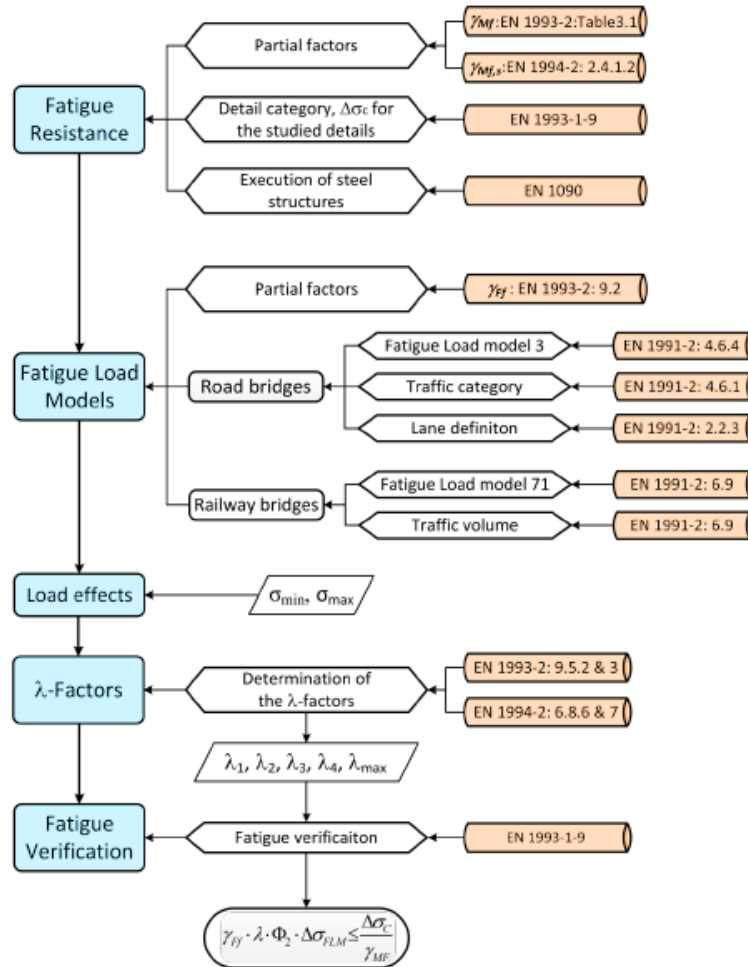
Figure 2.5: Overview of the application of the λ−coefficient method (Al-Emrani et al., 2014).

2.3.2.1 Factor λ_1

The factor λ_1 takes into account the effect of span length together with the position of the loads at which the load response has maximum value, i.e. by using influence lines/areas. EN 1993-2 defines the mid-span and support section over bridge spans to be able to examine the critical influence lines/areas when determining the λ_1 factor. The code defined locations to be used for determining the critical length of the influence lines for moments and shear for a continuous span is shown in Figure 2.6. The definition for other locations for both moments and shear is also given in Section 9.5 in EN 1993-2.
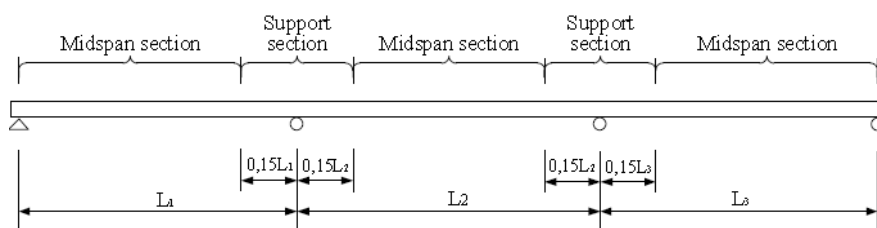
Figure 2.6: Location of mid-span or support section (source EN 1993-2).

The recommended λ_1 values to be used in bridge design for road and railway bridges are given in the Eurocode. As stated earlier, the damage equivalent factor λ_1 for both road and railway bridges is depended on the span length. It is worth remarking that EN 1991-2 states that "the National Annex may give the relevant values for the factor λ_1".

Factor λ_1 for road bridges

The λ_1 factor for road bridges is defined for the details subjected to stresses from FLM 3 and for the bridge span lengths from 10m to 80m. In case of road bridges with longer spans it is accepted that a linear extrapolation can be performed to obtain the λ_1 value. This procedure may also be applied to road bridges with shorter spans than 10m for the bending moments over the support. However, in case of moment at mid span the extrapolated λ_1 value (see Figure 2.7) may give conservative result.
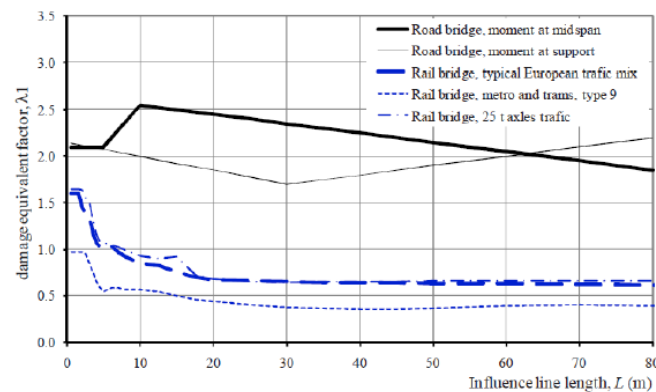
Figure 2.7: The factor λ_1 for road and railway bridges as a function of the critical influence line length (Nussbaumer, 2006).

The major factors when determining the λ_1 factor are the location of the studied detail to take into account the effect of the length of the influence line/area and the type of load effect acting on this detail: bending moment or shear force. A summary of the rules in EN 1993-2, 9.5.2 when determining the λ_1 factor for road bridges is given in Figure 2.8.

Studied region	Length of the span, [m]	λ_1 - factor	Remarks
At mid-span side	$10 \leq L \leq 80$	$2,55 - 0,7 \cdot \dfrac{L-10}{70}$	--
At intermediate support	$10 \leq L \leq 30$	$2,0 - 0,3 \cdot \dfrac{L-10}{20}$	$L = L_1 + L_2$
At intermediate support	$30 \leq L \leq 80$	$1,70 + 0,5 \cdot \dfrac{L-30}{50}$	$L = L_1 + L_2$

Figure 2.8: Damage equivalent factor λ_1 for road bridge details (Al-Emrani et al., 2014).

2.3.2.2 Factor λ_2

The factor λ_2 is a coefficient that takes into account the annual traffic flow and the traffic composition on the actual bridge. In bridge design, the number of heavy vehicles per year and per slow lane for road bridges (N_{obs}) and the amount of freight transported per track and per year for railway bridges should be specified by a competent authority.

Factor λ_2 for road bridges

According to EN 1993-2, the factor λ_2 considering the actual bridge traffic flow and composition should be calculated as follows:

$$\lambda_2 = \frac{Q_{ml}}{Q_0} \cdot \left(\frac{N_{obs}}{N_0}\right)^{1/m}$$

(Eq. 2.19)

where:

Q_{ml} is the average gross weight (kN) of the lorries in the slow lane

Q_0 is the equivalent weight (kN) of the reference traffic

N_0 is the annual number of lorries for the reference traffic

N_{obs} is the annual number of lorries in the slow lane

m is the slope of S-N curve; the largest m value in case of bilinear curve.

The average gross weight of the lorries in the slow lane can be calculated by the following formula:

$$Q_{ml} = \left(\frac{\sum n_i \cdot Q_i{}^m}{\sum n_i}\right)^{1/m}$$

(Eq. 2.20)

where:

n_i is the number of lorries of gross weight Q_i in the slow lane

Q_i is the gross weight of the lorry "i" in the slow lane

m is the slope of S-N curve; the largest m value in case of bilinear curve.

As stated earlier, EN 1993-2 is using the Auxerre traffic as the reference traffic data and recommends therefore using $N_0 = 0.5E6$ and $Q_0 = 480kN$ when calculating the λ_2 factor (for this specific case the factor λ_2 is equal to 1.0). Based on these two reference values, the factor λ_2 for any Q_{ml} and N_{Obs} can be obtained from Table 9.1 of EN 1993-2.

2.3.2.3 Factor λ_3

The λ_3 factor considers the design life of the bridge and according to EN 1993-2, this factor used for both road and railway bridges should be calculated as following:

$$\lambda_3 = \left(\frac{t_{Ld}}{100}\right)^{1/m}$$

(Eq. 2.21)

Where t_{Ld} is the design working life of the structure in years and m is the slope of the S-N curve.

The λ–coefficient method in Eurocode and the corresponding fatigue load models were derived based on a reference design life of 100 years. The λ_3 factors give the possibility of modifying the design life in years as given in EN 1993-2, 9.5.2(3) and 9.5.3(6).

2.3.2.4 Factor λ_4

Factor λ_4 for road bridges

The factor λ_4 considers the vehicles interactions and accounts the multilane effect. In other words, the λ_4 factor takes into account the interactions between lorries simultaneously loading on several lanes defined in the design (multilane effect) and should be according to EN 1993-2 calculated using the following formula:

$$\lambda_4 = \sqrt[m]{\sum_{j=1}^{k} \frac{N_j}{N_1} \cdot \left(\frac{\eta_j \cdot Q_{mj}}{\eta_1 \cdot Q_1}\right)^m}$$

(Eq. 2.22)

where:

k   is the number of lanes with heavy traffic

N_j is the number of lorries per year in lane *j*

Q_{mj} is the average gross weight of the lorries in lane *j*

η_j is the influence line for the internal force that produces the stress range (see Figure 2.9)

m   is the slope of S-N curve; the largest *m* value in case of bilinear curve.

This expression shows that the factor λ_4 is equal to 1.0 when considering a single bridge lane.
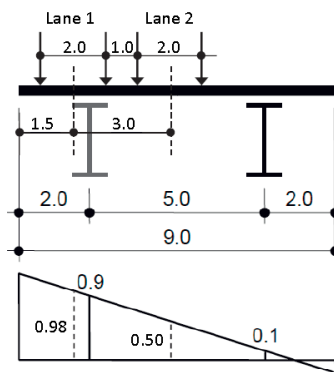
Figure 2.9: Example of transverse distribution of two-girder bridge cross-section in function of lateral load positions (Al-Emrani et al., 2014).

2.3.2.5 Factor λ_max

The final λ factor is obtained by multiplying the above mentioned individual λ–factors. An upper limit value has also to be considered defined. This is made through the factor λ_max which mainly takes into account the fatigue limit of the detail under consideration. The limitation of the damage equivalent factor value for railway bridges is based on the load model which gives an upper bound value while this factor for road bridges is on the same basis as the simulations for the λ_1 factor.

Factor λ_max for road bridges

The λ_max factor for road bridges for the span lengths from 10m to 80m is defined only for the sections subjected to the fatigue stresses caused by bending moment. This is clear as the S-N curves for shear effects do not have a defined CAFL. However, when using the λ-equivalence concept FLM 3 does not generate an upper limit value to establish a suitable λ_max value. The limiting λ value is therefore established by simulating the road traffic. Similar to the λ_1 factor given in EN 1993-2, the maximum λ values are depended on the length of the bridge span and also the location of the detail under consideration. EN 1993-2 presents therefore two graphs to determine the λ_max factor which are shown in Figure 2.10.

2.3.2.6 Factor λ_v

For shear studs, $\lambda_{v,2}$, $\lambda_{v,3}$, $\lambda_{v,4}$ factors should be determined using the relevant equations, but using a slope coefficient m = 8, or exponent 1/8, in place of those given to allow for the relevant fatigue strength curve for headed studs in shear. Regarding λ_max, the conservative values given in Figure 2.10 may be used.
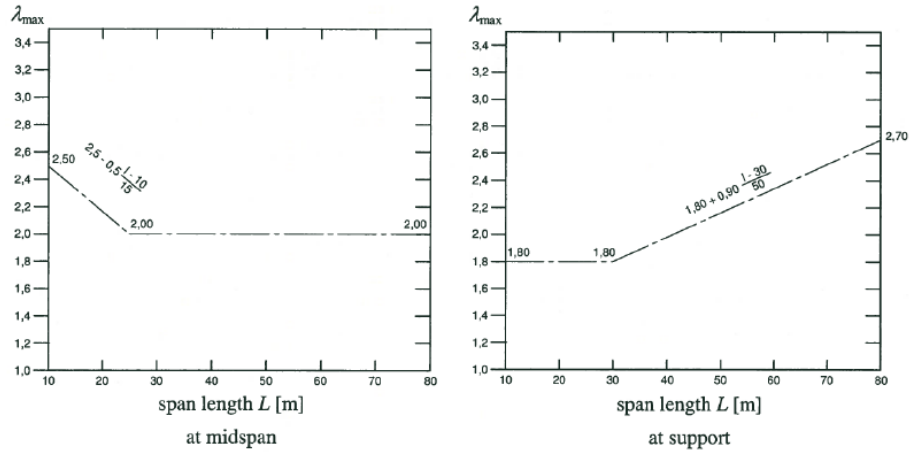
Figure 2.10: λ_{max} factor for road bridge sections subjected to bending stresses (Al-Emrani et al., 2014).

2.3.2.7 Fatigue assessment on shear connectors

The shear connection fatigue assessment is based on nominal stress ranges according to EN 1994-2. In steel-concrete composite girders two different situations should be considered:

1) Where the girder top flange is always in compression (Case 2 of section 2.2.2), the fatigue assessment should be made by checking the following criterion:

$$\gamma_{Ff} \cdot \Delta\tau_{E,2} = \frac{\Delta\tau_C}{\gamma_{Mf,s}} \qquad (Eq.\ 2.23)$$

2) Where the maximum stress in the top flange is tensile, the following interaction should be also verified (Cases 1 and 3 of section 2.2.2):

$$\frac{\gamma_{Ff} \cdot \Delta\sigma_{E,2}}{\Delta\sigma_C/\gamma_{Mf}} + \frac{\gamma_{Ff} \cdot \Delta\tau_{E,2}}{\Delta\tau_C/\gamma_{Mf,s}} \leq 1.3 \qquad (Eq.\ 2.24)$$

Also fulfilling:

$$\gamma_{Ff} \cdot \Delta\sigma_{E,2} \leq \frac{\Delta\sigma_C}{\gamma_{Mf}} \quad \text{and} \quad \gamma_{Ff} \cdot \Delta\tau_{E,2} \leq \frac{\Delta\tau_C}{\gamma_{Mf,s}} \qquad (Eq.\ 2.25)$$

where:

$\Delta\sigma_{E,2}$ is the normal stress range in the steel flange and γ_{Ff} and γ_{Mf} are the partial factors for fatigue loading and strength respectively;

$\Delta\sigma_C$ is the detail's category;

$\gamma_{Mf,s}$ is the partial factor for fatigue strength for shear studs, taken with the recommended value from EN 1994-2, 2.4.1.2 (6): $\gamma_{Mf,s}$ = 1.0;

$\Delta\tau_{E,2}$ is the range of shear stress due to fatigue loading related to the cross-section area of the shank of the stud, determined with the uncracked properties of cross-section, even in sections considered as cracked for global analyses;

$$\Delta\tau_{E,2} = \lambda_v \cdot \Delta\tau \qquad (Eq.\ 2.26)$$

The maximum shear stress range $\Delta\tau$ is calculated according to the procedure from section 2.2.3.

The expression on (Eq. 2.26) represents the range of shear stress due to fatigue loading related to the cross-section area of the shank of the stud, determined with the uncracked properties of cross-section, even in sections considered as cracked for global analyses.

2.3.2.8 Main shortcomings in the use of the damage equivalent factor method

The damage equivalence factors based on the Eurocodes presents some shortcomings, which could be summarized as follows:

- ✓ the definition of critical influence line length is non-exhaustive, and defined case by case;

- ✓ the effect of simultaneity in which several trucks stand on a bridge simultaneously either in the same lane or in several lanes is neglected;

- ✓ λ and λ_{max} obtained for different bridge influence lines are widespread;

- ✓ the safety margin for some bridge cases are over-conservative and for some cases are non-conservative.

2.3.3 Fatigue design with the Damage Accumulation Method

Load effects generated by traffic loads on bridges are generally very complex. Not only are the stress ranges generated by these loads of variable amplitudes, but also other parameters that might affect the fatigue performance of bridge details such as the mean stress values and the sequence of loading cycles are rather stochastic.

In order to treat such complex loading situations there is a need to represent the fatigue load effects caused by the "actual" variable amplitude loading in term of equivalent constant amplitude loading. In other words, a complex loading situation such as the one shown in Figure 2.11 should be represented as one or more equivalent constant amplitude loads, so that the latter will cause equivalent fatigue damage as the real loading history. Two steps are needed:

1. Transformation of the variable amplitude loading into a representative constant amplitude loading, this is usually done by some kind of cyclic counting method.

2. Using the new set of representative constant amplitude loading to perform the fatigue design or analysis, this is done either:

   - directly, by applying the Palmgren-Miner damage accumulation rule, or

   - by using the equivalent stress range concept.

The rules concerned with the fatigue design of bridges in Eurocode allow for the application of any of these two methods. The simplified λ-method in Eurocode is an adaption of the general equivalent stress range concept corrected by various λ-factors, while a direct application of the Palmgren-Miner rule can alternatively be used for both railway and road bridges.
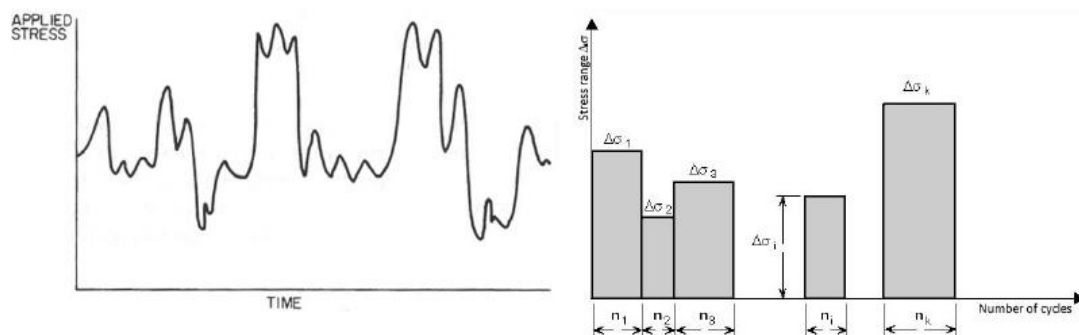
Figure 2.11: An example of variable amplitude loading and stress histogram resulting from the application of cyclic counting method (Al-Emrani et al., 2014).

The most common cycle counting methods are the "rainflow" and the "reservoir" stress counting methods. In general, these two methods do not lead to exactly the same result. However, in terms of fatigue damage both counting procedures give very close results, especially for "long" stress histories.

2.3.4   Palmgren-Miner damage accumulation

As known, an S-N curve represents the relation between the stress range $\Delta\sigma$ (or $\Delta\tau$) in a specific detail and the total number of cycles to failure, N. In other words, a specific detail with a certain fatigue strength (represented by an S-N curve) will fail after N cycles of a stress range $\Delta\sigma$. At failure, the fatigue life is consumed and the total fatigue damage in the detail would then be 100%, or $D = 1.0$. If the same detail is now loaded with a number of stress cycles $n < N$ at the same stress range, the fatigue damage accumulated in the detail would then be:

$$D = \frac{n}{N} = \begin{cases} 1.0 \ \ when \ n = N \\ < 1.0 \ \ when \ n \ < N \end{cases}$$

(Eq. 2.27)

With this in mind, if the detail is subjected to a number i of loading blocks each with a constant amplitude stresses $\Delta\sigma_i$ which is repeated n_i number of times, then the total fatigue damage accumulated in the detail would be the sum of the damage caused by the individual loading blocks:

$$D = \sum_i D_i = \sum_i \frac{n_i}{N_i}$$

(Eq. 2.28)

2.3.5   The application of the damage accumulation method

Annex A in EN 1993-1-9 gives information on the application of the damage accumulation method in the fatigue design of steel structures. What concerns bridges the use of damage accumulation method is suggested in two cases:

1. When actual traffic data is available. This is covered in Annex B of EN 1991-2.

2. Along with the traffic load models derived for this purpose. These are LM4 for road bridges (EN 1991-2, 4.6.5) and train types 1 to 12 in Annex D of EN 1991-2 of Eurocode.

For both road and railway bridges, the traffic load models to be used with the damage accumulation method are intended to reflect the real "heavy" traffic on European road and railway networks. The variation in traffic intensity and vehicle (or train) types on individual bridges is covered by defining different "traffic types" or "traffic mixes" for road and railway traffic respectively. These are also a subject for adaption and modification by the countries through their national annexes.

In the following, the traffic load models proposed in EN 1991-2 for fatigue verification with the cumulative damage concept will be shortly introduced. A summary of the main steps involved in the application of this method is then made.

2.3.5.1 Application to road bridges

The traffic load model to be used with fatigue verification of road bridges according to the damage accumulation method is LM4. This model is composed of 5 standard lorries which are assumed to simulate the effects of real road traffic on the bridge. The definition of each lorry is given by the number of axles, the load on each axle as well as the axle spacing which are reproduced in Table 2.2. The number of heavy vehicles, N_{obs} per year and per slow lane (observed or estimated) applies also for fatigue verification with the damage accumulation method. Indicative figures for N_{obs} and the recommended values for different traffic categories are given in EN 1991-2 4.6.1(3).

The fatigue verification procedure should be performed – for those details that are determinant for the fatigue performance of the bridge – according to the following steps:

1. Establish the bridge specific data for fatigue verification. Besides the design life of the bridge this includes:

   a. the "traffic category" with the associated number of heavy lorries in the slow lane, Nobs [EN 1991-2, 4.6.1(3)],

   b. the "traffic type" with the associated percentage of lorries, Table 4.7 in EN 1991-2.

2. For the detail in hand, obtain the influence line for relevant load effects (shear or bending stresses).

3. By passing the load model over the influence line, establish the time history response (i.e. stress vs. time, or time step)

4. Construct the stress histogram by mean of a cycle-counting method.

5. Select an appropriate fatigue category and establish the corresponding S-N curve ($\Delta\sigma_C$ at 2E6 cycles, $\Delta\sigma_D$ at 5E6 cycles and $\Delta\sigma_L$ at 100E6 cycles).

6. Use the stress histogram either to:

   a. Calculate a total damage:

$$
D_i = \begin{cases} \dfrac{n_i}{5E6} \cdot \left(\dfrac{\gamma_{Ff} \cdot \gamma_{Mf} \cdot \Delta\sigma_i}{\Delta\sigma_D}\right)^3 & if \ \gamma_{Ff} \cdot \Delta\sigma_i \geq \dfrac{\Delta\sigma_D}{\gamma_{Mf}} \\[4mm] \dfrac{n_i}{5E6} \cdot \left(\dfrac{\gamma_{Ff} \cdot \gamma_{Mf} \cdot \Delta\sigma_i}{\Delta\sigma_D}\right)^5 & if \ \dfrac{\Delta\sigma_L}{\gamma_{Mf}} \leq \gamma_{Ff} \cdot \Delta\sigma_i < \dfrac{\Delta\sigma_D}{\gamma_{Mf}} \end{cases}
$$

(Eq. 2.29)

   and verify that:

$$
D = \sum_i D_i \leq 1.0
$$

(Eq. 2.30)

   b. Calculate the equivalent stress at 2E6 cycles:

$$
\Delta\sigma_E = \left(\frac{\sum n_i \cdot (\gamma_{Ff} \cdot \Delta\sigma_i)^3 + \sum n_j \cdot (\gamma_{Ff} \cdot \Delta\sigma_j)^3 \cdot \left(\frac{\gamma_{Ff} \cdot \gamma_{Mf} \cdot \Delta\sigma_j}{\Delta\sigma_D}\right)^2}{\sum n_i + \sum n_j}\right)^{1/3}
$$

(Eq. 2.31)

   from (Eq. 2.15):

$$
\Delta\sigma_{E,2} = \Delta\sigma_E \cdot \left(\frac{N}{2E6}\right)^{1/3}
$$

(Eq. 2.32)

   and verify that:

$$
\frac{\Delta\sigma_{E,2} \cdot \gamma_{Ff} \cdot \gamma_{Mf}}{\Delta\sigma_C} \leq 1.0
$$

(Eq. 2.33)

The procedure is illustrated in Figure 2.12.
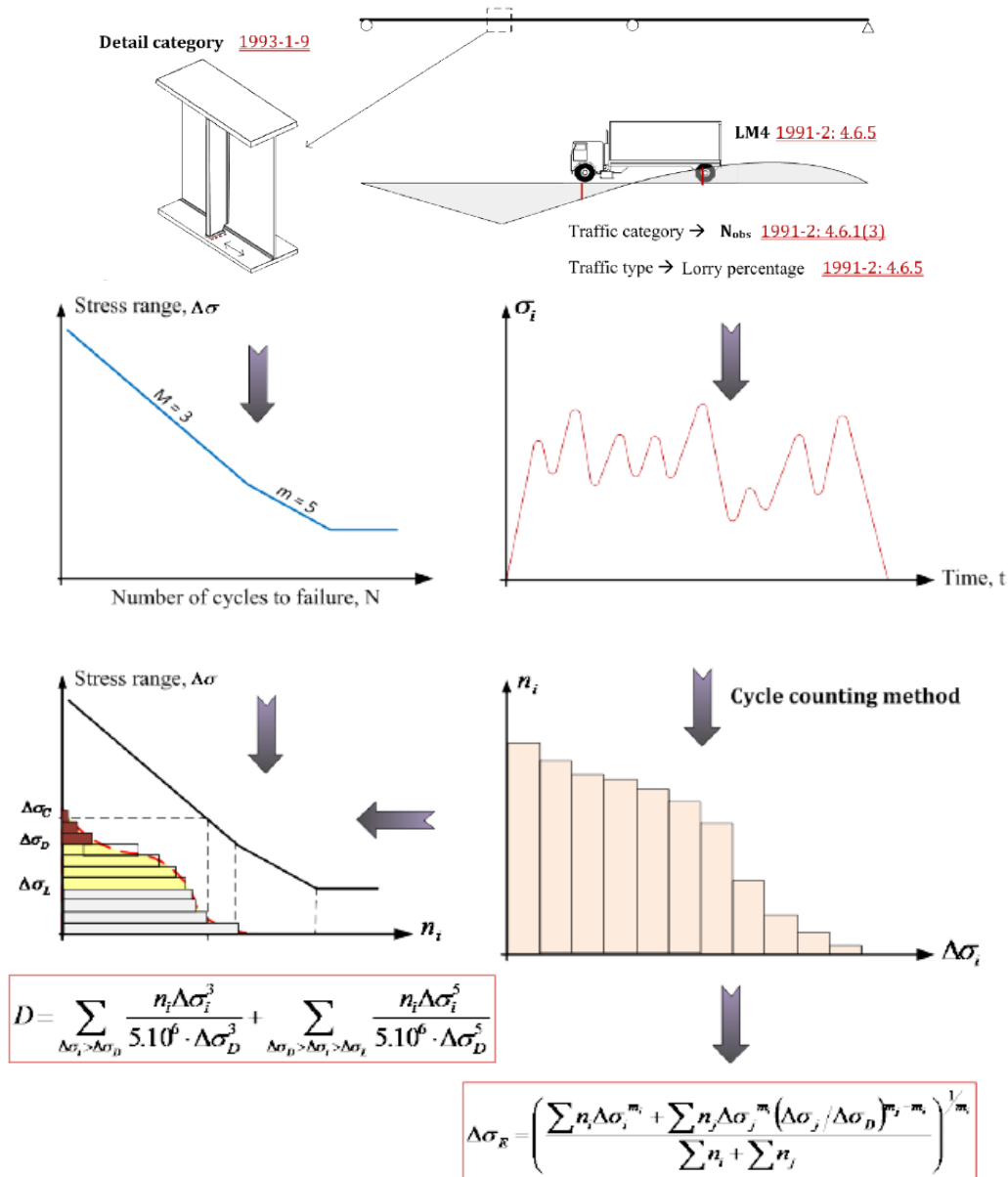
Figure 2.12: The application steps of cumulative damage method (Al-Emrani et al., 2014).

2.3.6 Fatigue strength

2.3.6.1 Set of fatigue strength curves (EN 1993-1-9)

The statistical analysis of the test results on a specific structural detail allows for the definition of one fatigue strength curve. Numerous fatigue tests programs on different details in steel have shown that the fatigue strength curves are more or less parallel. Fatigue strength is thus only a function of the constant *C*, see (Eq. 2.34), which value is specific to each structural detail.

$$logN = logC - m \cdot \log(\Delta\sigma)$$ *(Eq. 2.34)*

Since there are many different details, so is the number of the different strength curves, and this is unusable for design in practice. The solution is the classification of the different structural details in categories with a corresponding set of fatigue strength curves.

Classified structural details may be described in different EN 1993 associated Eurocodes (EN 1993-1-9, EN 1993-2, EN 1993-3-2, etc.) but they all refer to the same set of fatigue strength curves, as given in the

generic part 1-9. Each detail category corresponds to one S-N curve where the fatigue strength $\Delta\sigma$ is a function of the number of cycles, N, both represented in logarithmic scale. The set is composed of 14 S-N curves, equally spaced in log scale. The set has been kept the same over the last decades; it comes from the ECCS original work of drafting the first European recommendations (ECCS, 1985). The set is reproduced in Figure 2.13.
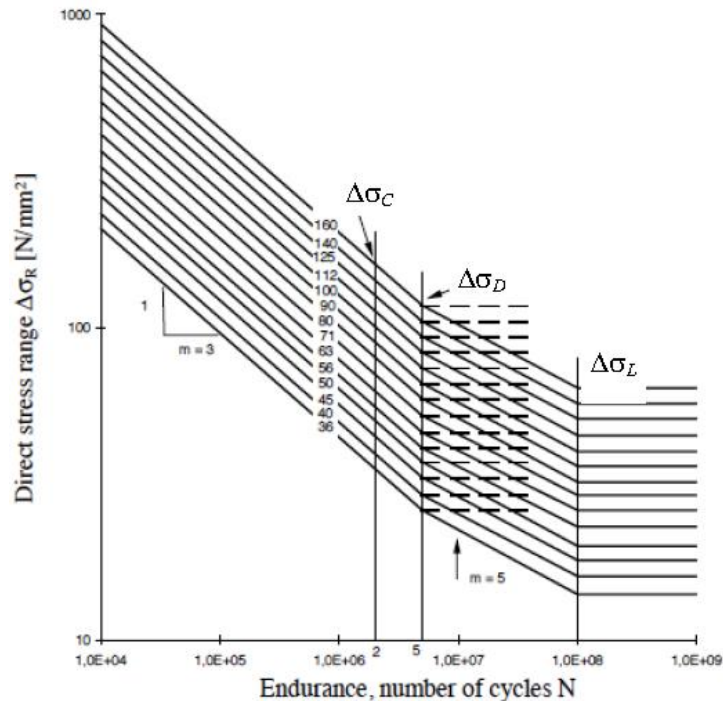
Figure 2.13: Set of fatigue strength (S-N) curves for normal stress ranges (Nussbaumer et al., 2011).

The spacing between curves corresponds to a difference in stress range of about 12% (values corresponding to the detail categories were rounded off), i.e. 1/20 of an order of magnitude on the stress range scale. All curves composing the set are parallel and each curve is characterized, by convention, by the detail category, $\Delta\sigma_C$ (value of the fatigue strength at 2 million cycles, expressed in N/mm2). It is also characterized by the constant amplitude fatigue limit (CAFL), $\Delta\sigma_D$, at 5 million cycles, which represents about 74% of $\Delta\sigma_C$. The slope coefficient m is equal to 3 for lives shorter than 5 million cycles. For constant amplitude stress ranges equal to or below the CAFL, the fatigue life is infinite.

The CAFL is fixed at 5 million cycles for all detail categories. This is not exactly the case in real fatigue behaviour but has advantages for damage sum computations. Other codes use different values.

Under variable amplitude loadings, the CAFL does not exist, but still has an influence. Thus, a change in the slope coefficient is made, the value m = 5 being used between 5 million and 100 million of cycles. This last value corresponds to the cut-off limit, $\Delta\sigma_L$, which corresponds to about 40% of $\Delta\sigma_C$. By definition, all cycles with stress ranges equal to or below $\Delta\sigma_L$ can be neglected when performing a damage sum. The reason for this is that the contribution of these stress ranges to the total damage is considered as being negligible. It should be emphasised that the double slope S-N curve (and the cut-off limit), compared to the unique slope curve, represents better the damaging process due to cycles below the CAFL.

If a structural detail configuration from a type of structure can be found in the tables of the relevant EN 1993 associated Eurocodes, and the description and requirements for this detail correspond, then the fatigue strength can be derived from the standard fatigue resistance S-N curves given in EN 1993, generic part 1-9.

Note that these fatigue curves are based on representative experimental investigations. They include the effects of:

- ✓ stress concentrations due to the detail geometry (detail severity),
- ✓ local stress concentrations due to the size and shape of weld imperfections within certain limits,
- ✓ stress direction,
- ✓ expected crack location,
- ✓ residual stresses,
- ✓ metallurgical conditions,
- ✓ welding and post-welding procedures.

Additional stress concentrations due to geometry and not included in the classified structural details, e.g. misalignment, large cut-out in the vicinity of the detail, have to be accounted for by the use of a stress concentration factor.

For shear stress ranges, the statistical analysis of the test results on specific structural details with fatigue cracks developing under shear have shown differences with those under direct or normal stress ranges. Firstly, the fatigue strength curves slope coefficient is higher than under direct or normal stress ranges, leading to a slope coefficient m = 5. Secondly, there is no well-defined constant amplitude fatigue limit and thus the curve has no CAFL. Thirdly, as for the other S-N curves, there is a cut-off limit at 100 million cycles. There are only a few details in shear only (EN 1993-1-9, Table 8.1, details 6, 7 and 15, Table 8.5, details 8, 9) so only two fatigue strength curves are needed to classify them as shown in Figure 2.14. However, there is a third, very special, S-N curve for studs in shear (detail 10, Table 8.5), with a slope coefficient m = 8, no CAFL and no cut-off limit, also shown in Figure 2.14. A cut-off limit would not change significantly the fatigue verification since the slope coefficient is very high, which explains why it is not specified.

Each curve is characterized by convention, again, by the detail category, $\Delta\tau_C$ (value, expressed in N/mm^2, of the fatigue strength at 2 million cycles). The curve with a unique slope coefficient, m = 5, is used up to 100 million cycles. This number of cycles corresponds to the cut-off limit, $\Delta\tau_L$. This means, again, by definition, that all cycles having stress ranges below $\Delta\tau_L$ can be neglected when performing a damage sum for the same reason as explained before.
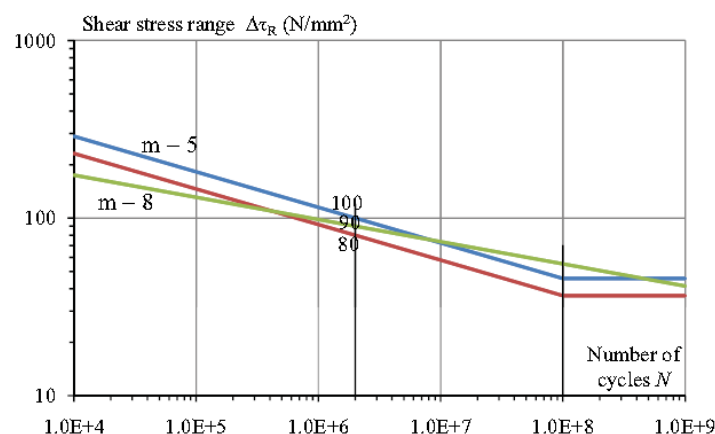
Figure 2.14: Set of fatigue strength curves for shear stress ranges (Nussbaumer et al., 2011).

2.3.7 Partial factors

The partial factors γ_{Ff} and γ_{Mf} are taken to cover the dispersions on the side of the actions effects and the determination of the fatigue strength. When these concern structures subject to fatigue loading in particular, the following uncertainties have to be considered:

- the definition of the operating load, and/or the estimation of the stress ranges during the service life, resulting from it;

- the determination of the cycle peaks;

- the presence of flaws in the material and in the connections, i.e. the quality of the used materials and the welded joints;

- the evaluation of the notch effect and thus the process of crack growth in a design detail;

- the applicability of the Miner's rule or of linear damage accumulation method (i.e. to get an equivalent constant amplitude stress range).

The partial factors are directly related to the calculation assumptions and the risk assessment of a failure. The vulnerability of people and environment must be reduced to an acceptable residual risk.

The failure due to fatigue is a long-continuous process in which a crack forms in a member, and grows until the remaining cross section can no longer resist the applied static load. The assessment of acceptable residual risk consists of determining whether such a crack can be detected at an early stage, whether the member or the overall structure permits a certain crack, and whether any effective measures to stop the crack growth can be taken.

The EN 1991 assumptions on the action effects result in a recommended value for the partial factor on the action effect side, γ_{Ff}, of 1.0. This factor is linked to the lifetime and loading assumptions of the structure or type of structure considered.

The partial factor for fatigue strength from EN 1991 takes into account:

- the chosen fatigue verification method (i.e. the strategy chosen) and

- the consequence of failure.

In fact, the fatigue strength factor does not assume a fixed single value, but can be adapted to the characteristics of the structure (e.g. redundancy, regular inspections) as well as the reliability in service and the damage consequences in case of failure. If the structure or details, for instance, exhibit fatigue cracking that can be detected and monitored, with predictable crack propagation and limited damage consequences, the partial factor γ_{Mf} is set to 1.0. If these conditions are not fulfilled, for example because the detail cannot be inspected, the partial factor γ_{Mf} value must be increased. EN 1993-1-9 suggests appropriate values for γ_{Mf}, see Table 2.3.

Verification method	Consequence of failure	
	CC1 and CC2*	CC3*
	Low consequence	High consequence
Damage tolerance	1.00	1.15
Safe life	1.15	1.35
* see EN 1990, annex B, Table B1		

Table 2.3: Recommended values for the partial factor γ_{Mf} (source EN 1993-1-9, Table 3.1).

2.4 TRAFFIC ACTIONS

Traffic represents external actions to consider for fatigue limit state analysis of bridges. However, the actual value of traffic load on bridges is very difficult to be modelled accurately because of its high

randomness nature. None of the traffic load models is thorough. Each model covers a range of span length and/or limit state of design depending on its assumptions. In fact, a few models are valid for both short spans and long spans bridges as far as it is valid for both ultimate limit state and fatigue limit state. Crespo-Minguillon and Casas [10] divided the methods to address the issue into three groups: 1) methods based on theoretical models, such as the theory of stochastic processes and the convolution or integration approach; 2) methods based on the simulation of static configurations of traffic; and 3) methods based on the simulation of real traffic flow.

For the methods based on the simulation of static configurations of traffic, Nowak [11] can be found. In these models, two traffic condition of congested and free-flow are analysed separately. The statistical parameters in these models (gross vehicle weight –hereinafter *GVW*–, vehicles geometry, distance between vehicles) are based on the recorded traffic data. Then the model extrapolates the results to obtain the maximum effects for a given service life [19].

The third group, which are the methods simulating real traffic flows on bridges, contains the most comprehensive approach for traffic load evaluations. The methods developed by Miki et al. [12] are within this group. These methods are more accurate than the other ones and can be applied to the analysis of the both serviceability and ultimate limit states without limitation of span length; however, they require a complicated simulation process that needs time-consuming computer calculation.

Accuracy of traffic flow simulations is highly dependent on real traffic statistical data such as GVW, vehicle geometry, axle's load, contribution of each vehicle type in total traffic, average daily traffic, percentage of trucks in traffic flow etc. If the statistical variation of all these parameters are determined properly, traffic actions can then be modelled accurately. Nowak [11] mentions that uncertainties involved are due to limitations and biases in the surveys. Also, the available data base is small in compare with the actual number of heavy vehicles in a 75 year lifetime. Finally, a considerable degree of uncertainty is due to unpredictability of the future traffic trends.

One important improvement in heavy vehicles loading knowledge has been achieved by application of Weigh-in-motion (hereinafter *WIM*). WIM devices are designed to capture and record truck axle weights and GVW as they drive over a sensor. Unlike older static weigh stations, current WIM systems do not require the trucks to stop, making them much more efficient and representative. The first WIM measurement and data collected in mid 1980's were not reliable, with estimated error 30-40%. But nowadays by advances in the technology of these devices, the estimated error is much lower.

Recently most traffic simulations are based on WIM measurements. Laman and Nowak [13] used WIM to determine damage due to fatigue loading on steel girders of road bridges, assuming one-by-one passage of trucks over bridge though. O'Connor and O'Brien [14] also assess the sensitivity of extreme loads to two methods of prediction: generalized codified loading models and the models based on WIM. Miao and Chan [15] studied how to analyse the obtained WIM data statistically and use results to calculate extreme daily bending moments.

In this work, traffic actions are modelled by simulating traffic flow with the program, which is developed and applied for this purpose (see section 3.7).

2.5   DYNAMIC ANALYSIS OF THE BRIDGE

The interaction between a bridge and the vehicles moving over the bridge is a coupled, nonlinear dynamic problem. Conventionally, most research has been focused on the dynamic or impact response of the bridge, but not of the moving vehicles. For the cases where only the bridge response is desired, the moving vehicles have frequently been approximated to the extreme as a number of moving loads. However, whenever the responses of both the bridge and moving vehicles are desired, models that can adequately account for the dynamic properties of the moving vehicles should be adopted.

The dynamic interaction between a bridge and the moving vehicles represents a special discipline within the broad area of structural dynamics. From the theoretical point of view, the two subsystems, i.e., the bridge and moving vehicles, can be simulated as two elastic structures, of which each is characterized by some frequencies of vibration. The two subsystems interact with each other through the contact forces, i.e., the forces induced at the contact points between the wheels and pavement surface (of the highway bridge). A problem such as this is nonlinear and time-dependent due to the fact that the contact forces may move from time to time, while their magnitudes do not remain constant, as a result of the relative movement of the two subsystems. The way by which the two subsystems interact with each other is determined primarily by the inherent frequencies of the two subsystems and the driving frequency of the moving vehicles.

In many cases, especially when the vehicle to bridge mass ratio is small, the elastic and inertial effects of the vehicles may be ignored and much simpler models can be adopted for the vehicles. One typical example is the simulation of a moving vehicle over a bridge as a single moving load, which has been conventionally referred to as the moving load model (Figure 2.15). Since the interaction between the two subsystems has been ignored, the moving load model is good only for computing the response of the larger subsystem, i.e., the bridge, but not of the smaller subsystem, i.e., the vehicle.
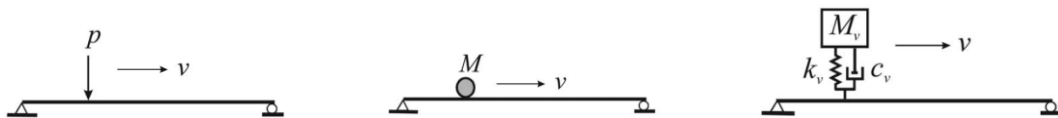
Figure 2.15: Moving load, Moving mass and Sprung mass models, respectively (Yang et al., 2004).

The moving load model is the simplest model that can be conceived, which has been frequently adopted by researchers in studying the vehicle-induced bridge vibrations. With this model, the essential dynamic characteristics of the bridge caused by the moving action of the vehicle can be captured with a sufficient degree of accuracy. However, the effect of interaction between the bridge and the moving vehicle was just ignored. For this reason, the moving load model is good only for the case where the mass of the vehicle is small relative to that of the bridge, and only when the vehicle response is not of interest.

More complex vehicle models have been studied (Yang et al. [18]), such as the moving mass model and the sprung mass model, also shown in Figure 2.15, where the DOF are increased and, with the aid of advanced computation technology, the problem could be solved more accurately.

Due to the complexity associated to the dynamic analysis of the loads, this project will not considered it in its scope of work; however, following the simplification from the Eurocodes, an impact coefficient φ will be included in the verification under fatigue, which accounts for the dynamic nature of the loads and the interaction between the vehicles and the bridge, among others.

2.6   LIFE CYCLE ASSESSMENT

Life cycle analysis (LCA) is a systematic procedure enabling for the identification of critical processes over the lifespan of a system. In relation to bridges, the initial stage of material production and the maintenance of the structure over its service life are usually considered to be critical processes, when environmental and user costs are considered together with the usual costs.

A methodology for integrated life cycle analysis of bridges was developed within the framework of the European research project SBRI with the aim to promote steel-composite bridges regarding sustainability.

According to Gervasio et al. [17], the reduction of the structural steel quantity by the use of high strength steel (S460) shows improvements in the results of the LCA compared to steels grade S355. Construction costs in parallel to the LCA also appear to be smaller when using HSS (reduction of around

4.5%), though the unit cost (€/kg) is higher. This research shows that solutions that might seem more expensive at the construction stage, can be more attractive at the end, when considering the life cycle of the structure. In this sense, the total life cycle cost (LCC) from the model with HSS shown a reduction of ~3% with respect to the same value using S355.

Therefore, it is concluded that the use of HSS has advantages in both environmental and economic criteria. Nevertheless, the behaviour of higher steel grades under fatigue does not present any advantage, since the steel grade is not considered within the main parameters governing the verification of this limit state.

3   PROGRAM

3.1   FLOWCHART

The program is structured as shown in the following flow-chart:
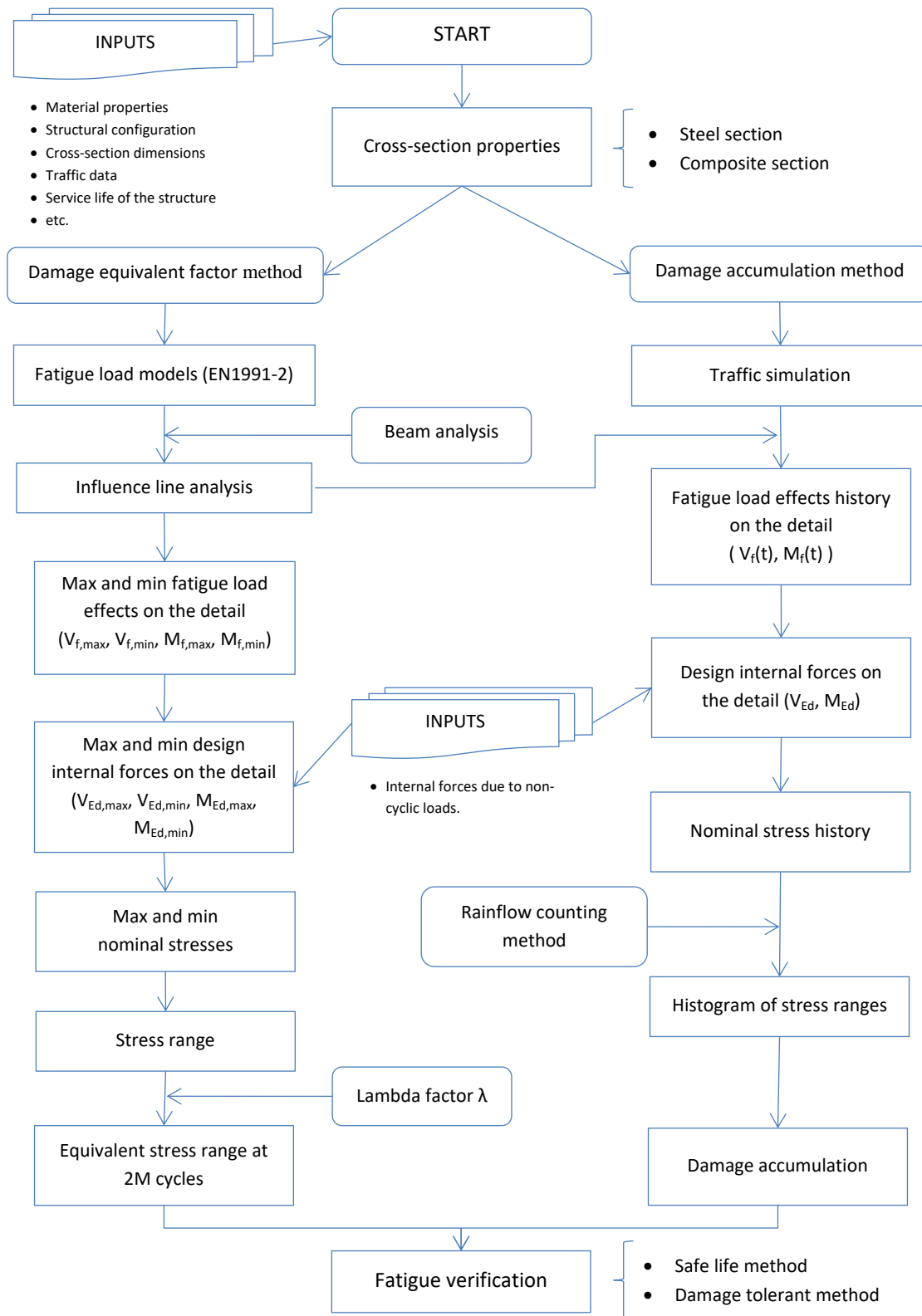
Figure 3.1: Program's flowchart.

3.2   INTRODUCTION

The program was developed in Python 2.7.12 and is structured in 4 interconnected files, each of them with several modules, which are listed below:

1. **Cross-section and detail verification to fatigue**
   Calculates the cross-section properties and checks the verification of the detail under fatigue using both damage equivalent and damage accumulation methods.

2. **Beam Analysis**
   Returns the load effects on the main girders (shear and bending moment).

3. **Influence line and FLM3**
   Calculates the shear and moment influence lines for a particular cross-section and applies the FLM3 in order to get the absolute maximum load effects for that section.

4. **Traffic simulation**
   Generates a random stream of heavy load traffic and evaluates its action effects on the structure.

The work will be presented following the usual steps from the design of a bridge, taking note of the particular points associated to the program's operation and features.

3.3   INPUTS

In order to initialize the program, it has to be fed with several inputs, which are stored in a database file and summarized in Table 3.1.

Table #	Table name	Parameters described in the table
1	Detail	• Position • Category [MPa]
2	Bridge data	• Number of girders • Distance between girders • Width of the deck • Number of lanes • Width of each lane • Number of traffic directions (1 or 2) • Number of slow lanes • Number of sidewalks • Width of sidewalks • Width of interior barriers • Thickness of concrete slab
3	Cross-sections	• Web height • Web thickness • Upper flange width • Upper flange thickness • Lower flange width • Lower flange thickness • Distribution of different cross-sections along the structure

4	Shear connectors	- Diameter of shank - Number of studs per cross-section - Long. distance between connectors - Transv. distance between connectors - Long distribution of each type of connector
5	Long. rebars	- Diameter - Transv. distance between rebars - Number of rows of rebars in the cross-section - Concrete covering
6	Concrete (material)	- Grade - Modulus of elasticity E_{cm} [MPa] - Characteristic compressive strength f_{ck} [MPa] f_{cm} [MPa] f_{ctm} [MPa] - Coeff. of thermal expansion α_{th} [1/°C] - Partial factor γ_c
7	Steel (material)	- Grade - Quality - Modulus of elasticity E_a [MPa] - Yield strength f_y [MPa] - Poisson's ratio v - Shear modulus G_a [MPa] - Coeff. of thermal expansion α_{th} [1/°C] - Partial factor γ_{M0}
8	Rebars (material)	- Grade - Class - Characteristic strength f_{sk} [MPa] - Partial factor γ_s
9	Shear connectors (material)	- Grade - Tensile strength [MPa] - Partial factor γ_{Mfs}
10	Other data	- Relative humidity - Partial factor for fatigue loading γ_{Ff}
11	Spans	Length of each span of the bridge
12	Traffic data	- Design life - Assessment method (safe life / damage tolerant) - Consequence of failure (low / high) - Traffic category (1 to 4) - Dynamic factor (in case it is a railway bridge) Trains per year per track

Table 3.1: INPUT tables

3.4 GENERAL DESCRIPTION OF THE BRIDGE

The program is designed to work for a composite steel-concrete multiple-girder-bridge with numerous continuous spans. The total length of the deck is defined as an input (see Table 3.1).

A few geometrical simplifications have been made: a) the horizontal and vertical road alignments are straight, and b) the top face of the deck is assumed to be flat.

The transverse cross-section of the slab and of the non-structural bridge equipments is considered symmetrical with respect to the axis of the bridge. The bridge deck has certain width and carries a defined number of traffic lanes, with constant width, either in one or two directions. The program also allows for internal and external shoulders, which generally give space for safety traffic barriers and/or sidewalks. For more details on the definition of the geometrical properties and its application refer to section 4.2.

Other parameters that are also user-defined include:

- centre to centre distance between main girders and the slab cantilevers on each side span;
- slab thickness.

As usually done in the deck longitudinal design, the slab is assumed to have an average constant thickness.

3.4.1 Structural steel distribution

The program allows for changes in the cross-sections along the bridge. Each type of cross-section with its parameters (e.g. web thickness, upper flange width, etc.) is user-defined and stored in the database with an ID.

Generally, section changes are aligned with the location of vertical stiffeners (as to simplify the fabrication process). In this work, the latter are also considered as inputs from the user.

Cross beams, which aim to give lateral stability to the bridge, will not be analysed for fatigue in this work, hence would not be included in the program. Similarly, longitudinal stiffeners are not taken into account for the main girders.

3.4.2 Execution scheme

The assumptions concerning the construction stages are important for the verification under fatigue. They are also needed to define the values of steel/concrete modular ratios. Finally, the calculation of internal moments and forces in the deck should take construction phases into account.

In the program, the construction phases include:

- installation of the steel structure of the deck;
- on-site pouring of concrete slab segments by casting them in a selected order.

Since the calculation of the internal forces due to non-cyclic loads is out of scope of this work (see section 3.6), the need to define the sequence of concreting just limits its functionality to the definition of the modular ratios, which would then allow us to get the cross-section properties (e.g. second moment of area) for the analysis under fatigue loads (long-term).

Therefore, some other parameters involved in the construction phase, are initially input to the program, such as:

- number of slab segments to be poured;
- time taken to pour and prestress each slab segment;

- time taken to complete the installation of non-structural bridge equipment, e.g. waterproofing, asphalt, safe barriers, etc.

3.5   MATERIAL PROPERTIES

In the development of this project, two different steel grades were considered for the main structure:

- S355

- S690 (High-strength steel)

The mechanical properties of each one, particularly the yield strength, would be defined by the thickness of the steel member (web, upper flange, lower flange) for each section, in accordance with EN 10025-3 (S355) and EN 10025-6 (S690).

Properties of the rest of the materials involved (concrete, steel for reinforcement and shear studs) are defined as inputs (see Table 3.1).

3.6   ACTIONS

The project focuses in the analysis of two sources of loads:

1) Fatigue Load Model 3 (FLM3) from EN 1991-2.

2) Loads due to traffic simulation.

Both cases will be treated independently. Fatigue load model 3 (FLM3) will be used for the verification under fatigue using the damage equivalent λ-factor method; whereas the traffic simulation will return a load history on a particular cross-section of one of the main girders, which will be used to assess critical details for fatigue using the damage accumulation method.

On the other hand, in this project only the cyclic loads concerning fatigue assessment were considered in the program. Therefore, when studying a real case scenario (see section 4), the load effects due to non-cyclic loads must be added to the results obtained from the program, in order to get the design load effects on the structure.

Further development of the program could include the analysis of non-cyclic loading and its interaction with cyclic loading on the structure.

3.6.1   Influence line module

As known from structural mechanics, the influence line is a graphic representation of the variation of a function (such as the shear or bending moments) at a specific point on a beam caused by a unit load placed at any point along the structure. In fatigue analysis, the influence lines allow us to study where should the loads be positioned in order to get maximum and minimum load effects in the cross-section where the detail under study is located.

Input data for this module is mainly related to the associated input data for the *Beam Analysis* module (see appendix A), since the latter will be the one used to get the load effects. Thus, the following information should be provided:

- Segments

- Supports

- OutPoints

- Point Loads [kN]: Point force equal to -1 for the influence line analysis

- Step [m]: indicates the intervals for the different positions of the point load during the influence line analysis.

The procedure followed in the program was the following:

1) Position the unitary point load at x = 0 (left end of the main girder);

2) Calculate shear and moment at the detail's cross-section using *Beam Analysis* module;

3) Store results in RAM;

4) Advance the load a distance equal to one step;

5) Repeat steps 3 to 4 until the load reaches the end of the bridge.

6) Finally store all the results of position, shear and moment in *results.db*.

For an example of its application, see section 4.5.

3.6.2 Fatigue Load Model 3 (FLM3)

The Eurocode proposes a load model for fatigue design and verification when considering a finite life of the structure, which is most commonly used in practice along with the simplified damage equivalent factor method. This load model is FLM3 and consists mainly of 1 heavy truck crossing the bridge, with the properties described in section 2.1.2.3. For details located near intermediate supports, a second vehicle with lower weight could be positioned on the bridge at a minimum distance of 40m with respect to the other truck.

This module uses the following inputs:

- Position of the detail under study along the bridge;

- Results from the *influence line* module;

- FLM 3 and its components:

    o Axles' weight

    o Distance between axles

- Transverse position of the slow lane (where the loads are supposed to be centered) with respect to the main girder under analysis.

First, the reaction on the main girder due to the transversal position of the loads is obtained using the simplified transversal distribution showed in Figure 2.9.

Then, considering the influence lines and the loads on the bridge, the program, using an iterative procedure, searches for the best longitudinal position where to allocate the loads along the main girder as to get maximum and minimum load effects. For this purpose, it analyses separately the heavier truck and the lighter one, getting their corresponding stresses. At last, it considers the superposition of both effects, but taking into account the minimum distance between the vehicles mentioned before.

Finally, it returns the value of the load effect and its longitudinal position along the bridge.

3.7 TRAFFIC SIMULATION

3.7.1 Introduction

In order to generate more realistic traffic loading, simulations of free-flowing traffic are performed. The objective is to get load effects (shear and moment) on the main girders, which result from loads coming from a random generated stream of traffic.

The general procedure in the simulation consists of the following steps:

1) Generate a stream of simulated truck traffic in one lane;

2) Calculate the bridge load effects for a stream of truck traffic.

Since the analysis of bridge loading involves several number of stochastic variables (e.g. vehicle's speed, gap between vehicles, traffic flows, etc.), the approach used in this work was to limit the number of random variables by fixing certain values as inputs. Further improvements could consider different statistical distributions to approach the behaviour of these variables (according to WIM and real data) more accurately (see section 2.4).

Then, the variables that were provided as user-inputs were the following:

- Minimum truck speed [km/h]

- Maximum truck speed [km/h]

- Minimum gap between vehicles [sec] (for safety matters)

- Period of time under study [hrs]

- Start of day period [hr]

- End of day period [hr]

- Minimum flow rate during day period [trucks/hr]

- Maximum flow rate during day period [trucks/hr]

- Minimum flow rate during night period [trucks/hr]

- Maximum flow rate during night period [trucks/hr]

- Time step [sec]

The limits on trucks' speed are according to the European regulations for motorways. The values adopted are 60 km/h (min) and 110 km/h (max), allowing for a 10% increase on the value of the maximum speed, in order to consider some exceptional cases.

The *Period of time under study* allows to define the number of hours to be covered by the simulation process (e.g. 1 hour, 24 hours -1day-, 720 hours -1month-, etc).

The simulation sets a division of the day into 2 time periods: night and day. Therefore, it is possible to consider different traffic volumes, depending on the time of the day. Moreover, the minimum and maximum parameters for the flow rates in both periods allow the user to circumscribe those variables within certain range (according to the site).

Finally, the *Time step* is used for the analysis of the load effects during the bridge crossing events.

Additionally, certain pre-defined truck types are used in the simulation. In this case, parameters corresponding to general lorries described in FLM4 (EN 1991-2) are considered in the program (see Table 2.2).

3.7.2 Stream of simulated truck traffic in one lane

3.7.2.1 Overview of simulation process

The steps in generating a stream of vehicles in a single lane may be summarized as follows:

1. random pick of flow-rate for day and night;

2. start clock (t = 0);

3. generate a truck:

   a. assign clock time to first axle of this truck (time of arrival on bridge);

   b. randomly pick one of the types of truck (from Table 2.2) and assign their main parameters (GVW, number of axles, wheelbase, distance between axles and load distribution to the axles);

European Erasmus Mundus Master
Sustainable Constructions under natural hazards and catastrophic events
520121-1-2011-1-CZ-ERA MUNDUS-EMMC

surcos

c. generate random vehicle speed;

d. if hour of day has changed, generate current flow rate (trucks / hr);

e. generate random gap (seconds) behind this truck based on current flow rate;

f. store details of this truck in memory (truck ID, speed, gap with following vehicle, time required to quit the bridge, start time, end time) for bridge-crossing programs to use;

g. advance clock to first axle of next truck, using the wheelbase and speed of this truck, and the gap behind this truck;

4. repeat step 3 for each truck, and continue until required stream of traffic has been generated.

The random selections of truck type, speed and gap behind each vehicle were performed using a normal distribution function.

For the selection of the truck type, the properties from Table 2.2 were used, with their set distribution as shown in the following table. Then, the program would pick randomly considering these weights.

ID	GVW	Axles	wheelbase	Dist axle 12	Dist axle 23	Dist Axle 34	Dist axle 45	Load axle1	Load axle2	Load axle3	Load axle4	Load axle5	Composition
	[kN]		[m]	[m]	[m]	[m]	[m]	[kN]	[kN]	[kN]	[kN]	[kN]	[%]
1	200	2	4.5	4.5	0	0	0	70	130	0	0	0	20%
2	310	3	5.5	4.2	1.3	0	0	70	120	120	0	0	30%
3	490	5	11	3.2	5.2	1.3	1.3	70	150	90	90	90	15%
4	390	4	11.2	3.4	6	1.8	0	70	140	90	90	0	25%
5	450	5	14.1	4.8	3.6	4.4	1.3	70	130	90	80	80	10%

Table 3.2: Truck types: properties and distribution.

Additionally, truck speed is assumed constant during the whole bridge crossing, unless it is higher than the speed of the previous truck. If the latter is the case, in order to avoid collision, the truck's speed is adjusted taking into account the gap between vehicles, until it reaches the same speed as the truck in front. Then, both trucks travel at the same speed.

The generation of the gap between vehicles (step 3e) is also performed randomly but according to the current hourly flow rate (either during day or night period). In other words, the program was developed considering that the sum of the gaps between vehicles equals to 1 hour and the number of vehicles that crossed the bridge in that period hour equals to the assigned flow-rate.

3.7.2.2 Outputs

The outputs of this first part are resumed in the following list:

− Number of truck

− Truck ID (associated to the truck_type from Table 3.2)

− Speed [km/h]

− Gap Time Truck [sec]: the gap between rear axle of front truck and front axle of the following.

− Time to end [sec]: time it takes the truck to cross the bridge.

− Start Time [sec]: time when the front axle of the truck enters the bridge.

− End Time [sec]: time when the rear axle of the truck exits the bridge.

When generating more than one stream of traffic, two additional parameters are added to the above, being:

- Stream ID: identification of each stream

- Direction: representing the sense of direction of the stream (either 1 or 2).

3.7.3 Bridge load effects for a stream of truck traffic

Once the stream of traffic is generated for each slow lane of the bridge, the load effects (mainly the shear V and bending moment M) on the main girders are calculated.

The process is summarized as follows:

1) combine the streams generated in each lane (see section 3.7.2) and get the stream of simulated traffic in the whole bridge;

2) identify the next crossing event – a continuous period of time when there is at least one axle on the bridge (from one or more trucks). Set the current time to the arrival time of the first axle in the crossing event;

   a. advance the clock by the set time step, until the end of the crossing event;

   b. calculate the total load effect for each time step for all axles on the bridge;

3) identify the maximum load effects for the crossing event;

4) repeat step 2 until the end of the traffic stream.

3.7.4 Definition of optimum fixed parameters

Several assumptions were considered when developing this simulation module, which really limit its application. For instance, the simulation is performed just taking into account two streams of truck traffic, with equal or opposite directions; moreover, there is no allowance for lighter vehicles (e.g. cars, vans etc.), since the main focus was to concentrate the heavier loads (e.g. trucks, lorries etc) which have the biggest impact on fatigue analysis. Further improvements could allocate a wider range of loads.

As mentioned in section 2.4, some research projects have developed sophisticated software tools which were calibrated according to relevant WIM data obtained from real traffic measurement on different sites. However, in this project the simulation was not calibrated, due to lack of data and limited time, since this would require a much deeper and thorough research. However, the simulation is still used as a simple generation of stochastic values (loads, gaps, distances etc), which proves to be good basis for an initial fatigue assessment.

The main issues encountered during the simulations were:

- the time that it took to run the simulation (both for the stream generation of traffic and the action effect analysis), and

- the amount of data that the CPU had to deal with, both in its RAM and when storing the information in the database.

These limitations raised the alarm on the initial parameters affecting the size of data generated, such as:

- the time of analysis implemented in the simulation (e.g. 1 month, 1 year, 10 years etc),

- the time step,

- the traffic flow (number of trucks per hour).

Therefore, a specific analysis was performed to study the impact of this variable on the results obtained from different simulations, changing one of the aforementioned values at a time and comparing their mean and standard deviation, trying to optimize the process.

A simple example, consisting on a simple supported beam with a span of 80m, was considered for this purpose, and the initial parameters used were the ones indicated in the following table. Particularly, the focus was centered in a detail located at mid-span, being the welded connection between the lower flange and the vertical stiffener.

min speed	max speed	min gap	time analysis	min flow day	max flow day	min flow night	max flow night	start time day	end time day	step
[km/h]	[km/h]	[sec]	[hrs]	[tr/hr]	[tr/hr]	[tr/hr]	[tr/hr]	[hr]	[hr]	[sec]
60	110	1.5	720	100	200	10	100	6	22	0.5

Table 3.3: Initial parameters used to test the traffic simulation on a simple example.

On a first approach, only variations on the time of analysis were performed, and the statistics are shown in Table 3.4.

#	Days of analysis	Time to complete load effect calculation	Total stream	Number of multiple crossing events	Δσ max	Damage	mean moment (total)	std deviation moment (total)
		[min]	[trucks]		[Mpa]		[kNm]	[kNm ^ 0.5]
1	7	3	39,883	5,857	25.438312	-	-1471.9997	2359.7196
2	30	11	170,306	25,331	25.438312	-	-1463.75	2357.48
3	60	24	338,309	49,995	25.438312	-	-1484.89	2366.07

Table 3.4: Statistics from traffic simulations with variations on time of analysis (example).

From the above, some conclusions could be drawn:

- The time of analysis is, generally, proportional to the simulation time, the total number of trucks crossing the bridge and the number of multiple crossing events. It is possible to see a linear relation between these variables.

- The maximum stress range is the same in all the simulations as expected, since it is not supposed to change with the time of analysis but with the type of loading (GVW). Moreover, since it remains below the cut-off limit (being equal to 32.4 MPa for a detail category 80).

- The mean moments are located within certain small range of values, and their value does not depend on the time of analysis (e.g. the simulation for 1 week gave similar mean value as the one for 2 months).

- The standard deviation confirms the theory that values are concentrated within certain range, not being affected by the time of analysis.

From the previous points, it is possible to conclude that running simulations for a smaller period of time (e.g. 1 month) would give similar results compared to those obtained from longer period of analysis, hence optimizing the global process. Therefore, the strategy will be to set the simulation period to 1 month.

The graph from Figure 3.2 shows that the means of the results obtained is practically the same, and all the values are within the same range if just one standard deviation is taken to each side (68% confidence).
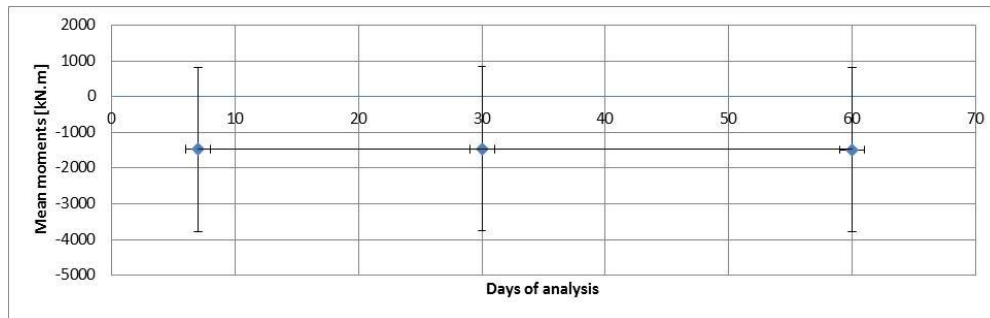
Figure 3.2: Mean moment vs days of analysis, considering standard deviation (example).

On a second approach, and following the previous conclusions, the time of analysis will be set to 1 month and only the traffic flow will be modified, as shown in the following table:

#	Days of analysis	min speed	max speed	min gap	time analysis	min flow day	max flow day	min flow night	max flow night	start time day	end time day	step
		[km/h]	[km/h]	[sec]	[hrs]	[tr/hr]	[tr/hr]	[tr/hr]	[tr/hr]	[hr]	[hr]	[sec]
1	30	60	110	1.5	720	100	200	10	100	6	22	0.5
2	30	60	110	1.5	720	300	700	40	300	6	22	0.5
3	30	60	110	1.5	720	500	900	60	600	6	22	0.5

Table 3.5: Simulations with different traffic flows (example).

The results are the following:

#	Time to complete load effect calculation	Total stream	Number of multiple crossing events	Δσ max	Damage	mean moment (total)	std deviation moment (total)
	[min]	[trucks]		[Mpa]		[kNm]	[kNm ^ 0.5]
1	11	170,306	25,331	25.438312	-	-1463.75	2357.48
2	127	567,595	277,652	25.438312	-	-1501.60	2367.58
3	174	837,012	569,057	25.438312	-	-1775.51	2462.27

Table 3.6: Statistics from traffic simulations with variations on traffic flow (example).

Some notes from the values shown in Table 3.6:

- Comparing simulation #1 and #3, increasing the total stream of truck traffic around 5 times affects the time to run the simulation by a factor of almost 16, hence being inefficient. This issue could be seen more clearly in the increase of the number of multiple crossing events, where the number of trucks over the bridge is substantially increased.

- The maximum stress range is similar in all the simulations as expected, since it is not supposed to change with the number of trucks crossing, but with the type of loading (GVW).

- The mean moments are located within certain small range of values for the first 2 simulations, whereas the third simulation, which had more dense traffic, shows an increase of around 20% in its mean.

Simulation number 3 presents a concentration of trucks on the bridge, with smaller distances between vehicles, therefore giving bigger values of load effects and dispersion. Since our interest is focused on free-flowing traffic, the third case is discarded.

Additionally, it is possible to conclude that increasing the traffic flow within the free-flowing traffic range does not affect the maximum stress range obtained, though having a great impact on the efficiency of

the simulation (increase on time of calculation). Thus, the simulations will be limited to the traffic flow proposed for simulation 1.

Finally, the step of analysis will now be modified in order to analyse its impact on the simulation, as shown in the following table:

#	Days of analysis	min speed	max speed	min gap	time analysis	min flow day	max flow day	min flow night	max flow night	start time day	end time day	step
		[km/h]	[km/h]	[sec]	[hrs]	[tr/hr]	[tr/hr]	[tr/hr]	[tr/hr]	[hr]	[hr]	[sec]
1	30	60	110	1.5	720	100	200	10	100	6	22	0.5
2	30	60	110	1.5	720	100	200	10	100	6	22	1
3	30	60	110	1.5	720	100	200	10	100	6	22	0.1

Table 3.7: Simulations with different time steps (example).

The results are the following:

#	Time to complete load effect calculation	Total stream	Number of multiple crossing events	Δσ max	Damage	mean moment (total)	std deviation moment (total)
	[min]	[trucks]		[Mpa]		[kNm]	[kNm ^ 0.5]
1	11	170,306	25,331	25.438312	-	-1463.75	2357.48
2	9	169,631	25,146	25.438312	-	-1348.43	2298.53
3	35	167,661	24,703	25.438312	-	-1560.95	2394.45

Table 3.8: Statistics from traffic simulations with variations on time step (example).

Some notes from the values shown in Table 3.8:

- The time to complete the calculation is not proportional to the reduction of the time step;

- As expected, the total stream does not change with the time step, since it just depends on the time of analysis and the traffic flow. The same applies for the number of multiple crossing events.

- The maximum stress range is the same in all the simulations as expected, since it is not supposed to change with the number of trucks crossing, but with the type of loading (GVW).

- The simulation with a step of 1 sec returns values of mean moment and accumulated damage which, compared to simulations with smaller time steps, seem to be a bit inaccurate.

- Smaller time steps (e.g. 0.01 sec) showed problems in the computer due to memory errors, thus not being able to get values to compare with.

The last observation leads to the conclusion that the time step to be used should be lower or equal than 0.5 sec. From the figure, it is seen that, compared to 0.5, using a step of 0.1 sec returns similar mean moments around 6-8 % bigger, though demanding more computer effort and, thus, taking more time to complete the simulation. Therefore, it is concluded that the optimal time step is 0.5 sec and is the one to be used during the simulations.

3.7.5 Example

With the purpose of showing the operation of the simulation module, a simple example is presented, using the same properties of the Case study (see section 4) with the following initial parameters:

European Erasmus Mundus Master
Sustainable Constructions under natural hazards and catastrophic events
520121-1-2011-1-CZ-ERA MUNDUS-EMMC

ᒣᑌᒣᑌᒣ

Days of analysis	min speed	max speed	min gap	time analysis	min flow day	max flow day	min flow night	max flow night	start time day	end time day	step
	[km/h]	[km/h]	[sec]	[hrs]	[tr/hr]	[tr/hr]	[tr/hr]	[tr/hr]	[hr]	[hr]	[sec]
30	60	110	1.5	720	100	200	10	100	6	22	0.5

Table 3.9: Initial parameters used for simple example on traffic simulation.

The results of the total stream obtained for a simulation of 1 hour of traffic are:

# truck	stream ID	direction	truck ID	speed [km/h]	gap time truck [sec]	time to end [sec]	start time [sec]	end time [sec]
1	1	1	2	96.42	193.651	13.65	0.000	13.650
2	2	2	4	83.57	108.386	15.99	0.000	15.990
3	2	2	3	71.56	95.152	18.66	108.869	127.529
4	1	1	4	83.79	203.735	15.95	193.856	209.806
5	2	2	1	91.14	106.669	14.40	204.574	218.974
6	2	2	1	64.18	118.867	20.45	311.421	331.871
7	1	1	4	104.85	301.200	12.75	398.073	410.823
8	2	2	4	88.72	114.567	15.06	430.540	445.600
9	2	2	2	96.97	116.999	13.57	545.562	559.132
10	2	2	2	62.73	125.276	20.98	662.766	683.746
11	1	1	2	94.3	161.978	13.95	699.657	713.607
12	2	2	1	82.33	160.419	15.94	788.357	804.297
13	1	1	5	98.02	294.437	13.74	861.846	875.586
14	2	2	5	109.15	121.304	12.34	948.974	961.314
15	2	2	4	91.16	112.450	14.66	1070.742	1085.402
16	1	1	3	75.57	196.834	17.67	1156.800	1174.470
17	2	2	2	101.23	157.301	13.00	1183.635	1196.635
18	2	2	2	77.24	107.915	17.04	1341.132	1358.172
19	1	1	2	85.31	195.687	15.42	1354.158	1369.578
20	2	2	5	81.7	139.736	16.48	1449.303	1465.783
21	1	1	1	106.31	245.482	12.34	1550.078	1562.418
22	2	2	3	75.22	140.207	17.76	1589.660	1607.420
23	2	2	1	68.63	137.371	19.12	1730.394	1749.514
24	1	1	4	91.74	318.091	14.57	1795.712	1810.282
25	2	2	4	63.21	184.393	21.14	1868.000	1889.140
26	2	2	3	109.08	129.844	12.24	2053.031	2065.271
27	1	1	3	85.79	353.655	15.57	2114.242	2129.812
28	2	2	1	81.82	76.251	16.04	2183.238	2199.278
29	2	2	5	78.51	121.414	17.15	2259.687	2276.837
30	2	2	2	73.97	149.549	17.79	2381.748	2399.538
31	1	1	3	88.64	210.529	15.07	2468.359	2483.429
32	2	2	2	97.99	137.596	13.43	2531.565	2544.995
33	2	2	1	72.15	103.625	18.19	2669.363	2687.553
34	1	1	2	100.44	294.752	13.10	2679.335	2692.435
35	2	2	2	76.98	136.581	17.09	2773.213	2790.303
36	2	2	4	102.04	147.550	13.10	2910.051	2923.151
37	1	1	2	97.05	191.872	13.56	2974.284	2987.844
38	2	2	3	67.18	129.719	19.88	3057.997	3077.877
39	1	1	4	87.45	267.701	15.28	3166.360	3181.640
40	2	2	4	79.57	135.075	16.79	3188.305	3205.095
41	2	2	1	83.24	138.873	15.76	3323.886	3339.646

Table 3.10: Results of total stream of for 1 hour of simulated traffic.

3.8   GLOBAL ANALYSIS

Following EN 1994-2, 5.4.1.1(1), action effects in the structure are calculated by an elastic global analysis of each main girder considered independently. Torsional rigidity of the deck as well as interaction with the other parts of the structure are not considered in this analysis. This simplifies the calculation, though

giving less accurate results than using a more sophisticated approach such as a finite element grid model of the deck.

Furthermore, the model takes into account the construction stages (see section 3.4.2), the time dependent behaviour of concrete, its cracking and shear-lag effects in the slab.

During the global longitudinal bending analysis, the girders' neutral fibre changes between different models according to the cross-section mechanical properties (areas and second moments of area). This is due to the different modular ratios (creep effect) to be considered and to the fact that a given composite cross-section could be cracked or not.

However, for the fatigue assessment due to cyclic loading (variable actions) only 1 model was considered, which consisted of composite cross-sections made by the steel girders and the concrete slab, taking into account the short-term modular ratio n_0.

The cracking of concrete around the internal supports is taken into account by using the simplified method proposed in EN 1994-2, 5.4.2.3 (3), considering the reduced flexural stiffness $E_a I_2$ of the cracked section over 15% of the span on each side of internal support and the uncracked values $E_a I_1$ elsewhere.

In order to get the load effects, the *Beam Analysis* module was developed in the program, which is explained in more detail in appendix A.

3.9   CROSS-SECTION

The analysis of the cross-section properties is made of 2 main sections:

1) Steel cross-section,

2) Composite cross-section.

Since the fatigue assessment implies the analysis in the long-term, the section will always be considered as composite in the design/verification under fatigue. However, the properties of the steel cross-section play an important role in the definition of many properties of the composite cross-section (e.g. section class). Furthermore, a separate analysis of the steel section alone would allow, in the future, the opportunity to expand the program to a broader analysis, including ULS and SLS, which would certainly need to study the construction stage where only the steel section is involved.

In the case of the composite cross-section, some parameters are included in the calculation, which show the interaction of both materials, particularly the concrete's non-linearity. Those are the already mentioned:

- Shear lag effect,

- Concrete cracking,

- Creep.

3.9.1   Steel cross-section

Once defined the main dimensions of the steel cross-section (e.g. web thickness, upper flange width etc.), the module determines the following properties:

- Yield stress (f_y) of each steel part (web, upper flange and lower flange), according to table 5 of EN 10025-3, depending on the thickness of the part.

- Class of each steel part and, hence, of the steel cross-section.

- Area of the steel cross-section (A).

- Shear area of the steel cross-section (A_v).

- Position of the neutral axis of the steel cross-section with respect to the bottom fibre (*p.n.a.*).

- Second moment of area of the steel cross-section around its strong axis (I_y).

- Second moment of area of the steel cross-section around its weak axis (I_z).

3.9.2 Local buckling – Determination of cross-section classes

Following clause 5.5.1(1) of EN 1994-2, the composite cross-section class is defined by the class of the steel cross-section according to EN 1993-1-1. Thus, cross sections are classified on a scale of 1 to 4 based on the slenderness (width/thickness noted *c/t*) of the different compressed panels.

For cross-sections Class 1 or 2, the design bending resistance shall be determined by rigid plastic theory. For Class 3 cross-sections, elastic analysis should be adopted; for Class 4 cross-sections elastic analysis with effective width properties should be applied.

In hogging bending zones (continuous beams), tensile stresses in concrete are neglected and the cross-section resistance is due to steel girders and longitudinal steel reinforcement included in the effective width of the slab.

The procedure followed for each steel part (upper flange, web and lower flange) is:

1. Check if the part is in compression, by analysing both the bending moment sign (positive or negative) and the position of the neutral axis of the cross-section.

2. If the part is partially or fully compressed, the ratio c/t is compared to the limits set in Table 5.2 of EN 1993-1-1 and, thus, the class of the element is defined.

For setting the web's class, a deeper study has to be considered, since it is generally submitted to both compression and bending due to different locations of the neutral axis. Therefore, additional parameters are taken into account, such as α and ψ (see Table 5.2 of EN 1993-1-1), which will take part in the definition of the class.

Finally, the class of the cross-section is equal to the highest class of its steel parts.

It should be noticed that, generally, in sections submitted to sagging bending moments the neutral axis is located within the concrete slab, hence being the steel girder fully tensioned. In this case, it is concluded that the cross-section is class 1.

3.9.2.1 Class 4 – Effective properties

Local instability effects (buckling) are taken into account by considering the effective properties of class 4 steel parts, following the procedure from EN 1993-1-5, section 4.3.

As mentioned before, the program just deals with plate elements without longitudinal stiffeners (EN 1993-1-5, 4.4), while future developments could include them in the calculation.

Following the Eurocode, parameters such as the buckling factor k_σ, plate slenderness λ_p, reduction factor ρ, effective width b_{eff} etc. are calculated in order to obtain the effective mechanical properties of the slender element and, then, of the steel cross-section.

3.9.3 Shear lag

According to clause 5.4.1.2 of EN 1994-2, the effect of shear lag on the beam's flanges could be addressed by using an effective width of the elements. Additionally, it is stated that one b_{eff1} should be considered for the mid-spans and one b_{eff2} for the supports of a continuous beam, according to (Eq. 3.1).

$$b_{eff} = b_0 + \sum_i b_{ei}$$

(Eq. 3.1)

where:

$$b_{ei} = min\left(\frac{L_e}{8}, b_i\right)$$

(Eq. 3.2)

being L_e the equivalent length, whose value is defined according to Figure 3.3.
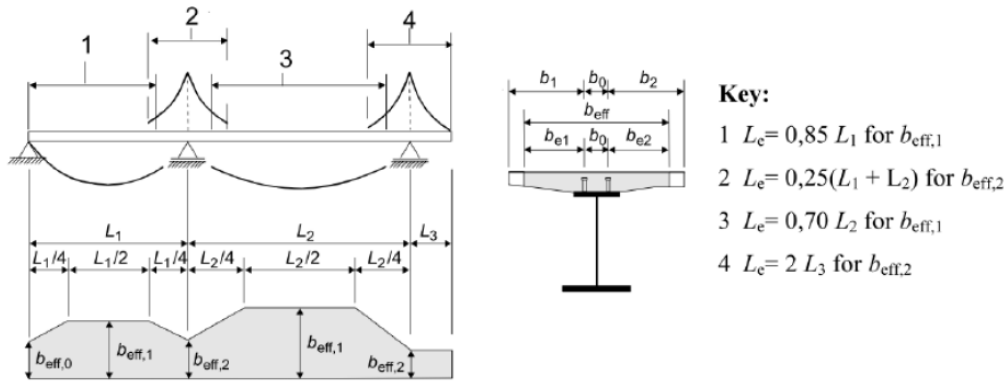
Figure 3.3: Equivalent spans, for effective width of concrete flange (EN 1994-2).

3.9.4 Concrete cracking

In order to consider the concrete cracking in hogging bending moments areas (continuous beams), and taking into account the simplification procedure stated in clause 5.4.2.3(3) of EN 1994-2, it was considered the rigidity of a cracked cross-section of the beam in a length equal to 15% of the spans on each side of the internal supports, as well as the rigidity of the un-cracked cross-section for the remaining length of the beams.

Moreover, it is important to mention that when calculating the position of the neutral axis of the composite cross-section, the following assumptions were made:

- Concrete does not contribute in tension;
- Steel from reinforcement bars does not contribute in compression.

3.9.5 Creep (modular ratios)

Following EN 1994-2, 5.4.2.2, appropriate allowance was made for the effects of creep and shrinkage of concrete. The Eurocodes state that the effect of creep may be taken into account by using modular ratios n_L for the concrete. The modular ratios depending on the type of loading (subscript L) are given by:

$$n_L = n_0 \cdot (1 + \psi_L \cdot \varphi_t)$$

(Eq. 3.3)

where:

n_0 is the modular ratio E_a / E_{cm} for short-term loading;

E_{cm} is the secant modulus of elasticity of the concrete for short-term loading according to EN 1992-1-1: 2004, Table 3.1 or Table 11.3.1;

φ_t is the creep coefficient $\varphi(t,t_0)$ according to EN 1992-1-1: 2004, 3.1.4 or 11.3.3, depending on the age (t) of concrete at the moment considered and the age (t_0) at loading;

ψ_L is the creep multiplier depending on the type of loading, which be taken as 1.1 for permanent loads, 0.55 for primary and secondary effects of shrinkage and 1.5 for prestressing by imposed deformations.

Moreover, in order to calculate the creep coefficient and, thus, the modular ratios, it is also necessary to input the value of the relative humidity on site, which is included in the database (see Table 3.1).

All the methods included in the composite cross-section module are dependent on the modular ratio, which would certainly give different mechanical properties ($I_{y,eff}$, p.n.a., etc.) and, thus, result in different stresses in the structure.

3.9.6   Mechanical properties

For the calculation of the main mechanical properties of the composite cross-section, the following points had to be considered:

- The analysis was divided between cracked and uncracked sections, according to the bending moment acting on the cross-section.

- The effective properties of the cross-section (due to local buckling of the structural steel elements) were considered for sections class 4. The procedure to find the position of the neutral axis of the effective cross-section is summarized in Figure 3.4.

A clear example is shown in the case study, section 4.4.4.

3.10   DAMAGE EQUIVALENT FACTOR METHOD

A simple scheme with the main critical details is shown in Figure 3.5. On this project, focus is centered in the following details:

1. Welded connection between vertical stiffener and lower flange of the main girder (detail category 90) and

2. Welded connection of the shear head studs to the upper flange (detail category 80).

Despite this singularity on the analysis, it is important to mention that, as explained before, the program was designed with the purpose of being able to assess for fatigue any type of detail from the steel girder, since the inputs include the detail's category and its geometry.

3.10.1   Details under direct stresses

According to the bending moments acting on the cross-section, either causing tension, compression or both in the concrete slab, (Eq. 2.6) to (Eq. 2.8) were included in the program to calculate the maximum stress range acting on the detail under study.

Finally, the design of every detail must satisfy (Eq. 2.17), using the λ-factor obtained from (Eq. 2.18). An example of its application is presented in section 4.
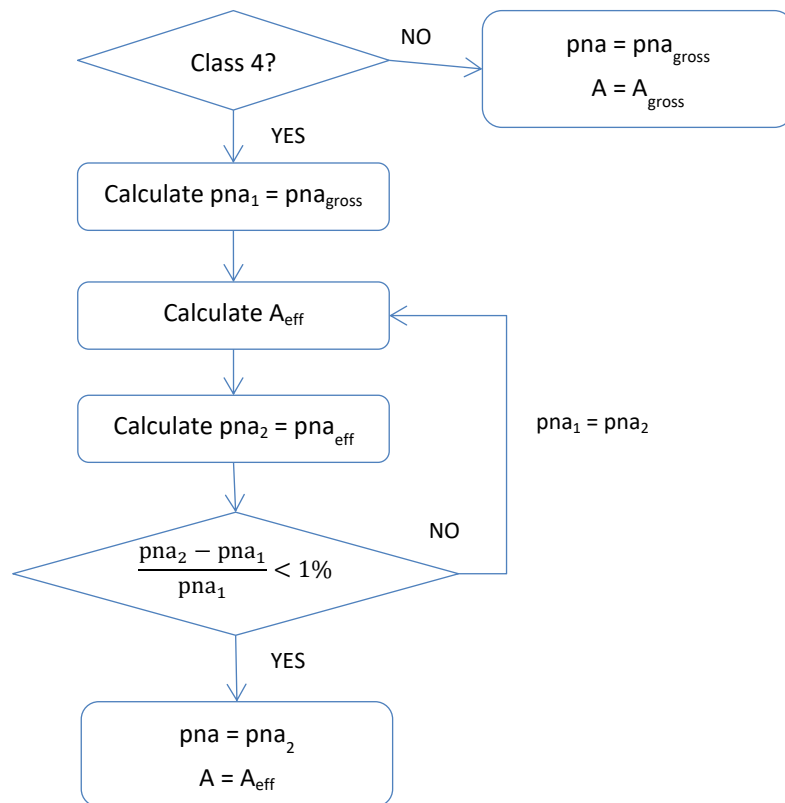
Figure 3.4: Iterative procedure to obtain the position of the neutral axis in class 4 cross-sections (effective).

3.10.2 Shear connectors

Same procedure is followed for the shear connectors in their assessment for fatigue, with the difference in the lambda factor used (λ_v instead of λ) and in the calculation of the equivalent stress range, as explained in section 2.2.3. Additionally, special attention should be paid for the cases where the maximum stress in the top flange is tensile, where the interaction criteria should be also verified (Eq. 2.24) and (Eq. 2.25).
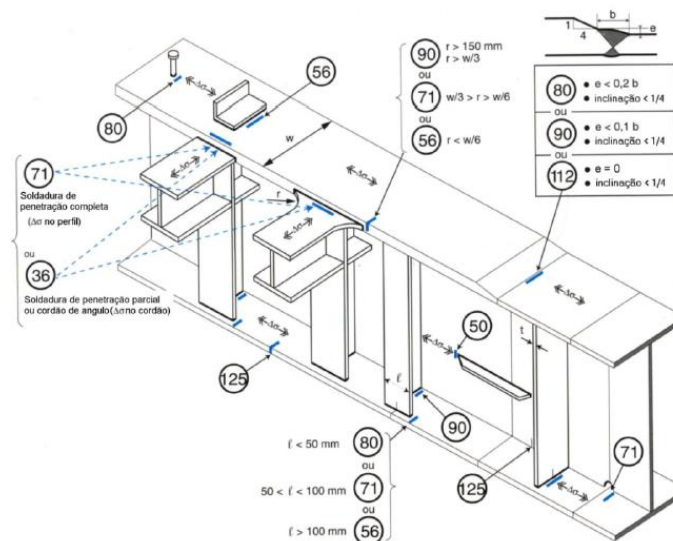
Figure 3.5: Typical detail categories (Adapt. from "Ponts Metalliques et Miixtes" – SETRA).

3.11 DAMAGE ACCUMULATION METHOD

From the raw data of load history obtained from the stream of simulated truck traffic, the program, first, identifies the peaks (or valleys) by means of a simple algorithm, and discards the values that are not wanted since they are not consecutively alternate. In the following simple example this concept is better explained.

Supposing that there is a stress history as the one shown in Table 3.11, then it is necessary to identify the peaks and valleys and discard the other values, before proceeding to the stress counting method. Following that purpose, column *check_1* stores the difference between the stress at that time and the stress at a previous time:

$$check\_1_i = \sigma_i - \sigma_{i-1} \qquad (Eq.\ 3.4)$$

Then, column *check_2* stores the ratio between the following value and the current value from column *check_1*:

$$check\_2_i = \frac{check\_1_{i+1}}{check\_1_i} \qquad (Eq.\ 3.5)$$

Finally, the last column checks if the value from *check_2* is positive or negative, assigning boolean *True* or *False* respectively. If the value is *True*, it means that it is a peak or a valley, and should be stored for further analysis; otherwise, the value is discarded (see Table 3.11 for a graphical representation, where the values highlighted in red are the ones discarded).

Once completed the purge, the program calculates the stress history (normal stresses) following the Theory of Elasticity:

$$\sigma = \frac{M}{I_y} \cdot d \qquad (Eq.\ 3.6)$$

where *d* is the distance from the neutral axis to the fibre where the detail is located.

Then, by means of the rainflow counting method (see appendix B), the stress ranges with their associated number of cycles are defined.

Time (s)	Stress (MPa)	check_1	check_2	TRUE = PEAK or VALLEY
0	-1000			TRUE
10	-900	100	18.000	FALSE
20	900	1800	-0.278	TRUE
30	400	-500	0.400	FALSE
40	200	-200	-1.500	TRUE
50	500	300	0.833	FALSE
60	750	250	0.600	FALSE
70	900	150	-0.467	TRUE
80	830	-70	5.143	FALSE
90	470	-360	-0.722	TRUE
100	730	260	0.000	TRUE
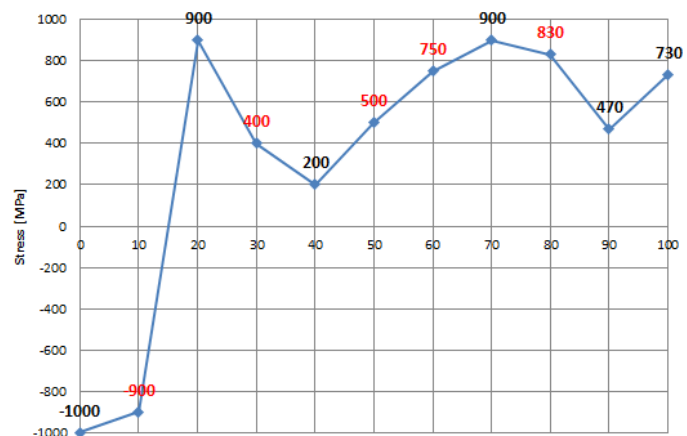
Table 3.11: Peak and valley slice algorithm (example).

As explained in section 2.3.5.1, the final damage equals to the sum of the proportional damage caused by each stress range. In the program, in order to obtain the accumulated damage on the detail for the whole service life of the bridge, the value obtained after 1 month of simulation (see section 3.7.4) was linearly extrapolated up to the end of the structure's life. Thus, in the case of a damage tolerant design method, it was possible to study the time where maintenance should take place as to repair the damage

and avoid failure of the structure. Following this concept and according to EN 1993-1-9, A.6(1), the accumulated damage should be always kept below 1.

As seen on Figure 3.6, the damage tolerant concept relies on major inspections and maintenance in order to reach the structure's design service life. Compared to the safe life design method where no major inspections are included during the service life, the former gives a cheaper structure, as well as having a significant lower impact in the down payment (reflected in the partial safety factors for fatigue strength).
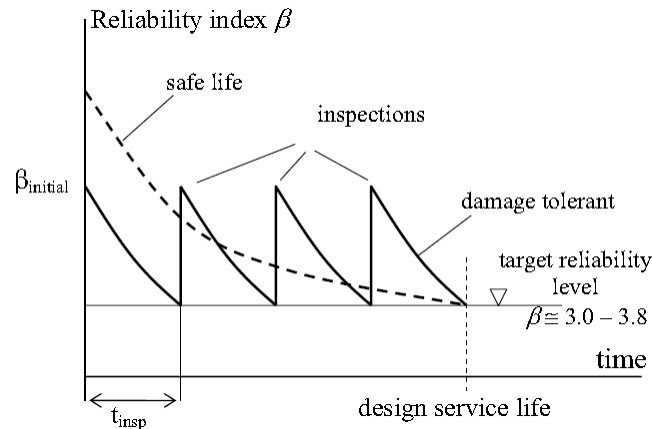
Figure 3.6: Schematic of fatigue reliability assuming damage tolerant and safe life methods and a failure with high consequence (Nussbaumer et al. [2]).

However, regular minor inspections should be carried more frequently as to detect and track possible cracks whose development could lead to potential structural problems.

4 CASE STUDY

4.1 INTRODUCTION

In order to test the program in a real scale, it was implemented into a case study. The project used for this purpose was the one from *OPTIBRI European Research Programme* [5].

First, a general description of the bridge, with its geometry, materials and cross-section is presented. Further on, aiming to synthetize this work, only the results from the application of the program will be shown, as well as their comparison with the values from the aforementioned project, with short comments and conclusions.

Two cases are studied within this project: one using normal steel grade S355, and the other using HSS S690. For each section, the results and parameters from both cases will be presented, in order to compare them and observe the differences, if any.

4.2 GENERAL DESCRIPTION

The road bridge is a composite steel-concrete girder bridge with a continuous multiple-span configuration, as shown in Figure 4.1.
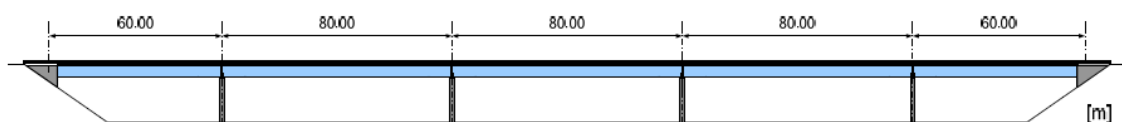
Figure 4.1: Elevation of the bridge deck and span distributions (source: OPTIBRI [5]).

The bridge is assumed to be straight in the horizontal plan, with a constant total depth along the entire span. The structure is made of 2 twin girders which are joined by diaphragms for lateral stability.

The transverse cross-section of the slab and of the non-structural bridge equipments is symmetrical with respect to the axis of the bridge. The slab shows a 2.5% superelevation either side of the bridge axis (see Figure 4.2). The bridge deck is 21.5 m wide and carries four traffic lanes, with 2 lanes 3.50 m wide in each direction, 2.0 m wide external shoulders with BN4 safety barriers, and 0.75 m wide internal shoulders with a central "New Jersey" barrier.
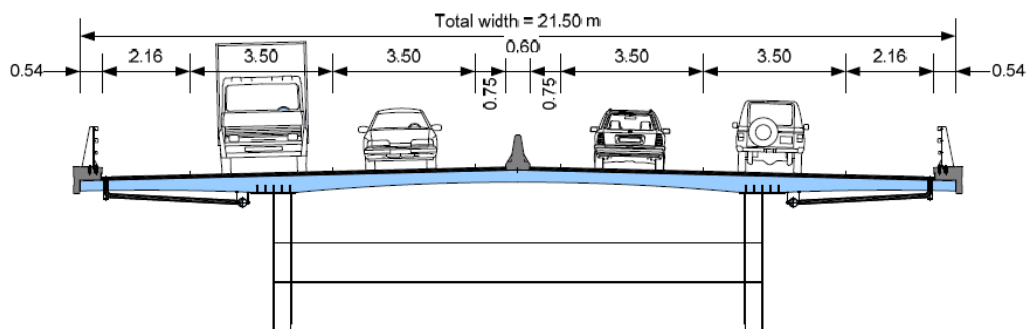
Figure 4.2: Cross-section of the deck with the road platform data (source: OPTIBRI [5]).

The centre to centre distance between main girders is 12 m and the slab cantilevers on each side span 4.75 m. The slab is transversely prestressed and its thickness varies from 0.40 m over the main girders to 0.30 m at mid-span and 0.25 m at the tip of the cantilevers.

The structural steel distribution for a typical span girder is presented in Figure 4.3. As usually done in the deck longitudinal design, the slab is assumed to have the average constant thickness of 0.32 m. For instance, for the model with S355, each main girder has a constant depth of 3800 mm and the variations

in thickness of the upper and lower flanges are found towards the inside of the girders. The lower flange is 1500 mm wide and its thickness varies from 120 mm at the supports to 50 mm at mid-span sections. The upper flange is 1300 mm wide and its thickness varies from 100 mm on supports to 35 mm at mid span. The web thickness varies from 26 mm to 18 mm. The web has only vertical stiffeners, spaced at 4.0 m at the span sections and 2.0 m near the supports.

The two main girders have transverse bracing at abutments and at internal supports. Intermediate brancings are well as every 7.5 m in side spans and every 8 m in inner spans. The cross-girders in span are made of built-up welded plate girder sections 1.0 m heigth at span sections and 2.0 m heigth at internal supports and abutments.

The vertical T-shaped stiffeners are duplicated and welded on the lower flange at supports whereas the flange of the typical span vertical T-shaped stiffeners has a V-shaped cutout for fatigue reasons. Additionally, flat stiffeners are placed between the Tee stiffeners, spaced by 2.0 m near supports and 4.0 m at span, to increase the web lateral support.
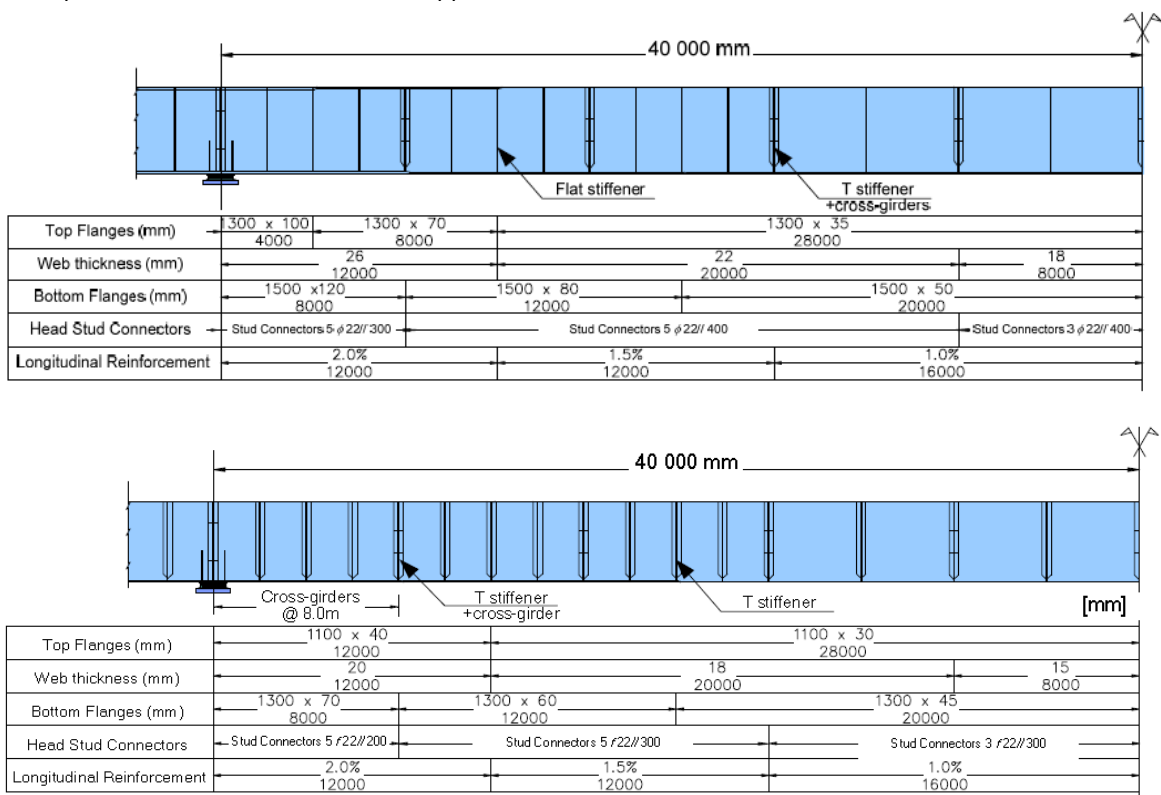
Figure 4.3: Structural steel distribution for the main girder typical span (S355 and S690, respectively) (source: OPTIBRI [5]).
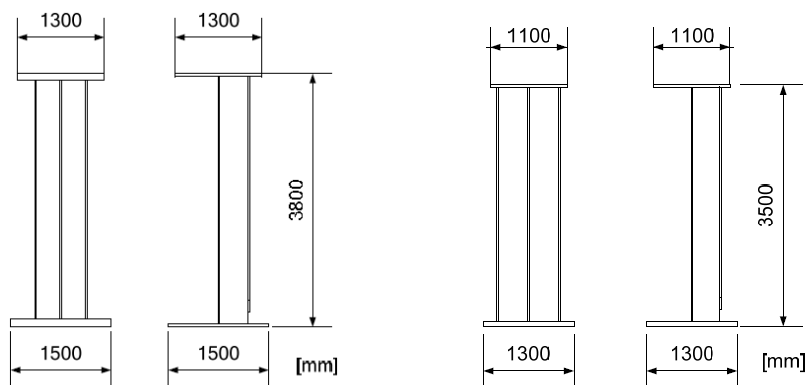
Figure 4.4: Detailing of main girders' cross-sections (S355 and S690, respectively) (source: OPTIBRI [5]).

According to the structural steel configuration (Figure 4.3), different types of sections are defined along the main girder for each span, and their properties (see following tables) are used as inputs for the program.

Table: cross_sections

ID	h_w_mm	t_w_mm	b_UF_mm	t_UF_mm	b_LF_mm	t_LF_mm
	Filter	Filter	Filter	Filter	Filter	Filter
1	3580.0	26.0	1300.0	100.0	1500.0	120.0
2	3610.0	26.0	1300.0	70.0	1500.0	120.0
3	3650.0	26.0	1300.0	70.0	1500.0	80.0
4	3685.0	22.0	1300.0	35.0	1500.0	80.0
5	3715.0	22.0	1300.0	35.0	1500.0	50.0
6	3715.0	18.0	1300.0	35.0	1500.0	50.0

Table: cross_sections_S690

ID	h_w_mm	t_w_mm	b_UF_mm	t_UF_mm	b_LF_mm	t_LF_mm
	Filter	Fil...	Filter	Filter	Filter	Filter
1 1	3390.0	20.0	1100.0	40.0	1300.0	70.0
2 2	3400.0	20.0	1100.0	40.0	1300.0	60.0
3 3	3410.0	18.0	1100.0	30.0	1300.0	60.0
4 4	3425.0	18.0	1100.0	30.0	1300.0	45.0
5 5	3425.0	15.0	1100.0	30.0	1300.0	45.0

Table 4.1: Types of cross-sections along the main girders (S355 and S690, respectively).

4.3 MATERIALS

- **Structural steel**

Two types of structural steel grades are used in OPTIBRI:

1. S355, normalized rolled weldable fine grain structural steels, and

2. S690, high yield strength steel in the quenched and tempered condition.

Material properties are obtained from EN 1993-1-1. In particular, the mechanical properties for S355 are taken from EN 10025-3, whereas the ones for S690 are given in EN 10025-6 (see Table 4.3).

Nominal thickness [mm]	≤ 16	> 16 ≤ 40	> 40 ≤ 63	> 63 ≤ 80	> 80 ≤ 100	> 100 ≤ 150
Minimum yield strength [MPa]	355	345	335	325	315	295
Tensile strength [MPa]	470					450

Table 4.2: Mechanical properties at ambient temperature for normalized steel.

Nominal thickness [mm]	≤ 50	> 50 ≤100	> 100 ≤150
Minimum yield strength [MPa]	690	650	630
Tensile strength [MPa]	770	760	710

Table 4.3: Mechanical properties at ambient temperature for quenched and tempered steel S690.

- **Concrete**

Normal concrete of class C35/45 is adopted for the slab. The main mechanical properties are according with EN 1992-1.

- **Reinforcing steel**

Reinforcement steel bars adopted in the project are high bond bars B500B with yield strength of 500 MPa (according with EN 10080). Other mechanical properties are obtained from EN 1992-1 and EN 1994-2.

- **Shear connectors**

Head stud connectors S235 with tensile strength of 450 MPa in accordance with EN 13918 and EN 1994-2 are adopted in the design.

4.4 CROSS-SECTION

4.4.1 Local buckling - steel cross-section

As an example, it will be shown the calculation of the effective properties of one of the steel cross-sections of the main girders (with S355), particularly the one at an intermediate support (x = 140m). The parameters describing the section are:

	WEB		UPPER FLANGE		LOWER FLANGE	
h_{web} [mm]	t_{web} [mm]	b_{uF} [mm]	t_{UF} [mm]	b_{LF} [mm]	t_{LF} [mm]
3580	26	1300	100	1500	120

$f_{y,web}$ [MPa]	$Class_{web}$	$f_{y,LF}$ [MPa]	$Class_{LF}$	$f_{y,UF}$ [MPa]	$Class_{UF}$	$Area_{gross}$ [cm2]	pna_{gross} [mm]
345	4030.8	295	1	315	1	4030.8	1677.29185

Table 4.4: Properties of steel cross-section (S355) at intermediate support (x = 140m).

The position of the neutral axis (*pna_mm*) is measured starting from the bottom fibre of the steel cross-section (see Figure 4.5).

The parameters to obtain the effective properties are calculated following EN 1993-1-5, section 4.4 and are presented as follows:

$$\varepsilon = \sqrt{\frac{235}{f_y [MPa]}} = 0.8253 \qquad (Eq.\ 4.1)$$

$$\bar{b} = h_{web} - 2 \cdot t_{web} = 3528 mm \qquad (Eq.\ 4.2)$$

$$\psi = \frac{b_{t,gross}}{b_{c,gross}} = \frac{-1996.70815}{1531.29185} = -1.303937 \qquad (Eq.\ 4.3)$$
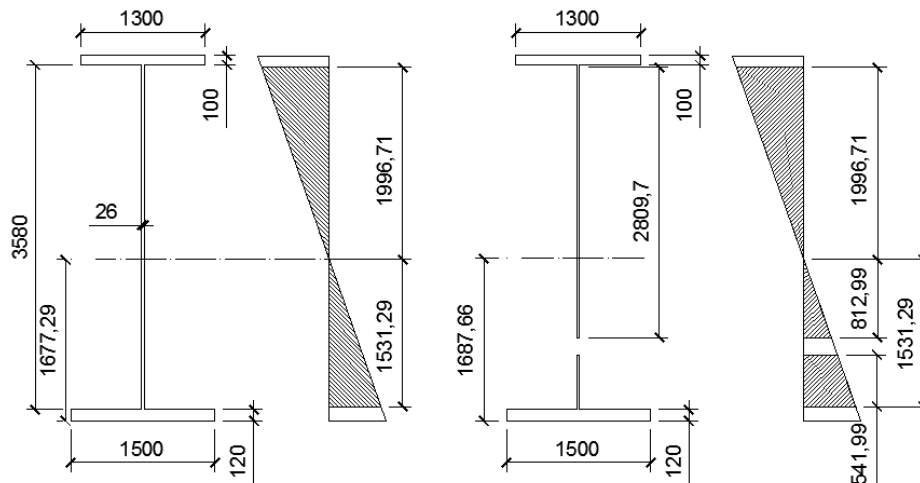
Figure 4.5: Steel cross-section at intermediate support (x = 140m), and reductions due to local buckling on the web.

$$k_\sigma = 5.98 \cdot (1 - \psi)^2 = 31.74259 \qquad \text{(Eq. 4.4)}$$

$$\overline{\lambda_p} = \frac{\overline{b}/t_{web}}{28.4 \cdot \varepsilon \cdot \sqrt{k_\sigma}} = 1.027552 \qquad \text{(Eq. 4.5)}$$

$$\rho = \frac{\overline{\lambda_p} - 0.055 \cdot (3 + \psi)}{\overline{\lambda_p}^2} = 0.8848387 \qquad \text{(Eq. 4.6)}$$

$$b_{c,eff} = \rho \cdot b_{c,gross} = 1354.95 mm \qquad \text{(Eq. 4.7)}$$

In the following table, the results obtained before are compared to the ones given by the program, as to detect its accuracy.

Source	ψ	k_σ	λ_p	ρ	b_{eff} [mm]	$b_{eff,1}$ [mm]	$b_{eff,2}$ [cm2]	b_t [mm]
Hand calculation	-1.30	31.74	1.03	0.88	1354.95	541.98	812.97	1996.71
Program	-1.30	31.74	1.03	0.88	1354.98	541.99	812.99	1996.71
Difference [%]	-2.14E-06	-7.73E-06	2.88E-03	-2.59E-03	-2.32E-03	-2.32E-03	-2.32E-03	5.01E-07

Table 4.5: Effective properties parameters of cross-section (S355) at intermediate support (x = 140m). Comparison between hand calculation and program.

Once obtained the effective widths of class 4 compression elements, which in this case is just confined to the web, the effective properties (e.g. pna_{eff}, A_{eff}, $I_{y,eff}$ etc.) could be calculated.

As mentioned before, since in this project only the long-term effects are of interest, where the composite cross-section plays the main role, the effective properties will be determined taking into account the composite behaviour (see section 4.4.4).

4.4.2 Creep (modular ratios)

The creep effect may be considered in the analysis by taking the appropriate modular ratio for the concrete rendering the steel-concrete composite section into an equivalent steel section.

For short term actions, like traffic loads, or for the analysis of the structure at traffic opening, the modular ratio may be obtained by direct relation between the steel and concrete elastic moduli (Eq. 3.3).

The concrete slab is casted in segments. Hence, each segment has a different age at loading. However, for simplification, EN 1994-2 allows the use of one average value (t_0) for the determination of the creep coefficient. Considering the estimated minimum time to complete the concrete slab (144 days) and the time to finish the execution and assembly of non-structural equipments (45 days), it is assumed a mean value of 95 days for the age of concrete at loading (t_0).

Thus, the modular ratios for long term actions are as presented in the next table:

Load case	Program	OPTIBRI	Diff. [%]
Short-term actions	6.163	6.2	-0.60
Shrinkage	14.219	14.3	-0.57
Non-structural bridge equipment	15.634	15.7	-0.42

Table 4.6: Modular ratios for different load cases.

The absolute differences are less than 1% and are due to round-off, hence the values obtained from the program are validated.

4.4.3   Shear-lag effect (effective width)

The shear lag effect is calculated following the procedure from section 3.9.3, and according to EN 1994-2. The results are shown in the following table, for different cross-sections.

Detail's position [m]	L_{eff} [m]	b_0 [m]	b_{e1} [m]	b_{e2} [m]	Effective width [m]		
					Program	OPTIBRI	Diff. [%]
140	40	0.80	4.35	5.00	10.15	10.15	0.0
144					10.15	10.15	0.0
148					10.15	10.15	0.0
152					10.15	10.15	0.0
156					10.15	10.15	0.0
160					10.15	10.15	0.0
164	56			5.55	10.75	10.75	0.0
168					10.75	10.75	0.0
172					10.75	10.75	0.0
176					10.75	10.75	0.0
180					10.75	10.75	0.0

Table 4.7: Concrete effective width (shear-lag effect).

4.4.4   Composite cross-section properties

4.4.4.1 Cracked properties

For the cracked cross-section, the effective properties of the steel section plus the steel reinforcement were taken into account. The area of the collaborating reinforcement was calculated as:

$$A_{bars} = rows\ of\ bars \cdot \frac{b_{eff}}{sep_{bars} + d_{bar}} \cdot \left(\frac{\pi \cdot d_{bar}{}^2}{4} \right)$$

(Eq. 4.8)

In the following tables, the main mechanical properties of the cracked composite cross-section at different locations are presented.

Table: composite_cracked_section_properties

	Position_mm	status	class_cr	pna_cr_mm	A_cr_cm2	Iy_cr_cm4
	Filter	Filter	Filter	Filter	Filter	Filter
1	140000	cracked	4	1969.94	4435.17	1.371e+08
2	144000	cracked	4	1796.13	4103.78	1.246e+08
3	148000	cracked and uncracked	4	2109.17	3417.07	1.040e+08
4	152000	cracked and uncracked	4	1852.35	2865.22	8.903e+07
5	156000	cracked and uncracked	4	1852.35	2865.22	8.903e+07
6	160000	cracked and uncracked	4	3422.11	1361.49	9.293e+07
7	164000	cracked and uncracked	4	3435.36	1390.34	9.374e+07
8	168000	cracked and uncracked	4	3435.36	1390.34	9.374e+07
9	172000	cracked and uncracked	4	3553.97	1265.2	9.302e+07
10	176000	cracked and uncracked	4	3553.97	1265.2	9.302e+07
11	180000	cracked and uncracked	4	3553.97	1265.2	9.302e+07

Table 4.8: Composite cracked cross-section mechanical properties (with S355).

Table: composite_cracked_section_properties

	Position_mm	status	class_cr	pna_cr_mm	A_cr_cm2	Iy_cr_cm4
	Filter	Filter	Filter	Filter	Filter	Filter
1	140000	cracked	4	3309.67	1189.64	1.047e+08
2	144000	cracked	4	3309.67	1189.64	1.047e+08
3	148000	cracked and uncracked	4	3303.51	1189.18	8.216e+07
4	152000	cracked and uncracked	4	3334.32	1039.82	8.115e+07
5	156000	cracked and uncracked	4	3334.32	1039.82	8.115e+07
6	160000	cracked and uncracked	4	3330.11	1037.7	5.008e+07
7	164000	cracked and uncracked	4	3340.34	1067.39	5.044e+07
8	168000	uncracked	0	0.0	0.0	0.000e+00
9	172000	uncracked	0	0.0	0.0	0.000e+00
10	176000	uncracked	0	0.0	0.0	0.000e+00
11	180000	uncracked	0	0.0	0.0	0.000e+00

Table 4.9: Composite cracked cross-section mechanical properties (with S690).
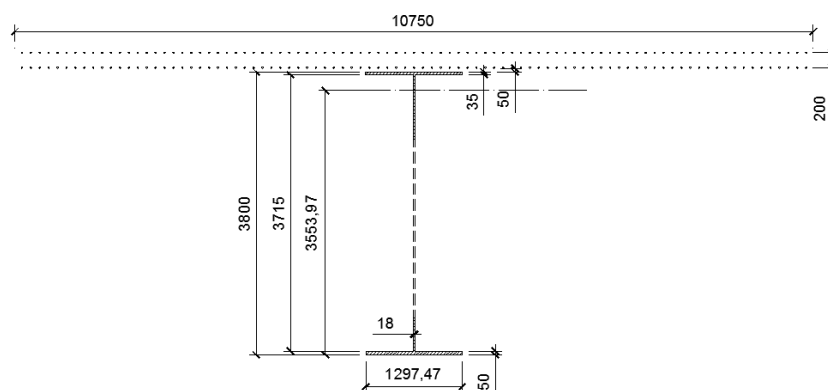
Figure 4.6: Composite cracked effective cross-section (S355) at mid-span (x = 180m).

In Table 4.9, it is possible to observe that the last 4 entries show zero values, which is due to the fact that the section is considered as 'uncracked', thus not being applicable the 'cracked' properties.

A graphic representation of the cracked cross-section (S355) at mid-span (x = 180m) is shown in Figure 4.6.

4.4.4.2 Uncracked properties

On the other hand, for the uncracked cross-section, the effective properties of the steel section plus the concrete slab were considered, where the collaborating area of the latter was:

$$A_{conc} = d_{conc} \cdot \frac{b_{eff}}{n_0}$$

(Eq. 4.9)

where d_{conc} represents the slab thickness.

In the following table, the main mechanical properties of the uncracked composite cross-section at different locations are presented.

Table: composite_uncracked_section_properties

	Position_mm	status	class_n0	pna_n0_mm	A_n0_cm2	Iy_n0_cm4
	Filter	Filter	Filter	Filter	Filter	Filter
1	140000	cracked	0	0.0	0.0	0.000e+00
2	144000	cracked	0	0.0	0.0	0.000e+00
3	148000	cracked and uncracked	3	3756.34	8329.58	8.307e+07
4	152000	cracked and uncracked	4	3117.95	8429.92	1.718e+08
5	156000	cracked and uncracked	4	3117.95	8429.92	1.718e+08
6	160000	cracked and uncracked	4	3306.59	7993.12	1.267e+08
7	164000	cracked and uncracked	4	3333.78	8304.68	1.279e+08
8	168000	cracked and uncracked	4	3333.78	8304.68	1.279e+08
9	172000	cracked and uncracked	1	3820.33	7455.84	1.227e+08
10	176000	cracked and uncracked	1	3820.33	7455.84	1.227e+08
11	180000	cracked and uncracked	1	3820.33	7455.84	1.227e+08

Table 4.10: Composite uncracked cross-section mechanical properties (with S355).

Table: composite_uncracked_section_properties

	Position_mm	status	class_n0	pna_n0_mm	A_n0_cm2	Iy_n0_cm4
	Filter	Filter	Filter	Filter	Filter	Filter
1	140000	cracked	0	0.0	0.0	0.000e+00
2	144000	cracked	0	0.0	0.0	0.000e+00
3	148000	cracked and uncracked	4	3066.83	7727.7	1.062e+08
4	152000	cracked and uncracked	4	3072.31	7467.08	1.033e+08
5	156000	cracked and uncracked	4	3072.31	7467.08	1.033e+08
6	160000	cracked and uncracked	4	3159.49	7277.48	8.458e+07
7	164000	cracked and uncracked	4	3181.85	7589.04	8.523e+07
8	168000	uncracked	4	3181.85	7589.04	8.523e+07
9	172000	uncracked	4	3203.06	7381.03	8.212e+07
10	176000	uncracked	4	3203.06	7381.03	8.212e+07
11	180000	uncracked	4	3203.06	7381.03	8.212e+07

Table 4.11: Composite uncracked cross-section mechanical properties (with S690).
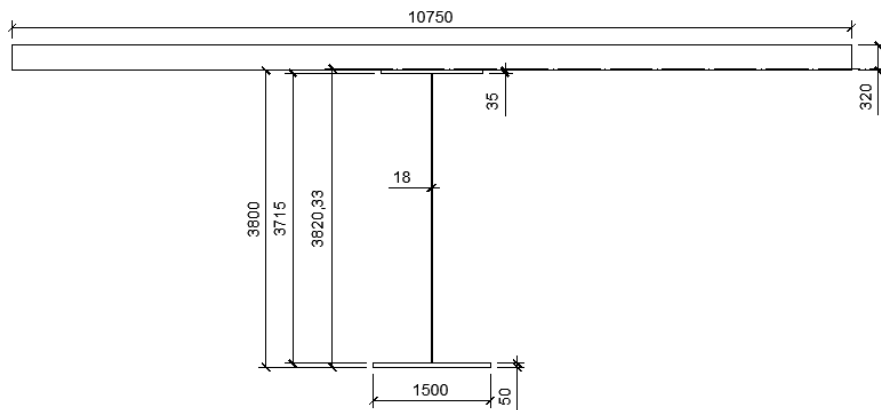
Figure 4.7: Composite effective uncracked cross-section (S355) at mid-span (x = 180m).

In Table 4.10, there is a sudden change from class 4 to class 1 at x = 172m, which is due to the change on the position of the neutral axis of the cross-section, from the steel section to the concrete slab.

A graphic representation of the uncracked cross-section (S355) at mid-span (x = 180m) is shown in Figure 4.7.

4.4.4.3 Comparison

Since there is no associated data for the model with S690, this section will show the comparison of the results only for the model with S355.

Section	Location	A [m2]		Diff [%]	Iy [m4]		Diff [%]
		Program	OPTIBRI		Program	OPTIBRI	
1	140.0 - 144.0	0.444	0.468	-5.13	1.371	1.423	-3.65
2	144.0 - 152.0	0.342	0.37	-7.57	1.04	1.094	-4.94
3	152.0 - 160.0	0.843	0.778	8.35	1.718	1.746	-1.60
4	160.0 - 172.0	0.799	0.759	5.27	1.279	1.314	-2.66
5	172.0 - 180.0	0.746	0.744	0.27	1.227	1.266	-3.08

Table 4.12: Comparison of cross-section mechanical properties between program and OPTIBRI (with S355).

It is possible to observe differences in the results obtained, which could be due to:

- Precision in the modular ratio used (round off);
- Position of the neutral axis, cross-section class and calculation of effective properties.

Furthermore, the differences are mostly negative, meaning that the program gives more conservative values of the cross-section. This could be due to the iteration and precision used when calculating the effective properties.

Additionally, it was detected that in OPTIBRI project the sections were reduced to 5 types, whilst, as shown in Table 4.1, the number of cross-sections are 6.

4.5   INFLUENCE LINES

In order to focus the attention, further comparisons of the results will be limited to 2 cross-sections:

- At intermediate support (x = 140m),
- At mid-span (x = 180m).

Thus, the module is run for this cases and the graphical representation of the influence lines for moment and shear are shown in Figure 4.8 and Figure 4.9, respectively.

Additionally, the step used in the calculation was 0.1m, since it was proven to give sufficiently refined results as to take all the positions of the moving load.
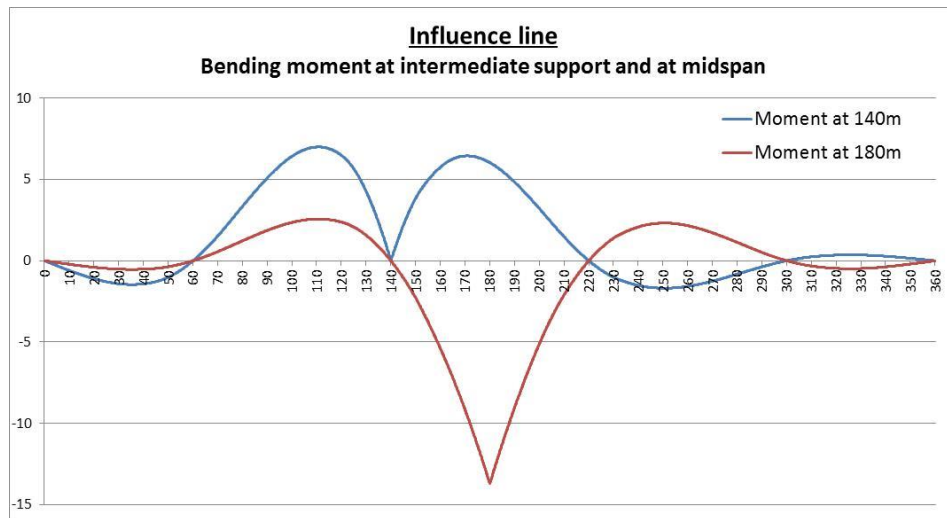
Figure 4.8: Influence lines for moment for detail located at intermediate support (blue) and at midspan (red).
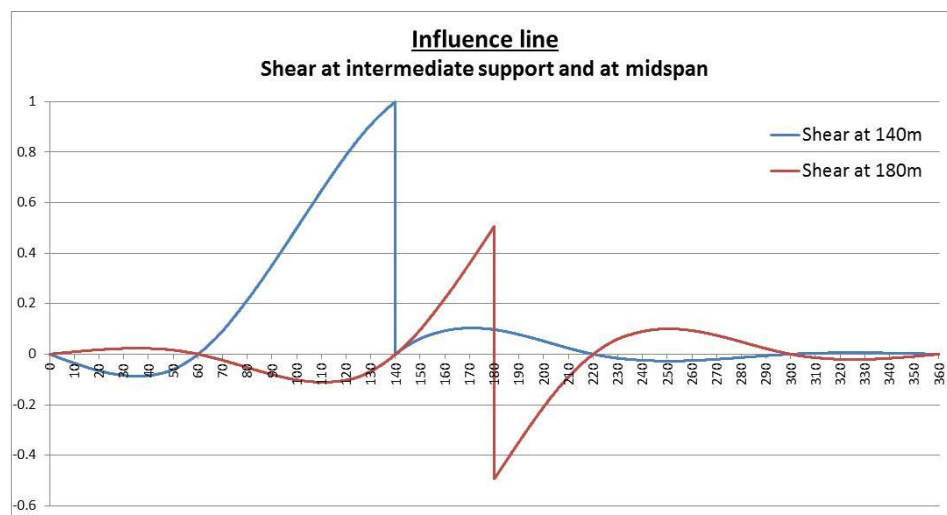
Figure 4.9: Influence lines for shear for detail located at intermediate support (blue) and at midspan (red).

As seen from Figure 4.8 to get the maximum bending moments in the detail located at an intermediate support it is necessary to load spans 2 (60-140), 3 (140-220) and 5 (300-360); whereas to get the minimum values, spans 1 (0-60) and 4 (220-300) should be loaded. Similar procedure is followed with the influence line for shear.

4.6   ACTIONS
4.6.1   Fatigue Load Model 3 (FLM3)

Following section 3.6.2, and once defined the influence lines (previous section), the load effects corresponding to FLM3 are obtained using the program.

As mentioned before, this load model consists in a single truck crossing the bridge, although a second smaller vehicle could be added and govern the calculation of a detail at an intermediate support, respecting the minimum distance stated in the Eurocodes (40m).

In Table 4.13 the values obtained with the program are compared to the ones used in OPTIBRI project:

Position [m]	V_{max} [kN]			V_{min} [kN]			M_{max} [kNm]			M_{min} [kNm]		
	Program	OPTIBRI	Dif. [%]	Program	OPTIBRI	Dif. [%]	Program	OPTIBRI	Dif. [%]	Program	OPTIBRI	Dif. [%]
140	519.84	500	4.0	-46.16	-50	-7.7	769.39	778	-1.1	-4168.31	-4134	0.8
180	232.75	215	8.3	-228.42	-220	3.8	5986.42	6019	-0.5	-1584.78	-1541	2.8

Table 4.13: Comparison between load effects obtained from program and OPTIBRI.

From the above, it is possible to observe a difference between the results from the program and the ones from OPTIBRI, which could be attributed to the different cross-section properties used during the calculation.

For further comparisons, the load effects from OPTIBRI will be used in order to avoid the impact of this difference when studying the verification for fatigue.

4.6.1.1 Design actions

Since non-cyclic loads are not calculated in this project (out of the scope of work), they will be considered as inputs from external analysis.

In this case, the following values are obtained from the OPTIBRI report:

Section [m]	140	144	148	152	156	160	164	168	172	176	180
$M_{c,max,Ed}$ [kNm]	-7371	-3510	-56	2992	5634	8520	11292	13448	14988	15912	16220
$M_{c,min,Ed}$ [kNm]	-43666	-37814	-32578	-27958	-23954	-4840	-3011	-1588	-1074	-464	-261

Table 4.14: Design bending moments due to non-cyclic loads (OPTIBRI).

Finally, the design bending moments are calculated using (Eq. 2.4) and (Eq. 2.5).

Section [m]	140	144	148	152	156	160	164	168	172	176	180
$M_{Ed,max,f}$ [kNm]	-6593	-2836	1461	5484	9002	12725	16173	18805	20718	21889	22239
$M_{Ed,min,f}$ [kNm]	-47800	-41358	-35647	-30617	-26352	-7064	-5099	-3539	-2888	-2142	-1802

Table 4.15: Design bending moments on the main girder.

The shear forces due to FLM3 are presented in the following table:

Section [m]	140	144	148	152	156	160	164	168	172	176	180
$V_{FLM3,max}$ [kN]	500	481	455	412	383	366	324	305	279	240	215
$V_{FLM3,min}$ [kN]	-50	-50	-52	-58	-63	-80	-117	-135	-157	-196	-220

Table 4.16: Shear forces due to FLM3.

4.7 DESIGN USING DAMAGE EQUIVALENT FACTOR METHOD

4.7.1 DIRECT STRESSES

4.7.1.1 Factor λ_1

As explained in section 2.3.2.1, the factor λ_1 accounts for the span length (a relation which is function of the influence line length). Therefore, first it is necessary to define the different segments (mid-span and support section –see Figure 2.6–) and the critical influence line length, according to the bridge properties. The values of the critical influence line length should stay within the range stipulated in the Eurocodes for the application of the λ_1 factor (10m ≤ L ≤ 80m).

Finally, the factor is calculated for the different regions using the formulas from Figure 2.8 and the results are shown in Table 4.17.

Position range [m]	Region	Critical influence line length [m]	λ_1
0.0 – 51.0	Mid-span	60	2.05
51.0 – 72.0	Intermediate support	70	2.10
72.0 – 128.0	Mid-span	80	1.85
128.0 – 152.0	Intermediate support	80	2.20
152.0 – 208.0	Mid-span	80	1.85
208.0 – 232.0	Intermediate support	80	2.20
232.0 – 288.0	Mid-span	80	1.85
288.0 – 309.0	Intermediate support	70	2.10
309.0 – 360.0	Mid-span	60	2.05

Table 4.17: Regions, critical influence line length and factor λ_1.

4.7.1.2 Factor λ_2

According to (Eq. 2.19), factor λ_2 depends on traffic type and volume.

The following values are used:

✓ N_{obs} = 2E6 lorries per year and per slow lane. This indicative number was obtained from EN 1991-2, Table 4.5, for motorways with 2 lanes in each direction.

✓ The mean weight for this traffic is taken from FLM4 for long distance traffic (EN 1991-2, Table 4.7), and it is calculated following (Eq. 2.20).

Lorry	Q_{weight} [kN]	% Composition	N_{obs}
1	200	20	0.4E+6
2	310	5	0.1E+6
3	490	50	1.0E+6
4	390	15	0.3E+6
5	450	10	0.2E+6

Table 4.18: Data for traffic mean weight calculation.

The value obtained is: Q_{m1} = 445.4 kN,

and, finally, the factor results: λ_2 = 1.224

4.7.1.3 Factor λ_3

This factor depends on the design life of the bridge t_{Ld} (in years) and is obtained by (Eq. 2.21). Since the design life of the bridge is 100 years, the factor is equal to $\lambda_3 = 1.0$.

4.7.1.4 Factor λ_4

Factor λ_4 accounts for the effect of heavy vehicles on the other lanes. Considering that the bridge has two slow lanes, one in each direction, (Eq. 2.22) becomes:

$$\lambda_4 = \sqrt[5]{1 + \frac{N_2}{N_1} \cdot \left(\frac{\eta_2 \cdot Q_{m2}}{\eta_1 \cdot Q_1}\right)^5}$$

Where:

$N_2 = N_1$ and $Q_{m1} = Q_{m2}$, are the number of lorries per year per slow lane and the average gross weight of the lorries in each lanes, respectively, which are the same for the two lanes;

η_1 and η_2 are the values of influence line for the internal forces that produce the stress range in the middle of the lane 1.

In this type of deck, with two girders at a large distance, the value of influence line η_2 is close to zero (η_2 = 8.63E-9) and thus it results that $\lambda_4 = 1.0$.

4.7.1.5 Factor λ_{max}

Finally λ_{max} such as λ_1 depends on the span length and it is obtained as follows:

✓ For midspan sections, with spans length L_i between 25 m and 80 m:

$$\lambda_{max} = 2.0$$

✓ For support sections, with adjacent spans between 30 m and 80 m:

$$\lambda_{max} = 1.80 + 0.9 \cdot \frac{L - 30}{50}$$

4.7.1.6 Factor λ

From the previous values, it is possible to calculate the equivalent lambda factor for each region:

Position range [m]	Region	Critical influence line length [m]	λ_1	λ_2	λ_3	λ_4	Π λ	λ_{max}	λ
0.0 – 51.0	Mid-span	60	2.05				2.51	2	2
51.0 – 72.0	Intermediate support	70	2.1				2.57	2.52	2.52
72.0 – 128.0	Mid-span	80	1.85				2.26	2	2
128.0 – 152.0	Intermediate support	80	2.2				2.69	2.7	2.69
152.0 – 208.0	Mid-span	80	1.85	1.224	1	1	2.26	2	2
208.0 – 232.0	Intermediate support	80	2.2				2.69	2.7	2.69
232.0 – 288.0	Mid-span	80	1.85				2.26	2	2
288.0 – 309.0	Intermediate support	70	2.1				2.57	2.52	2.52
309.0 – 360.0	Mid-span	60	2.05				2.51	2	2

Table 4.19: Factor λ.

The values obtained are exactly the same as the ones from the literature, since the calculation is straight and the same assumptions were considered.

4.7.1.7 Verification

Despite the program being able to assess on fatigue any critical detail from the girder bridge (see Figure 3.5), this work will just focus on one, aiming to show the program's operation and checking the results obtained. The one selected is the welded connection between the vertical stiffener and the lower steel flange (Detail 7 from Table 8.4 of EN 1993-1-9, Category 80).

First, the stress range is defined according to (Eq. 2.6) to (Eq. 2.8), depending if the concrete is always in tension, in compression or both.

Then, the equivalent stress range at 2M cycles is calculated:

$$\Delta\sigma_{E,2} = \Delta\sigma \cdot \lambda \cdot \phi \qquad (Eq.\ 4.10)$$

where the dynamic factor φ is set to 1.0 according to EN 1994-2, 6.8.6.1(7), and the lambda factor corresponds to the values calculated in the previous section.

Finally, in each section it is checked the fulfillment of (Eq. 2.17), considering that:

$$\frac{\Delta\sigma_C}{\gamma_{Mf}} = \frac{80}{1.35} = 59.26\ \text{MPa}$$

and the results are shown in Table 4.20 for S355 and in Table 4.21 for S690.

Section	140	144	148	152	156	160	164	168	172	176	180
$\sigma_{Ed,min,f}$	-5.579	-4.767	-6.282	-5.702	-5.240	-5.717	-5.361	-5.009	-5.574	-5.156	-4.735
$\sigma_{Ed,max,f}$	1.050	0.907	2.959	4.661	6.705	13.059	14.628	15.347	16.585	16.515	16.673
$\gamma_{Ff} \cdot \Delta\sigma_{E,2}$	17.833	15.261	24.856	27.875	23.889	37.552	39.979	40.714	44.318	43.343	42.817
Ratio	0.3009	0.2575	0.4194	0.4704	0.4031	0.6337	0.6746	0.687	0.7479	0.7314	0.7225

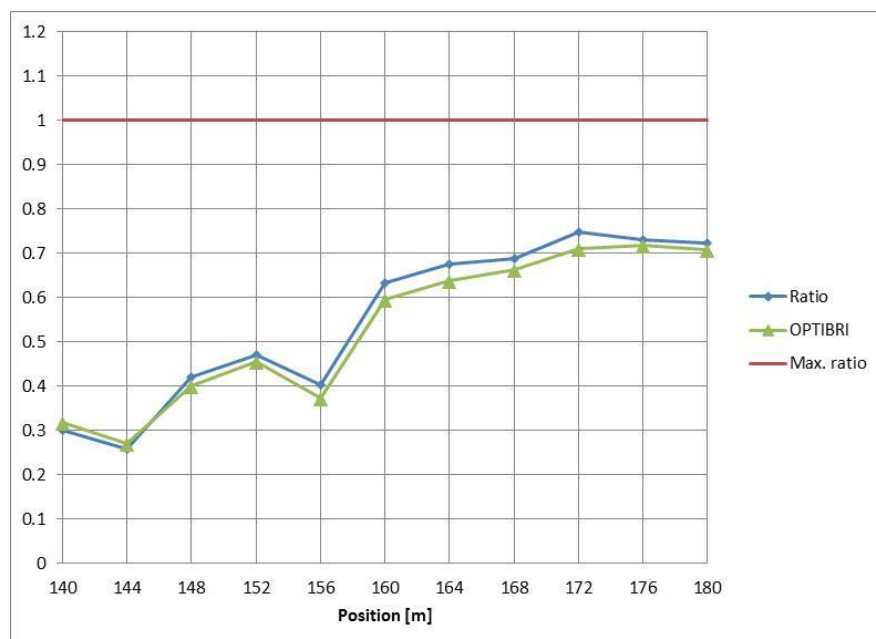*Table 4.20: Fatigue assessment of detail at bottom flange (equivalent damage factor method) using S355.*

Figure 4.10: Verification ratio of direct stresses on selected detail, using S355.

Section	140	144	148	152	156	160	164	168	172	176	180
$\sigma_{Ed,min,f}$	-11.587	-9.888	-7.765	-6.938	-6.419	-7.556	-7.104	-6.658	-6.487	-6.018	-5.553
$\sigma_{Ed,max,f}$	1.983	1.739	7.709	10.527	14.264	17.009	20.463	20.667	22.604	23.577	23.754
$\gamma_{Ff} \cdot \Delta\sigma_{E,2}$	36.502	31.276	41.625	46.981	41.365	49.130	55.133	54.651	58.183	59.191	58.614
Ratio	0.616	0.5278	0.7024	0.7928	0.698	0.8291	0.9304	0.9222	0.9818	0.9988	0.9891

Table 4.21: Fatigue assessment of detail at bottom flange (equivalent damage factor method) using S690.
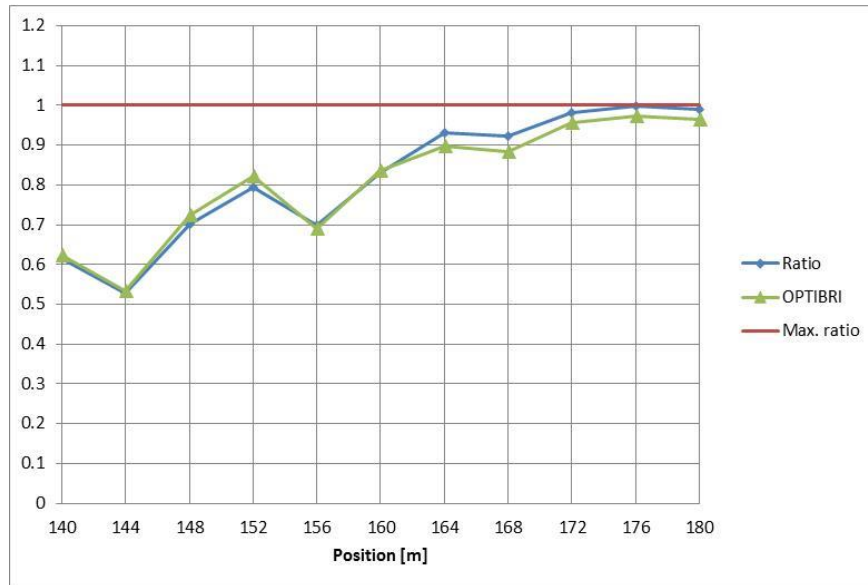
Figure 4.11: Verification ratio of direct stresses on selected detail, using S690.

In Figure 4.10 and Figure 4.11, the ratios are plotted and compared to the ones from OPTIBRI. It is noted that there are some differences in the values, which are associated to the different cross-section properties used in the calculation. This could be justified by the fact that both graphs show the same pattern, indicating that there is just some difference in the scale of the results.

The following tables show the differences found when comparing the values of $\gamma_{Ff} \cdot \Delta\sigma_{E,2}$ between the program and OPTIBRI, both for the scenarios with S355 and with S690.

Section	140	144	148	152	156	160	164	168	172	176	180
Program	17.833	15.261	24.856	27.875	23.889	37.552	39.979	40.714	44.318	43.343	42.817
OPTIBRI	18.889	16.074	23.778	27.037	22.148	35.259	37.778	39.259	42.148	42.519	41.926
Diff. [%]	-5.59%	-5.06%	4.53%	3.10%	7.86%	6.50%	5.83%	3.71%	5.15%	1.94%	2.13%

Table 4.22: Comparison of $\gamma_{Ff} \cdot \Delta\sigma_{E,2}$ values obtained from the Program and OPTIBRI, using S355.

Section	140	144	148	152	156	160	164	168	172	176	180
Program	36.502	31.276	41.625	46.981	41.365	49.130	55.133	54.651	58.183	59.191	58.614
OPTIBRI	36.889	31.630	42.889	48.741	40.889	49.556	53.259	52.370	56.667	57.630	57.111
Diff. [%]	-1.0%	-1.1%	-2.9%	-3.6%	1.2%	-0.9%	3.5%	4.4%	2.7%	2.7%	2.6%

Table 4.23: Comparison of $\gamma_{Ff} \cdot \Delta\sigma_{E,2}$ values obtained from the Program and OPTIBRI, using S690.

It seems that the differences obtained between this 2 methods are smaller when using S690, which could be explained by the fact that the effective properties are more defined and, thus, clearer in the latter. Once more, this hypothesis could not be proven here due to lack of details from the calculation performed during the case study.

Additionally, it is seen that, when using steel grade S690, the ratios are almost doubled close to the intermediate support, while reaching limit values close to mid-span. A graphical comparison between

both steel grades is shown in Figure 4.12. Is noticeable that, for the selected detail, when using S690 fatigue seems to be the governing limit state in the design (especially at mid-span), while it is not the case when using S355.
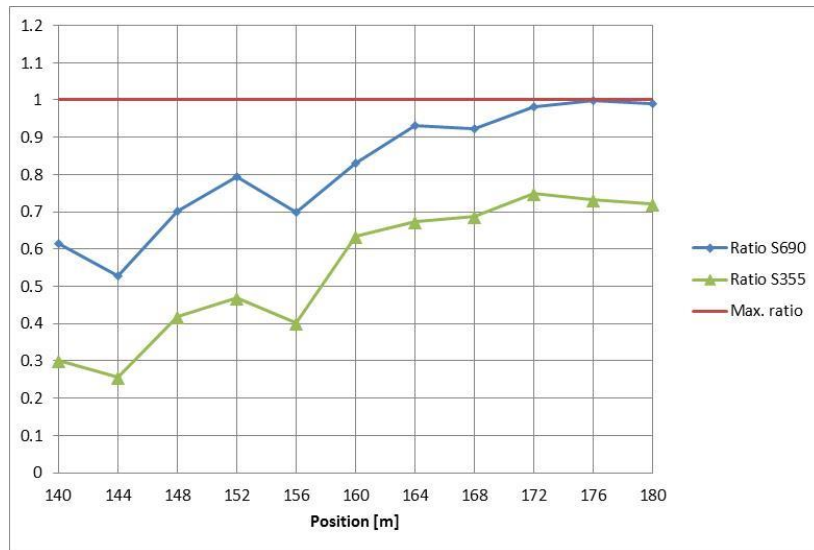
Figure 4.12: Verification ratio of direct stresses on selected detail placed at different locations. Comparison between S355 and S690.

4.7.2 Shear connectors

4.7.2.1 Factor λ_v

As explained in section 2.3.2.6, the factor λ_{v1} equals to 1.55 for road bridges with spans up to 100m, while factors λ_{v2} to λ_{v4} are determined as for the steel girders but using exponents of 8 and 1/8, to take account for the slope of the fatigue strength curve for headed studs m=8. Then, from (Eq. 2.19):

$$\lambda_{v2} = \frac{Q_{ml}}{Q_0} \cdot \left(\frac{N_{obs}}{N_0}\right)^{1/8} = 1.10$$

Applying (Eq. 2.21) the factor λ_{v3} equals to 1.0. Similar result returns (Eq. 2.22) for factor λ_{v4}. Finally, λ_{max} is the same as the one calculated in section 4.7.1.5.

From the previous values, it is possible to calculate the equivalent lambda factor for each region:

Position range [m]	Region	Critical influence line length [m]	λ_{v1}	λ_{v2}	λ_{v3}	λ_{v4}	$\Pi\,\lambda$	λ_{max}	λ_v
0.0 – 51.0	Mid-span	60						2	1.705
51.0 – 72.0	Intermediate support	70						2.52	1.705
72.0 – 128.0	Mid-span	80						2	1.705
128.0 – 152.0	Intermediate support	80						2.7	1.705
152.0 – 208.0	Mid-span	80	1.55	1.1	1	1	1.705	2	1.705
208.0 – 232.0	Intermediate support	80						2.7	1.705
232.0 – 288.0	Mid-span	80						2	1.705
288.0 – 309.0	Intermediate support	70						2.52	1.705
309.0 – 360.0	Mid-span	60						2	1.705

Table 4.24: Factor λ_v.

European Erasmus Mundus Master
Sustainable Constructions under natural hazards and catastrophic events
520121-1-2011-1-CZ-ERA MUNDUS-EMMC

surcos

The values obtained are exactly the same as the ones from the literature, since the calculation is straight and the same assumptions were considered.

4.7.2.2 Verification

According to EN 1993-1-9, the category details for shear studs fatigue assessment are:

- Detail 9 (Table 8.4) – Shear studs weld effect on base material. Detail category 80;

- Detail 10 (Table 8.5) – Shear cracks in the stud shank. Detail category 90.

First, the direct stresses are checked, for detail category 80. The results are shown in the following tables, both for the cases with S355 and with S690.

Section	140	144	148	152	156	160	164	168	172	176	180
$\sigma_{Ed,min,f}$	-5.519	-5.699	-0.161	-1.056	-0.952	-0.866	-0.761	-0.711	-0.030	-0.028	-0.026
$\sigma_{Ed,max,f}$	1.039	1.084	5.465	6.451	5.868	5.210	5.299	5.184	5.716	5.581	5.192
$\Delta\sigma_{E,2}$	17.706	18.313	15.192	20.269	13.639	12.152	12.120	11.790	11.491	11.217	10.435
Ratio	0.299	0.309	0.256	0.342	0.230	0.205	0.205	0.199	0.194	0.189	0.176

Table 4.25: Fatigue assessment of direct stresses in stud connector (equivalent damage factor method), using S355.

Section	140	144	148	152	156	160	164	168	172	176	180
$\sigma_{Ed,min,f}$	-8.307	-7.509	-6.119	-6.985	-5.911	-5.826	-5.720	-0.675	-0.610	-0.566	-0.522
$\sigma_{Ed,max,f}$	2.365	2.102	1.382	1.533	1.722	1.500	1.621	2.096	2.172	2.264	2.281
$\Delta\sigma_{E,2}$	28.815	25.951	20.252	22.998	15.266	14.653	14.684	5.543	5.565	5.660	5.605
Ratio	0.486	0.438	0.342	0.388	0.258	0.247	0.248	0.094	0.094	0.096	0.095

Table 4.26: Fatigue assessment of direct stresses in stud connector (equivalent damage factor method), using S690.

Secondly, the shear stresses are checked, for detail category 90. Using (Eq. 2.9) the longitudinal shear force per unit length at the steel-concrete interface due to FLM3 crossing ($\Delta v_{L,FLM3}$) is defined. Then, using (Eq. 2.10) and (Eq. 2.23) the equivalent shear stress range at 2M cycles is obtained.

The strength is calculated taking into account the partial factor for fatigue strength under shear:

$$\frac{\Delta\tau_C}{\gamma_{Mf,s}} = \frac{90}{1.0} = 90 \text{ MPa}$$

Finally, the results are:

Section	140	144	148	152	156	160	164	168	172	176	180
$\Delta v_{L,FLM3}$	119.336	130.001	131.020	121.406	115.207	121.234	120.538	120.265	117.833	177.833	117.769
$\Delta\tau_{E,2}$	33.076	36.032	48.419	44.866	42.575	44.803	44.546	44.445	71.143	71.143	70.104
Ratio	0.368	0.400	0.538	0.499	0.473	0.498	0.495	0.494	0.790	0.790	0.779

Table 4.27: Fatigue assessment of shear stresses in stud connector (equivalent damage factor method), using S355.

Section	140	144	148	152	156	160	164	168	172	176	180
$\Delta v_{L,FLM3}$	158.026	152.547	148.406	140.340	133.742	138.477	137.800	137.487	135.111	135.421	134.800
$\Delta\tau_{E,2}$	29.200	28.187	41.133	38.897	37.069	38.381	38.194	38.107	62.414	62.557	62.270
Ratio	0.324	0.313	0.457	0.432	0.412	0.426	0.424	0.423	0.693	0.695	0.692

Table 4.28: Fatigue assessment of shear stresses in stud connector (equivalent damage factor method), using S690.

The last check corresponds to the interaction between both direct and shear stresses, and should be according to (Eq. 2.24). The results are:

Section	140	144	148	152	156	160	164	168	172	176	180
Ratio	0.666	0.709	0.794	0.841	0.703	0.703	0.699	0.693	0.984	0.980	0.955

Table 4.29: Fatigue assessment of interaction between direct and shear stresses in stud connector (equivalent damage factor method), using S355.

Section	140	144	148	152	156	160	164	168	172	176	180
Ratio	0.811	0.751	0.799	0.820	0.669	0.674	0.672	0.517	0.787	0.791	0.786

Table 4.30: Fatigue assessment of interaction between direct and shear stresses in stud connector (equivalent damage factor method), using S690.

From Table 4.29 and Table 4.30, it is possible to observe that every section verifies for fatigue on the interaction stresses, since the values are always kept below 1.3.
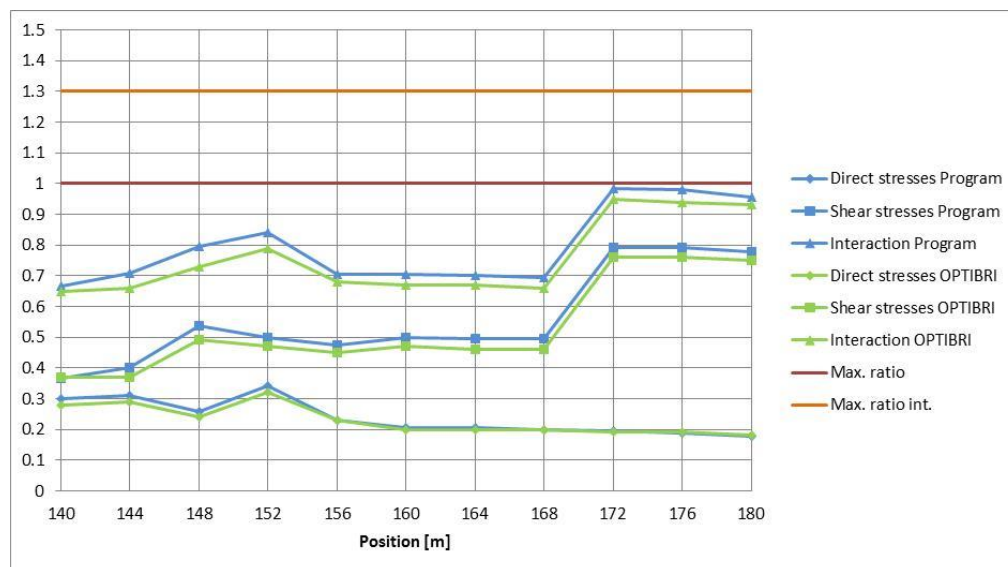

Figure 4.13: Verification ratio of shear head stud connector, using S355.

Comparison with the values from OPTIBRI show differences in the maximum and minimum stresses due to the different cross-section properties used in the calculation, though the results seem to be a good approximation.

4.8   DESIGN USING DAMAGE ACCUMULATION METHOD

Since OPTIBRI project just verified the details under fatigue using FLM3 and the damage equivalent factor method, in this section the design/assessment will be presented for the case study, though without comparison of results.

As mentioned when explaining the influence line module (section 4.5), just 2 sections will be studied, corresponding to a detail located at an intermediate support (x = 140m) and one at mid-span (x = 180m), both using S355 and S690.

4.8.1   Traffic simulation

For the hourly flow-rate day and night periods, the following means and standard deviations were obtained for the initial conditions:

Days of analysis	min speed	max speed	min gap	time analysis	min flow day	max flow day	min flow night	max flow night	start time day	end time day
	[km/h]	[km/h]	[sec]	[hrs]	[tr/hr]	[tr/hr]	[tr/hr]	[tr/hr]	[hr]	[hr]
28	60	110	1.5	720	100	200	10	100	6	22

Table 4.31: Initial conditions.

	Mean	St. Dev.
hourly_flow_rate_day [tr/hr]	150	28.83
hourly_flow_rate_night [tr/hr]	55	25.95

Table 4.32: Mean and standard deviation for day and night flow-rates.
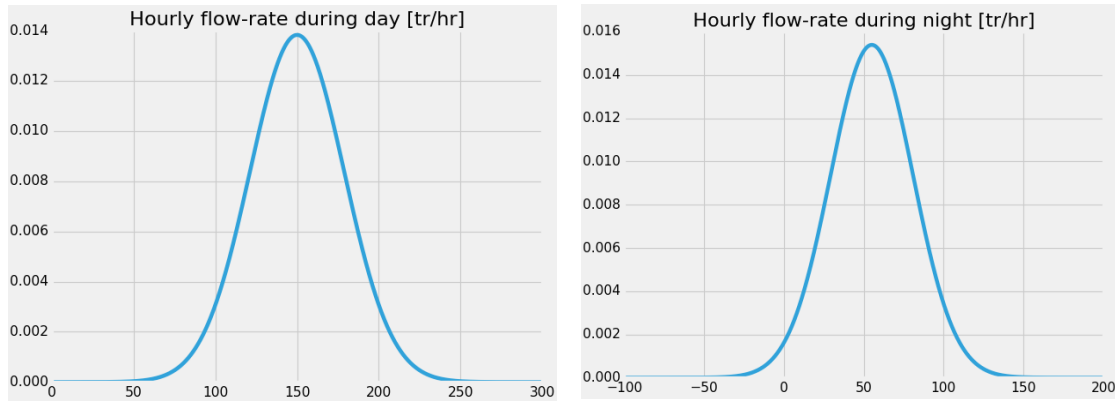
Figure 4.14: Charts showing the normal distribution on day and night flow-rates.

Regarding the speed, it presents the following statistical parameters:

	Mean	St. dev.
Truck speed [km/hr]	84.9	14.44

Table 4.33: Mean and standard deviation for truck speed.
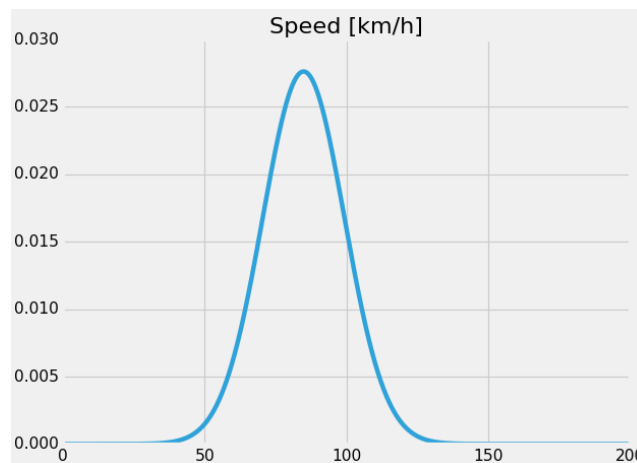
Figure 4.15: Chart showing the normal distribution on the truck speed.

4.8.2 Damage

The simulation run for a time period of 1 month and the results showed a maximum stress range of:

$\Delta\sigma_{max}$ [MPa]	S355	S690
At intermediate support	6.247	14.321
At mid-span	24.505	30.667

Table 4.34: Maximum stress range on selected detail after 1 month simulation, using S355 and S690.

Both details refer to the welded connection between lower flange of the girder and vertical stiffener. Here, it is important to mention that the detail corresponds to category 80, which, according to EN 1993-1-9, shows values of:

- $\Delta\sigma_C / \gamma_{Mf}$ = 80 MPa / 1.35 = 59.26

- $\Delta\sigma_D / \gamma_{Mf}$ = 0.737 * $\Delta\sigma_C / \gamma_{Mf}$ = 43.67 MPa (Constant Amplitude Fatigue Limit)

- $\Delta\sigma_L / \gamma_{Mf}$ = 0.405 * $\Delta\sigma_C / \gamma_{Mf}$ = 24 MPa (Cut-off Limit)

The cumulative damage for each case is shown in the following table:

	1 month		50 years		100 years	
Cumulative damage	**S355**	**S690**	**S355**	**S690**	**S355**	**S690**
At intermediate support	0	0	0	0	0	0
At mid-span	8.524 E-4	9.946 E-4	0.511	0.597	1.023	1.194

Table 4.35: Cumulative damage on selected details, using S355 and S690.

It is possible to observe from Table 4.34 that, for the detail located at an intermediate support, the maximum stress range stays below the value of the cut-off limit, which explains the zero-values observed in Table 4.35 for that same detail.

As seen in section 3.7.4, the simulation for 1 month shows sufficient convergence for the maximum stress range detected, since the latter is dependent on the type of loads and their variation over time, which is not considered in this project. Therefore, the simulation run for the whole service life period of the structure will still show the same maximum stress range and, hence, the same zero-damage in the detail.

On the other hand, stresses at mid-span seem to reach values above the cut-off limit, thus getting some accumulated damage after the simulation. Using linear extrapolation, an approximate cumulative damage in the structure on that detail over the whole service life (100 years) could be obtained, which, as shown in Table 4.35, is clearly beyond the safety limits stablished on the codes.

Another test was performed, but this time considering an increase of 20% on the trucks' weight, and mixing the results with the ones obtained from the previous simulation. Therefore, the values from Table 3.2, are now:

ID	GVW	Axles	wheelbase	Dist axle 12	Dist axle 23	Dist Axle 34	Dist axle 45	Load axle1	Load axle2	Load axle3	Load axle4	Load axle5	Composition
	[kN]		[m]	[m]	[m]	[m]	[m]	[kN]	[kN]	[kN]	[kN]	[kN]	[%]
1	240	2	4.5	4.5	0	0	0	84	156	0	0	0	20%
2	372	3	5.5	4.2	1.3	0	0	84	144	144	0	0	30%
3	588	5	11	3.2	5.2	1.3	1.3	84	180	108	108	108	15%
4	468	4	11.2	3.4	6	1.8	0	84	168	108	108	0	25%
5	540	5	14.1	4.8	3.6	4.4	1.3	84	156	108	96	96	10%

Table 4.36: Truck types with increased GVW (20%).

On the following tables, the maximum stresses and accumulated damage are presented for the simulation with increased trucks' weight.

Δσ$_{max}$ [MPa]	S355	S690
At intermediate support	7.493	17.177
At mid-span	29.442	36.846

Table 4.37: Maximum stress range on selected details after 1 month simulation for an increased-weight scenario, using S355 and S690.

	1 month		50 years		100 years	
Cumulative damage	**S355**	**S690**	**S355**	**S690**	**S355**	**S690**
At intermediate support	0	0	0	0	0	0
At mid-span	9.4 E-4	12.69 E-4	0.564	0.761	1.128	1.522

Table 4.38: Cumulative damage on selected details for an increased-weight scenario, using S355 and S690.

Adding up the cumulative damage on the detail after 50 years from Table 4.35 and Table 4.38, the results show that the damage for the whole service life of the bridge is:

	100 years	
Cumulative damage	**S355**	**S690**
At intermediate support	0	0
At mid-span	1.075	1.358

Table 4.39: Cumulative damage on selected details for an mixed-weight scenario after 100 years, using S355 and S690.

The idea with the traffic mixture is to consider an increase on the trucks' weight along time, which is a more realistic approach. Comparing the results from Table 4.35 and Table 4.39, it is noticed that for the model with S355, there is an increase of ~5% on the damage, whereas for the model with S690, the increase goes up to ~14%, almost 3 times more. Thus, the use of HSS should be studied more carefully in the long term, since the reduced cross-section could lead to fatigue problems.

At this point, it is necessary to mention that the safe life design method used in OPTIBRI seems to be too strict, and therefore, it conditions the design. On a different approach, a smaller partial factor could be used and improve the strength of the details. The latter would implicate the consideration of inspection and maintenance programs which should be scheduled and carried out after certain years of service in order to detect and control the initiation and further propagation of cracks.

As we mentioned before, the traffic simulation presents numerous assumptions and limitations that restrict its application to simple cases. Moreover, calibration of the model should be performed to compare the results with real traffic as to analyse and adjust the variables according to different statistical distributions and validate the simulation.

5 CONCLUSIONS AND FUTURE WORK

5.1 CONCLUSIONS

Conclusions are arranged in accordance with the objectives stated in section 1. The main objective was to develop a new software tool which would allow to design and assess under fatigue any detail from a composite concrete-steel girder bridge, using both design approaches proposed by the Eurocodes: the damage equivalent factor and the damage accumulation methods. Moreover, a simulation of traffic was developed in order to represent the stochastic variables involved in a more 'realistic' loading scheme.

The second objective was to compare the results obtained from the aforementioned program with the ones from the case study OPTIBRI.

From the analysis, the following conclusions are drawn:

♦ The truck simulation consists on a more realistic approach compared to the fatigue load models mentioned in the Eurocodes, though it requires the accurate definition of many variables involved in the process. In this project, many simplifications were considered which limit the application and results. Additionally, no validation of the module was able to be performed due to lack of real traffic data and time constraints.

♦ The main initial parameters affecting the traffic simulation developed in this project are the period of time under analysis, the traffic flow and the time step.

♦ Using a stable generation of trucks throughout the simulation process, i.e. without increasing the size of the loads through the structure's service life, the simulation converges quickly to the maximum stress range, thus being independent on the time of analysis chosen.

♦ The effect of having several trucks on the bridge either in the same lane or in several lanes is important and it should be taken into account.

♦ The results from the program when studying the damage equivalent factor method show some differences with the ones from OPTIBRI, being attributed, mainly, to the calculation of the effective cross-section properties. However, the results showed a good approximation, hence, validating the program.

♦ A mixed-weight truck composition was proposed in order to study the impact of the increased GVW through time, and results showed that the effects were sensibly bigger in the model with HSS.

♦ Using the cumulative damage method, the resulting damage for the structure's service life for the detail under analysis (welded connection between lower flange of the girder and vertical stiffener at mid-span and at an intermediate support), exceeds the limit considered in EN 1993-1-9, meaning failure of the structure in the long-term. One alternative solution could be changing the design approach and considering inspection and maintenance programs to be performed during its service life, which would help detect and control the initiation and propagation of cracks due to fatigue. Another alternative could be improving the details by means of post-welded treatment.

♦ It was stated that the use of HSS has advantages in both environmental and economic criteria compared to normal steel grades (S355). However, the use of smaller quantities of steel and, thus, smaller cross-sections, affects the fatigue behaviour when submitted to cyclic loading, since the stresses registered in the structure are bigger. Therefore, further studies should be considered as to evaluate the overall advantage on the use of HSS over S355, particularly trying to improve the fatigue behaviour.

5.2 FUTURE WORK

There are still many improvements and future work that could be developed as to obtain more accurate and complete results. Based on the work presented and the conclusions drawn, the following main future work items are recommended:

- ♦ Calibration of the traffic simulation with real traffic data,

- ♦ Improve the simulation by tackling some of its limited parameters, such as:

  - o generate random trucks, using statistical approach of their main variables, e.g. GVW, number of axles, distance between axles etc.,

  - o model different number of slow lanes on the bridge,

  - o include overtaking or lane change within the length of bridge,

  - o include driver's behaviour etc.

- ♦ Improve the calculation of stress history from the action effects' history, by means of a Finite Element software, for instance.

- ♦ Include load effects from non-cyclic loading.

- ♦ Study the dynamic nature of the loading and its impact in the calculation.

- ♦ Structural improvements of the details by means of post-welded treatment and its impact on global performance of the bridge under fatigue.

- ♦ Expand the traffic simulation to include the calculation of load effect maxima for the entire service life of the bridge, including estimation of future vehicles configurations in the stream.

- ♦ Include other bridges configuration, such as arch, cable-stayed or suspended bridges.

European Erasmus Mundus Master
Sustainable Constructions under natural hazards and catastrophic events
520121-1-2011-1-CZ-ERA MUNDUS-EMMC

ᒓᑌᒐᑕᓍᒐ

REFERENCES

[1] M. Al-Emrani, M. Aygül. *Fatigue design of Steel and composite bridges*. Göteborg, Sweden. 2014.

[2] A. Nussbaumer, L. Borges, L. Davaine. *Fatigue design of steel and composite structures*. ECCS Eurocode Design Manuals. 1st edition, 2011.

[3] P. Croce. *Background to fatigue load models for Eurocode 1: Part 2 Traffic Loads*. Progress in Structural Engineering and Materials, 2001. p. 335-345.

[4] P. Croce et al. Guidebook 2 - Design of Bridges, ed. P. Croce. 2010, Prague: Czech Technical University.

[5] A. Reis, J. Oliveira Pedro, C. Baptista, F. Virtuoso, C. Vieira. *Optimal use of High Strength Steel grades within bridges (OPTIBRI)*. Research Programme of the Research Fund for Coal and Steel. European Commission.

[6] B. Enright. *Simulation of traffic loading on highway bridges*. PhD thesis, College of Engineering, Mathematical and Physical Sciences of University College Dublin, 2010.

[7] EN1991-2. *Eurocode 1 - Actions On Structures - Part 2: Traffic Loads On Bridges*. European Committee for Standardization, Brussels, 2002.

[8] EN1993-1-9. *Eurocode 3: Design of steel structural - Part 1-9: Fatigue*. European Committee for Standardization, Brussels, 2005.

[9] EN1993-2. *Eurocode 3 - Design of steel structures - Part 2: Steel Bridges*. European Committee for Standardization, Brussels, 2006.

[10] C. Crespo-Minguillon and J. R. Casas. *A comprehensive traffic load model for bridge safety checking*. Structural Safety, 19(4):339–359, 1997.

[11] A. S. Nowak. *Live load model for highway bridges*. Structural Safety, 13(1-2):53–66, 1993.

[12] C. Miki, Y. Goto, H. Yoshida, and T. Mori. *Computer simulation studies on the fatigue load and fatigue design of highway bridges*. Proc. of JSCE Structural Eng./Earthquake Eng, 2(1):37–46, 1985.

[13] J. A. Laman and A. S. Nowak. *Fatigue-load models for girder bridges*. Journal of Structural Engineering-ASCE, 122(7):726–733, 1996.

[14] A. O'Connor and E. J. O'Brien. *Traffic load modelling and factors influencing the accuracy of predicted extremes*. Canadian Journal of Civil Engineering, 32(1):270–278, 2005.

[15] T. J. Miao and T. H. T. Chan. *Bridge live load models from WIM data*. Engineering Structures, 24(8):1071–1084, 2002.

[16] W. McKinney. *Python for Data Analysis*. Published by O'Reilly Media Inc. First edition, USA, 2012.

[17] H. Gervásio et al., *Improved design of composite highway-bridges to enhance lifetime performance*. Life-Cycle of Structural Systems – Furuta, Frangopol & Akiyama (Eds). London, 978-1-138-00120-6. 2015.

[18] Y. B. Yang et al., *Vehicle-Bridge interaction dynamics*. ISBN: 978-981-256-717-8. 2004.

A   BEAM ANALYSIS

A.1   INTRODUCTION

This module aims to get the load effects on any type of beam configuration. Particularly, it was developed in this project in order to be able to define the shear and moment influence lines on particular cross-sections, which will then be used in both the simplified method and the damage accumulation one.

The main inputs of this module are:

- **Segments**: list including the properties of the cross-section along the beam, such as:
  - Position [m]: place where the cross-section changes its properties
  - E.I [kN.m^2]: Product of the Modulus of Elasticity (E) and the Second Moment of Area of the cross-section around its strong axis (I).
  - G.A [kN]: Product of the Shear Modulus (G) and the Area of the cross-section.

- **Outpoints**: indicates the position of the cross-section where the load effects want to be obtained (could be one or multiple sections).

- **Supports**
  - Position [m]: place where the support is located.
  - Translational rigidity: sets the restriction on the vertical displacements at the support section. If equal to -1, it is infinitely rigid (translation restricted).
  - Rotational rigidity: similar to the previous one, but for rotations at the support. If equal to -1, the support is fully fixed.
  - Imposed displacements [m]: vertical imposed displacements at the supports.

- **Distributed Loads** (*DLoads*)
  - Starting point [m]: place where the load starts.
  - Ending poing [m]: place where the load finishes.
  - Load at starting point [kN]
  - Load at ending point [kN]

- **Point Loads** (*PLoads*)
  - Position [m]: place where the load is located.
  - Point force [kN]
  - Point moment [kNm]

Some limitations on the module are listed below:

- ✓ It does not include axial loading nor loads in the direction of the beam's weak axis.
- ✓ It does not consider any load or deflection in the direction of the cross-section's weakest axis
- ✓ The distributed loads just allows for either constant or linear distributed loads.

Finally, the output consists of a number of sections (according to Outpoints) with the following information:

1) Position [m];
2) Shear force [kN];
3) Bending moment [kNm];

4) Slope / Rotation [1/m];

5) Deflection [m].

A.2 OPERATION

First, it is important to mention the main methods that were developed and used in this module and their functions:

- *Macaulay*: Integrates shear and bending moments by using Macaulay's method to find slopes and deflections.

- *Cantilever*: calculates the shear, moment, slope and deflection for a cantilever beam.

- *SSSpan*: idem Cantilever but for a simple supported beam.

- *ConBeam*: idem SS beam but for a continuous beam.

All of them are closely interconnected and the list is sorted in ascending order of importance. In other words, the latter is the main module (*ConBeam*) and is the one used by the program to get the load effects in the main girders by means of interacting with the other methods. The process of calculation is summarized in the flowchart showed in Figure A.1.

A.2.1 Macaulay's method

Macaulay's method (also known as *double integration method*) is a technique used in structural analysis to determine the deflection and slopes of Euler-Bernoulli beams. Use of Macaulay's technique is very convenient for cases of discontinuous and/or discrete loading. Typically partial uniformly distributed loads (u.d.l.) and uniformly varying loads (u.v.l.) over the span and a number of concentrated loads are conveniently handled using this technique, and, thus, are covered in this project.

The starting point is the relation between bending moment and curvature from Euler-Bernoulli beam theory:

$$\frac{d^2v}{dx^2} = \frac{M}{E \cdot I}$$

(Eq. A.1)

where *v* is the deflection and *M*, the bending moment. This equation is simpler than the fourth order differential equation for displacements and can be integrated twice to find the deflection if the function M(x) is known.

The steps to follow are summarized in the next list:

1. Calculation of support reactions;

2. Take a section *x-x* at a distance far away from left hand support;

3. Calculate bending moments acting on section x-x (from left hand side);

$$My_{x-x} = \sum My_{\overline{x-x}}$$

$$E \cdot Iy \cdot \frac{d^2v}{dx^2} = \sum My_{\overline{x-x}_i}$$

4. Integrating the bending moment equation twice, we get:

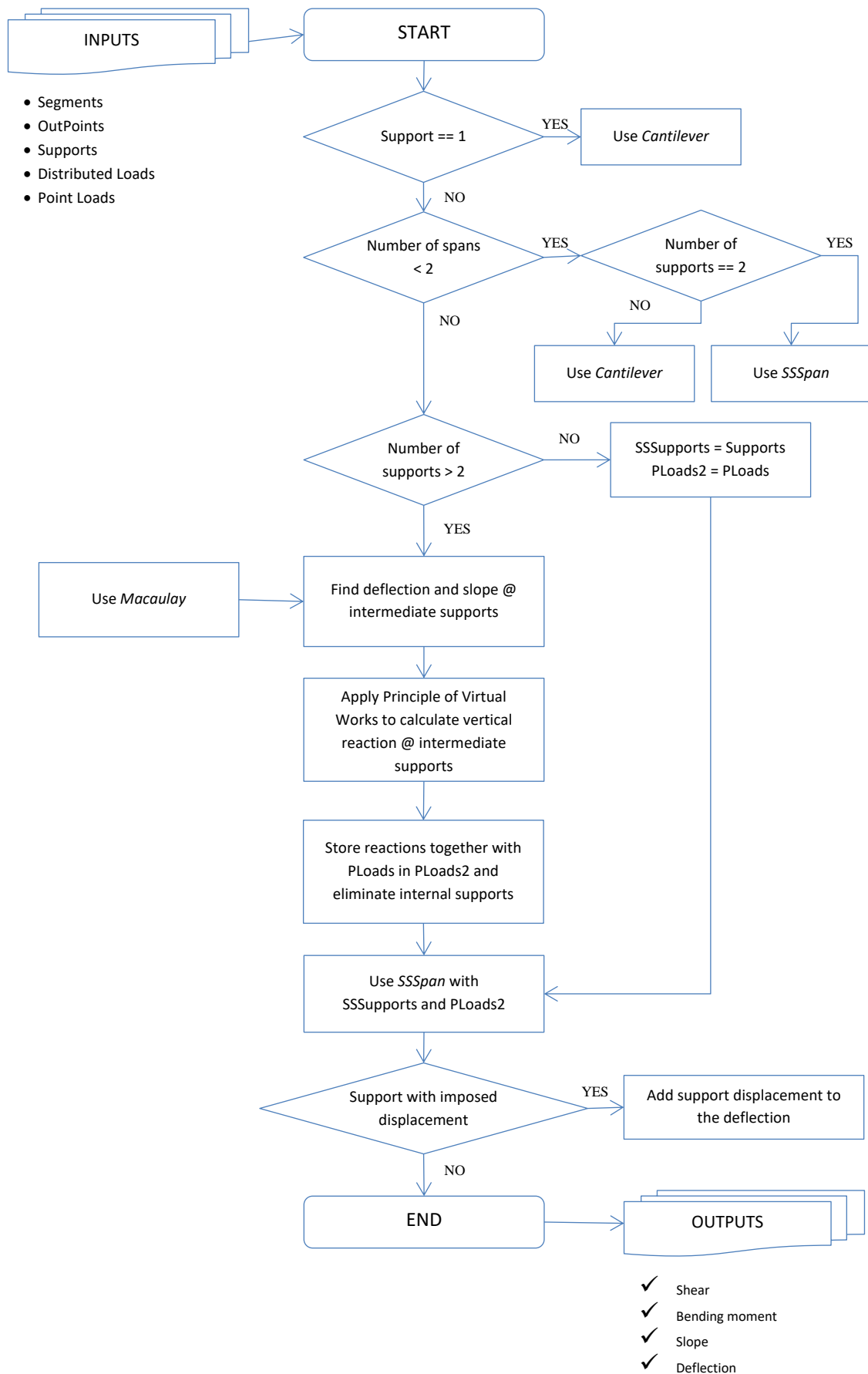$$E \cdot Iy \cdot v = \sum \iint My_{\overline{x-x}_i} \cdot dx^2 + C_{1_i} \cdot x + C_{2_i}$$

Figure A.1: Flowchart – Beam Analysis module.

5. Apply the boundary conditions to obtain the values of C1 and C2, and finally get the deflection and slope:

$$Deflection = v = \frac{\sum \iint My_{\overline{x-x}_i} \cdot dx^2 + C_{1_i} \cdot x + C_{2_i}}{E \cdot Iy}$$

$$Slope = \frac{dv}{dx} = \frac{\sum \int My_{\overline{x-x}_i} \cdot dx + C_{1_i}}{E \cdot Iy}$$

In the program, each type of load is treated separately and is briefly explained as follows.

Concentrated loads

The expression for the Bending Moment for all the loads on the left from section *x* is:

$$E \cdot I \cdot \frac{d^2v}{dx^2} = M = -W_1 \cdot x + R \cdot (x-a) - W_2 \cdot (x-b) - W_3 \cdot (x-c) \qquad \text{(Eq. A.2)}$$
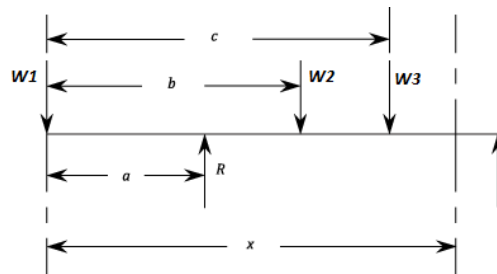

Figure A.2: Concentrated loads on a beam (Macaulay's example).

Integrating the previous expression:

$$E \cdot I \cdot \frac{dv}{dx} = -W_1 \cdot \frac{x^2}{2} + \frac{R}{2} \cdot (x-a)^2 - \frac{W_2}{2} \cdot (x-b)^2 - \frac{W_3}{2} \cdot (x-c)^2 + A \qquad \text{(Eq. A.3)}$$

And integrating once more:

$$E \cdot I \cdot v = -W_1 \cdot \frac{x^3}{6} + \frac{R}{6} \cdot (x-a)^3 - \frac{W_2}{6} \cdot (x-b)^3 - \frac{W_3}{6} \cdot (x-c)^3 + A \cdot x + B \qquad \text{(Eq. A.4)}$$

Where A and B are the constants of integration which are common to all sections of the beam.

Uniformly distributed loads

Supposing that a uniformly distributed load is applied from a distance *a* to a distance *b* measured from one end. Then in order to obtain an expression for the Bending Moment at a distance *x* from the end, which will apply for all values of *x*, it is necessary to continue the loading up to the section at *x*, compensating this with an equal negative load from *b* to *x* (see Figure A.3).
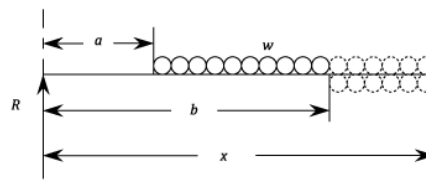

Figure A.3: Uniformly distributed loads on a beam (Macaulay's example).

Hence:

$$M = R \cdot x - \frac{w}{2} \cdot (x - a)^2 + \frac{w}{2} \cdot (x - b)^2 \qquad \text{(Eq. A.5)}$$

Each length of the loading acts at its centre of gravity.

For a < x < b:

$$M = R \cdot x - \frac{w}{2} \cdot (x - a)^2 \qquad \text{(Eq. A.6)}$$

The remaining steps of integration are the evaluation of the constants as shown in the previous section.

Concentrated bending moments

It is possible to express:

$$E \cdot I \cdot \frac{d^2 v}{dx^2} = M = -R \cdot x + M_0 \cdot (x - a)^0 \qquad \text{(Eq. A.7)}$$

$$E \cdot I \cdot \frac{dv}{dx} = -R \cdot \frac{x^2}{2} + M_0 \cdot (x - a) + A \qquad \text{(Eq. A.8)}$$

$$E \cdot I \cdot v = -R \cdot \frac{x^3}{6} + \frac{M_0}{2} \cdot (x - a)^2 + A \cdot x + B \qquad \text{(Eq. A.9)}$$
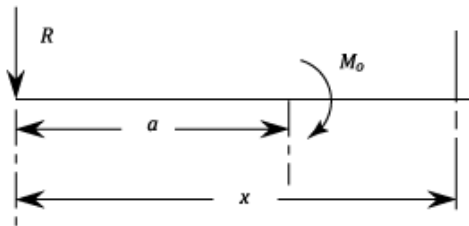

Figure A.4: Concentrated moment on a beam (Macaulay's example).

A.3   EXAMPLE

In order to have a clearer representation of its functionality, it will be applied to a simple example, a double-span continuous supported beam, and the results will be compared to the ones obtained using a FE software (Robot Structural Analysis).

The beam has 2 spans of 10m and 22m respectively (see Figure A.5), and the following inputs:

BEAM SEGMENTS		
Position @end	E * Iy	G * A
[m]	[kN.m^2]	[kN]
8.00	1.6667E+06	6.6667E+06
20.00	3.3333E+06	1.3333E+07
32.00	1.6667E+06	6.6667E+06
SUPPORTS			
---	---	---	---
Position	Translational rigidity	Rotational rigidity	Imposed displacement
[m]		[1/m]	[m]
0.00	-1	0	0
10.00	-1	0	0
32.00	-1	0	0

DISTRIBUTED LOADS			
Position @start	Position @end	Load/m @start	Load/m @end
[m]	[m]	[kN/m]	[kN/m]
2	4	10	20
16	18	10	20
26	28	10	20
POINT LOADS			
Position		Point Load	Point Moment
[m]		[kN]	[kN.m]
2		-100	0
6		0	100
14		-100	0
18		0	100
28		0	100
30		-100	0

Table A.1: Inputs for continuous beam (example).

The Outpoints chosen where every 2m step: (0, 2, 4, 6… 30, 32).

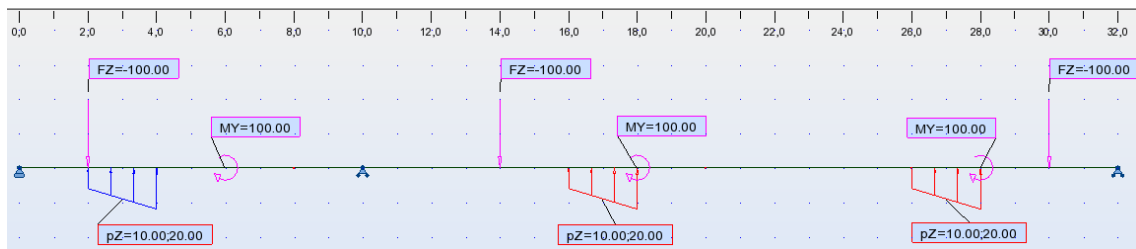The static configuration and loading on the beam could be seen in Figure A.5.

Figure A.5: Loading and static configuration of continuous beam (example).
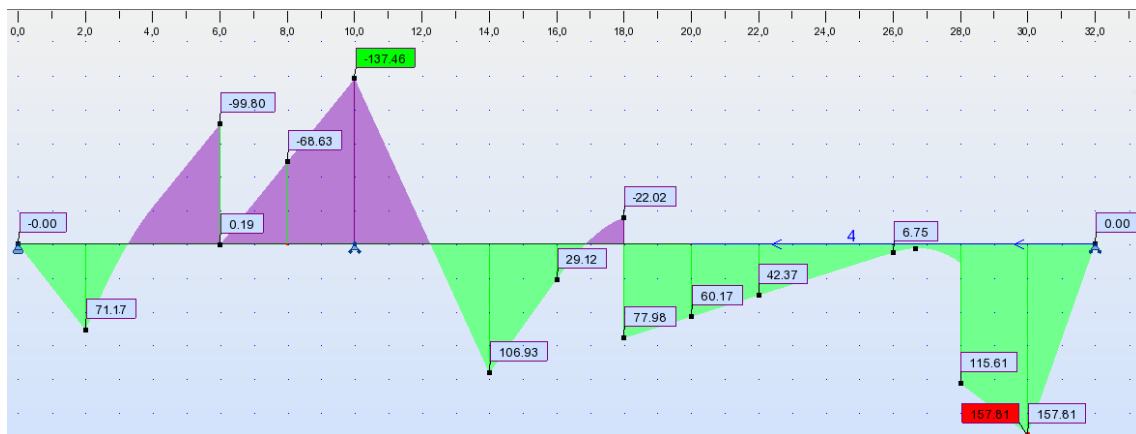

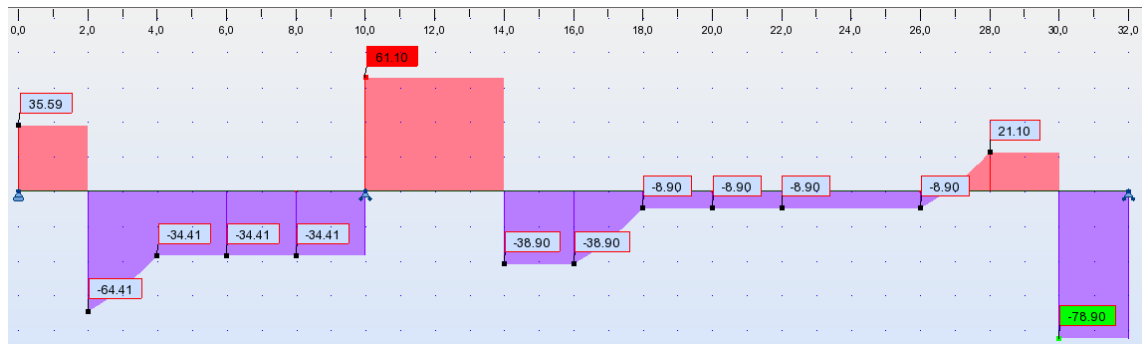*Figure A.6: Bending moments for continuous beam (example).*

Figure A.7: Shear for continuous beam (example).

The bending moment and shear diagrams obtained from the FE software are shown in Figure A.6 and Figure A.7 respectively. Finally, the comparison between the results from the program and the ones from the FE software, is detailed in Table A.2.

Position	Shear [kN]		Dif.	Moment [kN.m]		Dif.
[m]	ConBeam	FE	[%]	ConBeam	FE	[%]
0	35.5874	35.59	-7.42E-05	0.0000	0.00	0.00E+00
2	-64.4126	-64.41	4.10E-05	71.1747	71.17	6.63E-05
4	-34.4126	-34.41	7.67E-05	-30.9839	-30.98	1.26E-04
6	-34.4126	-34.41	7.67E-05	-99.8092	-99.80	9.19E-05
8	-34.4126	-34.41	7.67E-05	-68.6345	-68.63	6.49E-05
10	61.0967	61.10	-5.48E-05	-137.4597	-137.46	-1.96E-06
12	61.0967	61.10	-5.48E-05	-15.2664	-15.26	4.21E-04
14	-38.9033	-38.90	8.60E-05	106.9269	106.93	-2.91E-05
16	-38.9033	-38.90	8.60E-05	29.1202	29.12	6.73E-06
18	-8.9033	-8.90	3.76E-04	-22.0198	-22.02	-7.78E-06
20	-8.9033	-8.90	3.76E-04	60.1735	60.17	5.78E-05
22	-8.9033	-8.90	3.76E-04	42.3668	42.37	-7.58E-05
24	-8.9033	-8.90	3.76E-04	24.5601	24.56	3.99E-06
26	-8.9033	-8.90	3.76E-04	6.7534	6.75	5.04E-04
28	21.0967	21.10	-1.59E-04	15.6134	15.61	2.17E-04
30	-78.9033	-78.90	4.24E-05	157.8067	157.81	-2.10E-05
32	-78.9033	-78.90	4.24E-05	0.0000	0.00	0.00E+00

Table A.2: Results from Beam module compared to FE software (example).

Thus, it is possible to see a very good match (small difference) between both results, which indicates that the program gives accurate and trustful results.

B   RAINFLOW COUNTING METHOD

The rainflow-counting method is used in the analysis of fatigue data in order to reduce a spectrum of varying stress into a set of simple stress reversals. Its importance is that it allows the application of Miner's rule in order to assess the fatigue life of a structure subject to complex loading.

The algorithm consists of the following steps:

1. Reduce the time history to a sequence of alternated peaks and valleys.

2. Count the number of half-cycles by looking for terminations in the flow occurring when either:

    a. It reaches the end of the time history;

    b. It merges with a flow that started at an earlier peak; or

    c. It flows when an opposite peak has greater magnitude.

3. Repeat step 2 for the valleys.

4. Assign a magnitude to each half-cycle equal to the stress difference between its start and termination.

5. Pair up half-cycles of identical magnitude (but opposite sense) to count the number of complete cycles. Typically, there are some residual half-cycles.

B.1   EXAMPLE

A simple example is shown in order to explain how the algorithm works and compare hand calculation results with the ones obtained from the program.

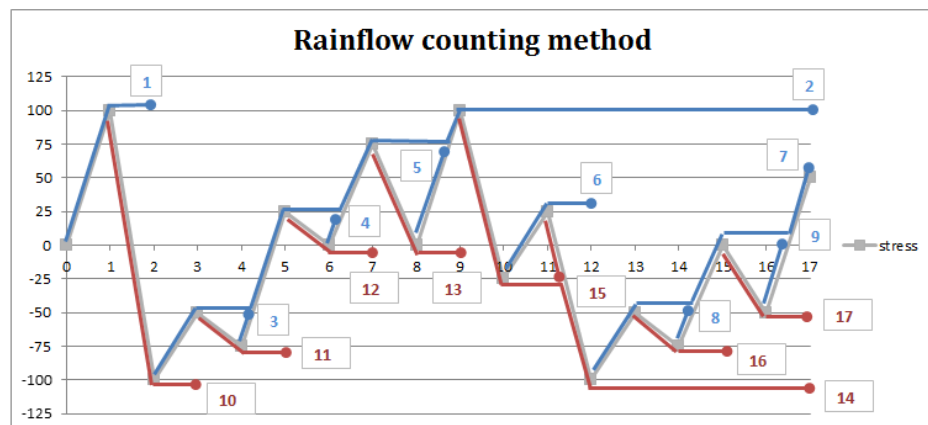| x	stress
0	0
1	100
2	-100
3	-50
4	-75
5	25
6	0
7	75
8	0
9	100
10	-25
11	25
12	-100
13	-50
14	-75
15	0
16	-50
17	50

Figure B.8: Example of rainflow counting method.

Every half-cycle is counted (see blue and red lines in Figure B.8) and the results for every stress range are shown in Table B.3.

#	From	To	Range
1	0	100	100
2	-100	100	200
3	-75	-50	25
4	0	25	25
5	0	75	75
6	-25	25	50
7	-100	50	150
8	-75	-50	25
9	-50	0	50
10	100	-100	200
11	-50	-75	25
12	25	0	25
13	75	0	75
14	100	-100	200
15	25	-25	50
16	-50	-75	25
17	0	-50	50

Range	Count
25	3
50	2
75	1
100	0.5
150	0.5
200	1.5

Table B.3: Results from rainflow counting method (hand calculation).

On the other hand, the results from the program show the following:

```
stresses = [   0  100 -100  -50  -75   25    0   75    0  100  -25   25 -100  -50  -75
   0  -50   50]

stress range = [  25.   50.   75.  100.  150.  200.]

number of cycles = [ 3.    2.    1.    0.5  0.5  1.5]
```

Figure B.9: Results from rainflow counting method (program).

Therefore, in this simple example it is possible to observe that the algorithm is well developed in the program and accurate results could be obtained as to be used, further on, for the damage calculation on the detail due to fatigue.